TO INVESTIGATE THE ACCURACY OF DOSE MEASUREMENT IN MEGA VOLTAGE BLOCKED BEAM γ-RADIATION AND TO DEVELOP AN EMPIRICAL RELATION FOR TREATMENT PROCEDURE

By

Md. Shamsuzzaman

A dissertation submitted in partial fulfillment of the requirement for the degree of M.Phil. in the department of Physics, Bangladesh University of Engineering & Technology, Dhaka.

Department of Physics

Bangladesh University of Engineering & Technology

Dhaka, Bangladesh

September 2006

BANGLADESH UNIVERSITY OF ENGINEERING & TECHNOLOGY (BUET)
DEPARTMENT OF PHYSICS, DHAKA-1000, BANGLADESH

Certification of thesis work

The thesis titled "***TO INVESTIGATE THE ACCURACY OF DOSE MEASUREMENT IN MEGA VOLTAGE BLOCKED BEAM γ-RADIATION AND TO DEVELOP AN EMPIRICAL RELATION FOR TREATMENT PROCEDURE***", submitted by **MD. SHAMSUZZAMAN,** Roll No: 100114003P, Session- October 2001, has been accepted as satisfactory in partial fulfillment of the requirement for the degree of **MASTER OF PHILOSOPHY (M. Phil.)** in Physics on **17 September 2006.**

BOARD OF EXAMINERS

1. Dr. Nazma Zaman, (Supervisor) — Chairman
   Professor, Department of Physics
   BUET, Dhaka-1000

2. Mr. M. Jahangir Alam (Co-Supervisor) — Member
   Senior Medical Physicist
   Delta Medical Centre Ltd
   Mirpur-1, Dhaka

3. Dr. Jiban Podder — Member
   Professor & Head
   Department of Physics
   BUET, Dhaka-1000

4. Dr. Md. Abu Hashan Bhuiyan — Member
   Professor
   Department of Physics
   BUET, Dhaka-1000

5. Dr. Nurul Alam — Member (External)
   Chief Scientific Officer
   Physical Science Division
   Bangladesh Atomic Energy Commission (BAEC)
   Dhaka

CANDIDATE'S DECLARATION

It is bereby declared that this thesis or any part of it has not been submitted elsewhere for the award of any degree or diploma.

Signature of the supervisors:

NZaman

(Dr. Nazma Zaman)
Supervisor
Professor
Department of Physics
BUET, Dhaka.

Jahangir Alam

(Md. Jahangir Alam)
Co-Supervisor
Senior Medical Physicist
Delta Medical Center Ltd.
Mirpur, Dhaka.

Signature of the Candidate:

(Md. Shamsuzzaman)

CONTENTS

Chapter-I Introduction

Chapter-II Review

List of Tables

List of Figures

Acknowledgement

With great pleasure I would like to express my hearted gratitude to my supervisor *Dr.Nazma Zaman*, Professor, Department of Physics, Bangladesh University of Engineering and Technology (BUET) for her continuous guidance and kind supervision throughout the progress of my research work. Her all-out support and guidance paved the way for a smooth jaunt and eventually helped me come up with fruitful findings.

I shall always remain grateful to my co-supervisor *Mr. Md. Jahangir Alam*, Senior Physicist, Delta Medical Center Ltd. Dhaka, for his constant guidance and whole hearted co-supervision throughout the research work, without which it would have been impossible for me to carry out this extensive experimental work.

I would like to convey my heartfelt gratitude to *Prof Jiban Podder*, Head, Department of Physics, BUET, for his keen interest and the unvarying inspection I received from him throughout the progress of my work. Special thanks also go to *Prof. Abu Hashan Bhuiyan, Prof.M. Mominul Huq* of the department for their valuable support during this work. I am also thankful to all other teachers of the department for their encouragement.

I am indebted to *Dr. Syed Reza Husain*, Chief Medical Physicist, Delta Medical Center Limited and Ex-director, Institute of Nuclear Medicine, BAEC, Dhaka, for his kind permission to use the facilities available in the Oncology Unit of DMCL at Mirpur and for valuable guidance, cordial and enthusiastic inspiration during the course of this research work.

I would like to express my heartfelt gratitude to *Prof. Gias Uddin Ahmad*, who constantly guided me through my co-supervisor during experimental work being presented at Delta Medical Center.

I would also like to express my sincere gratitude to *Mr. Md. Shakilur Rahman*, Senior Scientific Officer, SSDL, HP&RWMU, INST, Atomic Energy Research Establishment, for backing me up with his continuous encouragement and thus helping me complete the thesis work.

I would like to thank *Mr S. Roy*, Principle, Scientific Officer, Health Physics Division, Atomic Energy Center, Dhaka, BAEC, for his valuable suggestions.

From the core of my heart, I convey my gratitude to *Dr. S.M. Ali*, Managing Director, Delta Medical Center Ltd., for making available allout technical supports in the form of all possible equipment facilities of their establishment.

Abstract

Irregularly shaped fields are usually encountered in routine radiotherapy when radiation sensitive structures are shielded from the primary beam or when the field extends beyond the irregularly shaped patient body contour. The aims of the present work were (a) to investigate the accuracy of dose measurement in irregular photon fields encountered in routine radiotherapy practices. (b) to develop an Empirical relation for radiotherapy treatment procedure. For treatment planning in irregular photon fields usually encountered in routine radiotherapy practices eleven (11) irregular fields were simulated in solid perspex phantom to investigate the doses for photon beam of ^{60}Co teletherapy unit. It was expected that, these fields would almost cover the different irregular fields encountered in daily radiotherapy practices at different therapy establishments. The direct measurement dose values in irregular fields were compared with calculated dose values obtained by the use of Clarkson's method and newly developed Empirical relation of dose calculation in irregular photon fields. The Tables 3(I-XI) contain, directly measured dose values at various interested points in different irregular fields, the directly measured dose values at those points in the corresponding open fields, percentage difference of dose values between irregular (blocked) and open fields, calculated dose values at respective points using both Clarkson's method and Empirical relation, percentage difference of dose values between directly measured and calculated values. The calculated dose values of Empirical relation are in good agreement with the directly measured dose values at different points in irregular fields, So that, dose estimation in irregular fields could be approximated with reasonable accuracy from the calculated dose values of Empirical relation normalized to central axis beam dose data in respective open fields. The averaged of the mean percentage differences with 1sd between directly measured dose values at different points in irregular (blocked) fields and the corresponding dose values at those points in open fields of 3(i–xi) for ^{60}Co was found to be 16.76% ± 9.12 (range 2.45% – 49.20%) for ^{60}Co teletherapy unit. The mean value of the coefficients of correlation (r) between directly measured dose values in irregular fields and the calculated dose values by Clarkson's method and Empirical relation in the corresponding fields of 3(i–xi) for ^{60}Co were found to be 0.999 and 0.999 respectively. The averaged of the mean percentage differences with 1sd between directly measured dose

values and calculated dose values of Clarkson's method and Empirical relation were found to be 2.528% ± 1.622 (range 0.475% – 5.998%) and 2.527% ± 1.623 (range 0.475% – 5.998%) respectively. The corresponding uncertainty ±1.291%and ±1.291% between directly measured dose values and calculated dose values by Clarkson's method and Empirical relation were found statistically satisfactory, because according to the International Commission on Radiation Units and measurements (ICRU) the dose delivered to the target volume should be at least within ±5%[40]. The averaged of the mean difference 16.76% ± 9.12 (range 2.45% - 49.2%) between directly measured dose values at different points in irregular (blocked) fields and the corresponding points in respective open fields could be considered statistically significant in case of dose prescription for a patient receiving radiotherapy treatment with irregularly shaped photon fields. The important finding of this study is that the directly measured dose values in irregular fields are in good agreement with calculated dose values of Empirical relation so that the dose estimation in irregular fields could be approximated with reasonable accuracy from the calculated dose values of empirical relation normalized to central axis beam dose in open fields. This normalized central axis dose data was expected to be useful as reference data for dosimetry of irregular fields in routine radiotherapy practices. Moreover, it may be considered that, our dosimetric results may be useful as general guidelines, to optimize the radiation doses to the organs at risk during radiotherapy. On the basis of ALARA concept, exposure should be kept as low as reasonably achievable. It is suggested that shielding devices should be used in risk organs, especially gonad and lens of eye, whenever possible to reduce the potential risk due to the scattered radiation dose.

Chapter-I

Introduction

1.1 General

The aim of radiotherapy technique is to deliver a dose as high as possible to malignant cells (tumor) with minimum detriment to surrounding healthy tissues. From the view point of radiation protection on the basis of ALARA concept, one of the basic principles of using ionizing radiation in medical fields [5] is that the dose to surrounding tissues should be minimized by using the best available techniques and to take measures to reduce the doses as far as possible to other parts of the body as well as organs at risk. In addition, dose uniformity within the tumor volume and sparing of risk organs are important considerations in judging a treatment plan. But there is no available hospital based critical organ dose data for radiotherapy departments in our country. It is therefore necessary to have adequate consideration for the accuracy of absorbed dose in radiation therapy. The prime aim of radiotherapy used alone or in combination with other treatment modalities is to achieve cure from malignant diseases. Radiotherapy does however play an equally vital role in palliative treatment where although cure has not been achieved, relief from the symptoms produced by disease is possible.

Accurate patient dosimetry is only possible when sufficiently accurate patient data are available. Such data collection includes body contour, outline and density of relevant internal structures, location and extent of the target volume Acquisition of these data is necessary whether the dosimetric calculations are performed manually or with a computer. Also, application of central axis- depth dose data to dose calculation for the treatment of a patient is an another step from their determination in a water phantom and therefore involves the possibly of additional error.

Under these circumstances, the standard dose distribution data collected in ideal conditions from a phantom can not be applied directly for treatment without proper modifications or corrections for achieving best possible uniform dose distribution system. In radiotherapy technique, however, an ideal radiation field i.e . a cross-sectional area of a photon beam, every point inside which has equal number of incident photons per unit time and every point outside which has no incident photon at all can not be achieved in practice but attempts could be made to modify the physical construction of a therapy treatment unit to have radiation fields with satisfactorily acceptable condition.

Shielding of vital organs within a radiation field is one of the major concerns of radiotherapy. Considerable time and effort are spent in shaping fields not only to protect critical organs but also to avoid unnecessary irradiation hazards to the surrounding normal healthy tissues. Partial shielding to avoid irradiation of healthy normal tissues modifies the square or rectangular radiation beam. Whenever square or rectangular radiation beam is modified by partial shielding to avoid irradiation of healthy normal tissues, characteristics of the beam changes. this change occurs due to the change in contribution from scattered radiation. Modification of beam affects the dose received at point P (say). Dose measurement for any field other than rectangular. circular or square field may be time consuming, because basic data for calculations are usually available for square or rectangular fields. Clarkson's method (Clarkson's, 1941) is available to predict dose at point P (say) with the help of scattered air ratios (SAR) table. It is based on principle that the scattered component of the depth dose can be calculated separately from primary component. Apart from Clarkson's method; other authors have given different relations to calculate the dose for blocked beams (Day, 1950). This technique is not practical for routine calculations as calculations with this method are time consuming and it is not practical to use it in day-to-day applications.

1.2 Objective with Specific Aims of the Study

A comprehensive quality assurance program is necessary for the improvement of accuracy in dose delivery in radiation therapy. Again, the duties and responsibilities of a medical physicist in the field of radiotherapy is to draw out a radiotherapy treatment and dosimetry plan to ensure quality control and radiation protection.

The main objectives of the present study cover dose calculation and investigation procedures in irregular fields to avoid undesirable radiation hazard and ensure quality assurance(QA) for the accuracy in radiotherapy treatment planning [73,86].

Further to this, certain recommendations regarding dosimetry system in various irregular fields will be within the aim of the present work.

The primary aims of the present work are:

i. Simulation of different irregular fields in solid phantoms usually encountered in routine radiotherapy practices
ii. Modifications of photon beams from ^{60}Co to the shapes of different irregular fields simulated in solid Perspex phantoms.
iii. Investigation of doses along long axis (x-axis) in those irregular fields.
iv. Development of an empirical relation for the accuracy of treatment procedure.
v. Comparison of central axis depth dose data with doses calculated by using Clarkson's method and newly developed Empirical relation.

The overall objective of the present work is to establish certain systems as basic requirements for the calculation of doses in irregular fields to investigate the accuracy of the dose measurement in mega voltage blocked beam of γ-radiation.

1.3 Scope of the study

Shielding blocks play an important role in clinical application of radiotherapy. Application of radiotherapy for treatment of malignant diseases is primarily aimed to provide curative radiation dose to the treatment volume. The target or treatment volume is often irregular in shapes in contrary to the square or rectangular fields employed in standard dose distribution data collection[72]. Organ at risk also limits dose application to the treatment volume. Individual planning is needed to optimize each treatment by selecting an irradiation technique, beam incidence, radiation quality, dose weight, field size and shape to guarantee a certain dose and dose homogeneity to each target volume under optimal sparing of organs at risk[84]. The optimal treatment plan is one, which results in a uniform dose to the target volume while minimizing the dose to adjacent tissue. The oforesaid curative type patent's surface, tissue inhomogeniety and irregular shaped target volume to each target volumes etc are apparently the prevailing constraints in application of standard isodose data for calculation of patient's radiation dose in clinical situations. Radiotherapy without necessary corrections for those incompatibilities can not provide desired results. Dose required as well as dose tolerated is different for different target volumes depending primarily on the number of tissue cells, beam quality, dose distribution and dose application strategy (treatment planning) etc. Beam modifications according to the target shape tissue compensator for

curvature type surface and target tissue density values are essentially desired to meet clinical dosimetry requirements for adequate and homogeneous dose applications to the treatment volume. The shaping of treatment fields is primarily dictated by tumor distribution-local extensions as well as regional metastases. Not only the dose to vital organs should not exceed their tolerance but also the dose to normal tissue, in general, should be minimized. Sometimes, the accuracy and precision in clinical institutions and hospitals are not maintained within a narrow range , there can be a tendency to avoid normal tissue complications by lowering the prescribed dose. The consequence is a drastic decrease in the probability of tumor control[16].The only acceptable solution is improvement of accuracy and precision so that the right doses can be prescribed and applied.

1.4 Field Irregularity and Dose Distribution

Any fields other than the square, rectangular or circular fields may be termed irregular fields. These irregularly shaped fields are frequently encountered in radiotherapy practices. Irregular shaped fields, in fact, appear when radiation sensitive structures are shielded from the primary beam or when the field extends beyond the irregularly shaped patient's body contour Since basic standard dosimetric data are available for rectangular or square fields only, special methods including several corrections factors are necessary to use these basic data for calculation of dose in irregularly shaped fields. For certain specific irregular fields, some special methods are in general use. However, irregular fields are not universal rather it can be different for different clinical situations. Therefore, several approaches are in progress for making generally applicable methods for calculation of doses in individual irregular fields.

1.5 Radiosensitivity and Dose Fractionation

Radiosensitivity of cells is very common word in radiotherapy practices normally contemplated by the treatment planning team usually comprised of radiation oncologists, medical physicists, dosimetrists during making a blue print for therapy applications. The term " Radiosensitivity " means the relative vulnerability of cells to be damaged by ionizing radiation. Radiosensitivity is measurable in cell survival curves using the capacity of cells to reproduce following irradiation as the end point. Both normal and malignant tissues have

different sensitivities, mainly determined by their different growth rates. This is the basis of the law of Bergonie and Tribondeau (1904). The biological action of ionizing radiation is greater where the reproductive activity of the cell is higher, the longer the period of its mitosis and the less the degree of differentiation . It has been observed that the radiosensitivity of the rapidly dividing germ cells of the reproductive organs " Testis or Ovary " is high. fortunately the cells of a malignant tumour of the testis or ovary have even higher radiosensitivity, paving the way for application of radiotherapy to these highly radiosensitive organs. In contrast, a slow growing soft tissue sarcoma shares the low sensitivity of its parent tissue. However, adequate dose can be applied to the soft tissue sarcoma without causing extra dose burden to the critical organs by shaping the irradiation beam as per tumour outline so that irradiation beam zone excludes the vulnerable critical organs. The various tissues and organs have a wide spectrum of radiosensitivity. The highly sensitive tissues are readily damaged by fairly low doses while the most radioresistant organs can withstand much more higher dose without any obvious radiation induced effects. Radiosensitivity of different living tissues can be categorized as follows :

High - sensitivity

(1) The epithelium of the skin (Epidermis)
(2) The epithelial lining (inner surface) of the alimentary tract .
(3) The cells in the bone marrow which produces the blood cells i.e., the haematopoitic tissue.
(4) The reproductive cells of the testis and ovary

Intermediate sensitivity

Liver, Kidney, Lung and many glands.

Less – sensitive

Muscle, Bone, connective and nervous tissues etc.[8,20].

These radiosensitive organs lying close to the malignant tumours can be saved from unwanted exposure beyond their tolerance level by shaping the radiation fields using beam blocks so that it excludes these critical organs and exploiting the dose fractionation facility as well. It is well understood that different types of tissues respond differently to same amount of radiation exposure. Dose fractionation exploits this benefit of variable responses

of rapidly responding tumours and late responding normal tissues to ionizing radiation. Damage to DNA following irradiation is generally repaired over a period of hours. However, the degree of repair will vary from tissue to tissue. Slowly responding tissues (connective tissue and spinal cord) have a greater capacity for repair than tumour tissues as long as the gap between treatment fractions is at least 6 hours, which is the conventional daily fraction. Since cell killing is logarithmic rather than linear, the difference in survival between normal and tumour cells is increased exponentially. Ideally it is preferable to deliver a radiation dose over as short as possible within the limits of acute radiation tolerance Giving radiotherapy in several small fractionated doses at regular intervals during the day (multiple daily fractions) may help to overcome tumour repopulation. Conversely excessive prolongation of radical external beam irradiation between two fractions over 7 – 8 weeks may allow significant tumour reproduction [25,88,89]. Dose rate per fraction and number of fractions in therapy completion must also be taken into account so that possible acute radiation syndrome can be controlled well.

1.6 Rationality of Dose Risk

It would not be overwhelming to mention here that in routine clinical radiotherapy practices, radiation doses can not be lowered to that level so that there would certainly be no acute radiation syndrome. However, adapting necessary arrangements during treatment plan, the radiation doses to the organs outside the treatment volume are ascertained at least theoretically to a minimum and justificatiable level so that no unwanted radiation effect could happen. The special arrangements to do so, involves modification of the therapy beam according to the target volume in such a manner that organs at risk like: bone marrow, gonads, bladder, rectum, spine and GI tract etc. would be well spared from the radiation exposure while adequate and requisite dose with optimum uniformity could be delivered to the malignant tumor volume. For radiation protection, an upper limit must be established for permissible radiation exposures. This limit should be reflected as a risk that is acceptable to the exposed individuals and to the society in general, without depriving society of the benefits derived from judicious use of ionizing radiation. In addition, it should be recognized that dose should always be kept as low as reasonably achievable (ALARA) consistent with reasonable costs and convenience without compromising the benefits of radiation to the society[72,2,46].

1.7 Measurement of Ionizing Radiation

Radiation is invisible and thus its presence can not be detected directly. However, ionizing radiation produces observable effects in medium. through which it is passing. which in turn can be detected by several methods. In fact, measurement of these effects regarding to their to their extent is an indirect and only strategic method of measuring ionizing radiation In the early days of x-ray usage for diagnosis and therapy, attempts were made to measure ionizing radiation on the basis of their chemical and biological effectiveness Radiation effects on photographic emulsions. changes in the colour of some chemical compounds and reddening of human skin were related to the amount of radiation absorbed. For radiotherapy purposes, the reddening of skin during therapy application was related to a radiation unit known as skin erythema dose (SED) which was defined as that amount of x or γ-radiation that just produces reddening of the skin. However, this SED unit had many drawbacks and used as a crude estimation of radiation dose which depends on many factors such as type of skin, the quality of radiation, the extent of skin exposed to radiation. dose fractionation and skin reaction characteristics. With a view to avoid the aforesaid uncertainties and to have more appropriate and precise unit for the measurement of ionizing radiation, in 1928 ICRU (International Commission on Radiological Unit and Measurement) recommended adoption of two physical quantities "Roentgen" as exposure unit and " Rad " as absorbed dose unit. Although SED has been discarded in favour of ICRU recommended Roentgen and Rad, radiotherapy establishments having orthovoltage radiotherapy facilities are still using this skin erythema as an approximate index of the skin response to the given radiation treatment and considering reddening of the skin as limiting factor to the delivery of tumoricidal doses. However, departments having megavoltage beams with skin sparing facilities must not rely on observing the development of skin reaction for the assessment of radiation response to individual treatments.

The quality of ionizing radiation is most often expressed in terms of exposure (its ability to produce ionization in air) and absorbed dose (the amount of radiation energy imparted in a medium) [67,49,82].

The unit of exposure is roentgen which is a measure of the ionization ability of a photon beam (x or γ) in air with photon energy not higher than 3 MeV. This unit "Roentgen" was

originally defined as the amount of x or γ -radiation required to produce 1 esu (electrostatic unit) of charge of either sign in 1cc air at STP (standard temperature and pressure). The current definition of the unit "Roentgen" is equivalent to 2.58×10^{-4} coulomb/kg dry air at STP which is equal to the original definition if the charge is expressed in coulombs (1 esu = 3.333×10^{-10} coulomb) and the volume of air is charged to mass (1 cc of air at STP weights 1.293×10^{-6} kg). ICRU-1980 defines exposure (X) as the quotient of dQ/dm where dQ is the absolute value of the total charge of the ions of one sign produced in air when all the electrons (negatrons and positrons) liberated by photons in air of mass dm are completely stopped in air. Mathematically it is expressed as

$$X = \frac{dQ}{dm} \qquad \text{----------(1)}$$

The system International (SI) unit for exposure is coulomb per kg (C/kg) of air. It should be emphasized here that the quantity exposure with its unit "Roentgen" applies only to photon beam (x or γ) in an air medium. The exposure is a measure of the ionization in air only, and can not be used for photons having energies above 3 MeV. If the radiation is not a photon beam e.g. electron beam or if the medium is not air, e.g. tissue, then unit of exposure "Roentgen" can no longer be used. In such cases, another physical term "absorbed dose" is used which describes the quantity of radiation for all types of ionizing radiation including charged and uncharged particles, all materials and all energies thereby eliminating inherent limitations in the use of exposure unit "Roentgen" for quantitive measurement of ionizing radiation. The absorbed dose is a measure of radiation energy being absorbed per unit mass of the medium, which in turn measures the biologically significant effects produced as a result of the absorbed ionizing radiation. The most significant definition of the absorbed dose or simply the dose is the quotient $\frac{d\bar{e}}{dm}$ where $d\bar{e}$ is the mean energy imparted by ionizing radiation to material of mass dm[32]. The conventional (old) unit of absorbed dose is rad (an acronym for radiation absorbed dose) and represents the absorption of 100 ergs of energy per gram of the absorbing material. Thus we see that, the unit of absorbed dose "rad" is much more general than the exposure unit "roentgen" since it does not specify the type and energy of the radiation nor the type medium while exposure is confined only to photon (x or γ) having not more than 3 MeV and the medium is not air only. As the unit of energy

varies e.g , erg, joule, eV etc.. the unit of absorbed dose also varies accordingly. Thus

$$1\text{Rad} = 100\text{ergs/gm} = 10^{-2}\text{J/kg}$$

Recently adopted SI unit for absorbed dose is the Gray (Gy) and is defined as

$$1 \text{ Gray} = 1 \text{ J/Kg}$$

Thus the relationship between gray and rad is

$$1 \text{ Gy} = 100\text{rads} = 1 \text{ J/Kg}$$

$$\text{or } 1 \text{ rad} = 10^{-2} \text{ gy.}$$

Since gray is a larger unit, a sub unit, centigray (cGy) has often been used as being equivalent to rad.

1.8 Standard Field Ionization Chamber

Although many different types of measuring systems exist, there is no doubt that the one which uses an ionization chamber is usually the most satisfactory. To overcome energy related limitations along with other physical problems in using normal ionization chamber for measurement of exposure in roentgen, several attempts were made on designing standard field ionization chamber to this end. The wall materials used in an ionization chamber have a significant effect on the performance of the detector. Ionization chambers are usually made with wall and central electrode materials such as plastics or carbon that have effective atomic numbers close to those of air or water. A typical ionization chamber is the thimble chamber with "condensed air" walls, shown in fig.1 . Thimble chambers with air equivalent wall are in use instead of free air ionization chambers as replacement for measurement of exposure in roentgen. The condensed air is actually a solid material of the same effective atomic umber as air but 1000 times air density. This allows the size of the chamber to be significantly reduced. Since the density of solid air equivalent wall is much greater than that of the free air, the thickness required for electronic equilibrium in the thimble chamber is considerably reduced. The cap of the chamber is designed to be as thin as possible, but still thick enough to establish electronic equilibrium, so that as many electrons are captured as are reduced released in interactions. In practice, however, a thimble chamber is usually constructed with wall thickness of 1 mm or less and this is supplemented with close fitting build up caps of Plexiglas or other plastic of different thickness to bring the total wall thickness up to that needed to establish electronic equilibrium for the radiation in question.

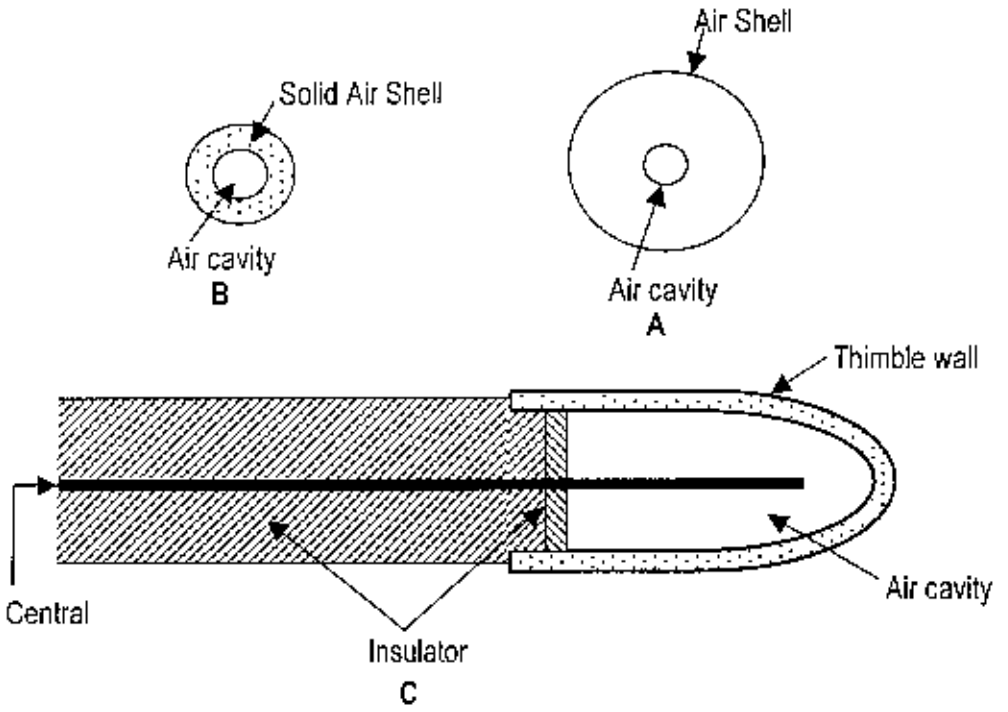

Fig.1: Schematic diagram illustrating the nature of the thimble chamber. A. Air shell with air cavity. B. Solid air shell with air cavity. C. the thimble chamber Courtesy of F M Khan. (Physics of Radiation Therapy, 2nd edition).

This thimble chamber is basically a condenser type chamber which is suitable for measuring exposure rate in air for relatively low energy photon beams (≤ 2 MeV).Although there are no basic limitations to their use for higher energy radiation, the design of the stem and excessive stem leakage create dosimetric problems, especially when making measurements in phantoms. In 1955, Farmer designed a chamber, which provides a stable and reliable secondary standard chamber for x and γ-rays for all energies in the therapeutic range. This chamber connected to a specific electrometer (to measure ionization charge) is known as the Baldwin-Farmer substandard chamber. The original design of the Farmer chamber was modified by Aird and Farmer with a view to have better (flatter) energy response characteristics and more constancy of design from one chamber to another. This type of chamber is usually used in almost all therapy establishments with reliable dosimetric performances. A typical Farmer with all dimensions is schematically shown in fig.2.

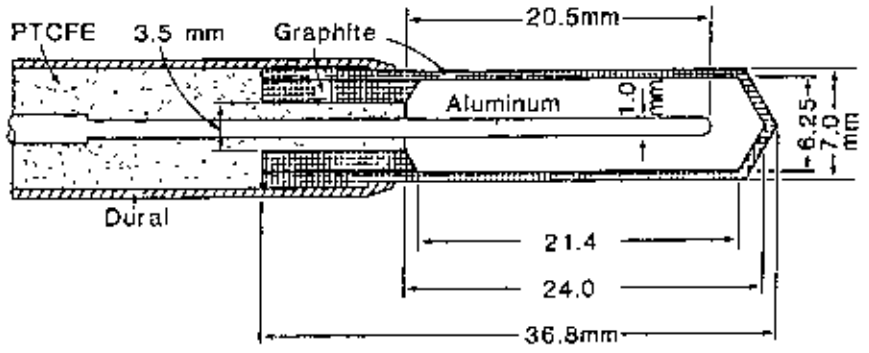

Fig.2: Farmer graphite/aluminum chamber. Nominal air volume 0.6 ml PTCFE Polytrichlorofluorethylene. Courtesy of F M Khan. (Physics of Radiation Therapy, 2nd edition).

1.9 Characteristics of Ion Chamber

When a chamber is attempted to use in practical situation for the measurement of exposure in roentgen, it is essential to examine whether it is capable of fulfilling the following desirable inherent characteristics:

(a). Variation of sensitivity or exposure calibration factor should be minimal over a wide range of energies.

(b). Chamber sensitive volume should be suitable to allow measurements for the expected exposures. The sensitivity (charged measured per roentgen) is directly proportional to the chamber's sensitive volume.

(c). Chamber sensitivity variation should be minimal with the direction of the incident beam. However, this effect can be minimized by using the chamber in the same configuration as specified under chamber calibration condition.

(d). Stem leakage should be minimal. A chamber is said to have stem leakage if it records ionization produced anywhere other than its sensitive volume.

(e). It should be evaluated that whether the chamber has been calibrated for exposure against a standard chamber for all radiation qualities of interest.

(f). Ion recombination loss should be minimal which could be a serious problem with high intensity or pulsed beam[23,26].

1.10 Exposure Measurement Technique

Exposure can be measured in roentgen with either a thimble or a Farmer type ionization chamber connected with appropriate electrometer, whereas Farmer type chamber is usually assumed to provide more stable and reliable dosimetric performances. However, each of them must have an exposure calibration factor N_c (say) that is traceable to primary standard dosimetry laboratory (PSDL) via secondary standard dosimetry laboratory (SSDL) for a given quality of radiation. The chamber is to be placed at the desired point of measurement with its axis perpendicular to the radiation beam axis as well as the same geometry as used during chamber calibration configuration as shown in fig.3.

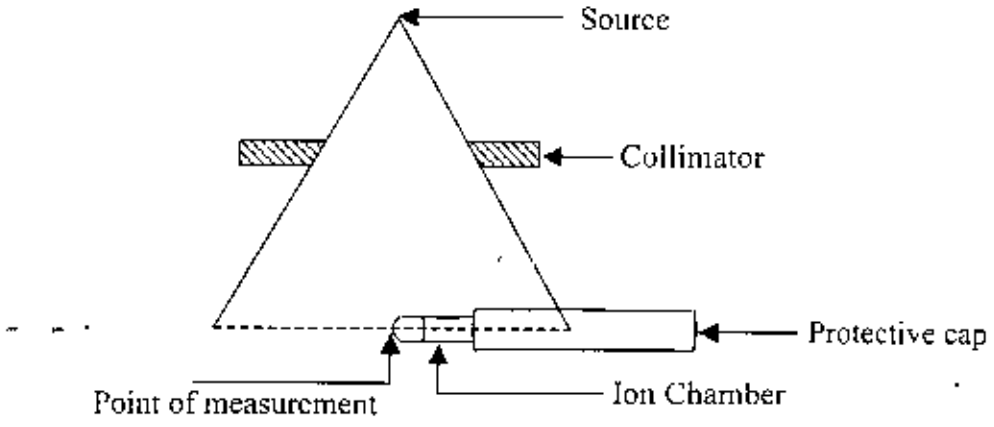

Fig.3: Geometry of exposure measurement with an ion chamber

For measurement in air, the effective point of measurement is usually specified to be the centre of the chamber cavity for cylindrical or thimble shaped chambers. After the application of the calibration factor, the dosimeter reading will give the value of air kerma at a point in air corresponding to the centre of the chamber, with the chamber replaced by air [79,80 27].Necessary precautions are to be taken to avoid media, other than air, in the vicinity of the chamber, which might scatter radiation. Suppose for a given exposure, the electrometer reading is M. This exposure reading can be converted to roentgen as follows:

$$X = M.N_c.C_{t,p}.C_s.C_{st} \qquad \text{----------(2)}$$

where $C_{T,P}$ is the correction for temperature and pressure, C_s is the correction for loss of ionization as a result of recombination, and C_{st} is the correction for stem leakage. The quantity obtained from the above expression is the exposure that would be expected in free air at the point of measurement in absence of the chamber. In other words, the correction for

any perturbation produced in the beam by the chamber is inherent in the chamber calibration factor N_c. For low-energy radiation such as applied in the superficial or orthovoltage range, no build up cap is required with the assumption that at this energy range. the chamber's wall thickness would be sufficient to provide necessary electronic equilibrium and also at this energy range, the chambers are usually calibrated without build up caps under the aforsaid assumption. However, for higher energies such as ^{60}Co (Cobult-60), a build up cap of lucide or other suitable material is to be used unless the chamber wall is already thick enough to provide electronic equilibrium. In either case. the correction to zero wall thickness is inherent in the chamber calibration factor N_c. It should be noted that no chamber should be used for measurement purpose unless its characteristics have not been clearly be evaluated and found acceptable [23]. The transfer of energy from a photon beam to the medium takes place in two stages The 1st stage (a) involves the interaction of photon with an atom. causing an electron or electrons to be set in motion. The 2nd stage (b) involves the transfer of energy from the high energy electron to the medium through excitation and ionization. A quantity called ***kerma*** has been introduced by ICRU to describe the initial photon interaction characteristics. Kerma stands for kinetic energy stands for kinetic energy released in the medium. [30].

Mathematically kerma is defined as $K = \frac{d\overline{E_{tr}}}{dm}$ ----------(3)

where $d\overline{E_{tr}}$ is the sum of the initial kinetic energies of all the charged particles (electrons and positrons) liberated by uncharged particles (photons) in a material of mass dm. Since kerma is a measure of energy per unit mass, its unit is same as for dose i.e., J/Kg and its SI unit is gray and its special unit is rad. For photon beam traversing a medium, kerma at a point is directly proportional to the mass energy transfer coefficient $\frac{\mu_{tr}}{\rho}$ i.e.. $K \propto \frac{\overline{\mu_{tr}}}{\rho}$ or

$K = \psi\left(\frac{\overline{\mu_{tr}}}{\rho}\right)$ where ψ is the photon energy fluence = φE

The other term, mean mass energy absorption coefficient $\overline{\frac{\mu_{tr}}{\rho}}$ is defined as the product of $\frac{\mu_{tr}}{\rho}$ and (1-g) where g is the fraction of the energy of secondary electrons that is lost to bremsstrahlung in the material. Thus

$$\left(\overline{\frac{\mu_{en}}{\rho}}\right) = \left(\overline{\frac{\mu_{tr}}{\rho}}\right)(1-g) \qquad \text{----------(4)}$$

Therefore $$K = \psi \frac{\left(\overline{\frac{\mu_{en}}{\rho}}\right)}{(1-g)} \qquad \text{----------(5)}$$

A major part of the initial kinetic energy of the electrons in low atomic number materials like air, soft tissue and water, is expended by inelastic collisions (ionization and excitation) with atomic electrons. Only a small part is expended in the radiative collisions with atomic electrons. Only a small part is expended in the radiative collisions with atomic nuclei (bremsstrahlung). Kerma can thus be divided into two parts

$$K = K^{col} + K^{rad} \qquad \text{----------(6)}$$

where K^{col} and K^{rad} are the collision and radiative parts of kerma.

Hence, we can have $K^{col} = \psi\left(\overline{\frac{\mu_{en}}{\rho}}\right)$

and $$\overline{K}^{rad} = \psi\left(\overline{\frac{\mu_{en}}{\rho}}\right)\left[\frac{\bar{g}}{(1-\bar{g})}\right] \qquad \text{----------(7)}$$

1.11 Relationship between Kerma and Exposure

Under conditions of electronic equilibrium, all the kinetic energy released in unit mass of air (air kerma) will be absorbed in the air providing none is lost in bremsstrahlung production. Thus, exposure is the ionization equivalent of collisional kerma in air i.e.,

$$\frac{dE_{tr}}{dm} = \frac{dE_{en}}{dm} \qquad \text{----------(8)}$$

or Dose in air $K_{air} = K_{air}^{col} = X\frac{\overline{W}_{air}}{e}$ ----------(9)

$\overline{W}_{air}$ is the average energy required to produce one ionization(one electron) in air and it is 33.97 eV/electron(an ion pair). If e is the magnitude of electronic charge $=1.602\times10^{-19}$ Coulomb, then $\frac{\overline{W}}{e}$ is the average energy required to produce per unit charge of ionization.

Since 1 eV = 1.602×10^{-19} joule, then $\frac{\overline{W}}{e} = 33.97$ J/C.

Therefore, Dose in air (air kerma), K_{air} =33.97 J/C.X(C/Kg) ----------(10)

$K_{air} = 33.97$ X.J/Kg ----------(11)

$$X = \Psi_{air}\left\{\frac{\overline{\mu}_{en}}{\rho}\right\}_{air}\left\{\frac{e}{\overline{W}}\right\}_{air} \quad \text{----------(12)}$$

But if the energy liberated, dE_{tr} is not absorbed then

$$\text{Dose in air} = K_{air}\left\{\frac{\overline{\mu}_{en}}{\rho}\right\}_{air} / \left\{\frac{\overline{\mu}_{tr}}{\rho}\right\}_{air} \quad \text{----------(13)}$$

The ratio $\left\{\frac{\overline{\mu}_{en}}{\rho}\right\}_{air} / \left\{\frac{\mu\overline{\mu}_{tr}}{\rho}\right\}_{air}$ accounts for the energy lost in bremsstrahlung production. (The ratio increases with energy, being approximately 1.003 for ^{60}Co photons). It follows that

$$\text{Dose in tissue} = K_{air}\left\{\frac{\overline{\mu}_{en}}{\rho}\right\}_{tissue} / \left\{\frac{\overline{\mu}_{tr}}{\rho}\right\}_{air} \quad \text{----------(14)}$$

$\left\{\frac{\overline{\mu}_{en}}{\rho}\right\}_{tissue} / \left\{\frac{\overline{\mu}_{tr}}{\rho}\right\}_{air}$ is approximately 1.10 for soft tissue over a wide range of photon energies

and therefore

Dose in soft tissue(Gray) = $1.10K_{air}$ (Gray)
= 1.10x33.97 J/C × X{C/Kg}

1.12 Absorbed Dose Calculation Technique

In any medium the measurement of exposure is the basis for the calculation of dose, provided the condition for charged particle equilibrium concept must be satisfied. In the presence of charged particle equilibrium, dose at a point in any medium is equal to the collision part of kerma. Dose to air under this condition is given by

$$D_{air} = \left(K^{col}\right)_{air} \cdot \frac{W}{e} \cdot X \qquad \text{----------(15)}$$

With units this expression can be expressed as

$$D_{air}\left(\frac{J}{Kg}\right) = X(R)2.58\times10^{-4}\,\frac{C}{Kg}\,R^{-1}.33.97\frac{J}{C} \qquad \text{----------(16)}$$

$$= 0.876.10^{-2}\,\frac{J}{Kg}.rad/10^{-2}\,J/Kg$$

$$D_{air} = 0.876rad \qquad \text{----------(17)}$$

Therefore, under electronic equilibrium, roentgen to rad conversion factor is 0.876.

All dosimetry should spicify the calibration depths or reference depths or reference depths as reference depths in a water phantom at which measurements are made to determine the dose rates from γ-ray or x-ray generators. For ^{60}Co γ-radiation, the calibration depth is chosen to be 5 cm while for high energy x radiation, the calibration depth is chosen to be beyond the peak of the central axis depth dose curve However, for high energy x-radiation, the effect of the changein phantom spectrum between 5 and 10 cm depth is small, so it would make little difference in practice when either of the alternative sets of depths is used[23,30,45,7].

1.13 Absorbed Dose to any Medium other than Air

The absorbed dose to a medium, other than air can be determined by using the calculated values of the photon energy fluence Ψ at any point in the medium and the weighted mean mass energy absorption coefficient $\overline{\frac{\mu_{en}}{\rho}}$ for a given photon beam quality. Suppose ψ_{med} is the photon energy fluence at the same point when a material other than air is interposed in the beam. Then, under conditions of electronic equilibrium, in either case, dose to air is related to the dose to medium by the following relationship:

$$\frac{D_{med}}{D_{air}} = \left[\left(\overline{\frac{\mu_{en}}{\rho}}\right)_{med} / \left(\overline{\frac{\mu_{en}}{\rho}}\right)_{air}\right].A \qquad \text{----------(18)}$$

Where $A=\Psi_{med}/\Psi_{air}$ is the ratio of photon energy fluence in two media and is termed as transmission factor.

We know that $$D_{air} = \frac{\overline{X}}{e}$$

Thus, $$D_{med} = \frac{\overline{X}}{e}\left[\left(\frac{\overline{\mu_{en}}}{\rho}\right)_{med} / \left(\frac{\overline{\mu_{en}}}{\rho}\right)_{air}\right].A$$

If, we express exposure X in roentgen and D_{med} in rad, we have

$$D_{med} = \left[0.876\left(\frac{\overline{\mu_{en}}}{\rho}\right)_{med} / \left(\frac{\overline{\mu_{en}}}{\rho}\right)_{air}\right].X.A \qquad \text{----------(19)}$$

The quality in brackets has frequency been represented by the symbol f_{med} so that

$$D_{med} = f_{med}.X.A \qquad \text{----------(20)}$$

Where $f_{med} = \left[\left(\frac{\overline{\mu_{en}}}{\rho}\right)_{med} / \left(\frac{\overline{\mu_{en}}}{\rho}\right)_{air}\right]0.876$. The quantity f_{med} or simply the f-factor is sometimes called the roentgen to rad conversion factor. This f is a function of the medium composition as well as the photon beam energy.

1.14 Measurement of Dose from the Exposure

In the case of low energy x-ray beams in the superficial or orthovoltage range, the ion chamber walls are thick enough to provide necessary electronic equilibrium and thus, in this energy range the ion chamber is usually calibrated without build up cap. However, in the case of high energy photon beams such as ^{60}Co, a build up cap is used over the sensitive volume (air) of the chamber so that the combined thickness of the chamber wall and the build up cap provide the required electronic equilibrium. Let the chamber be exposed to the beam with geometry as shown in fig.4 : a).b).c)

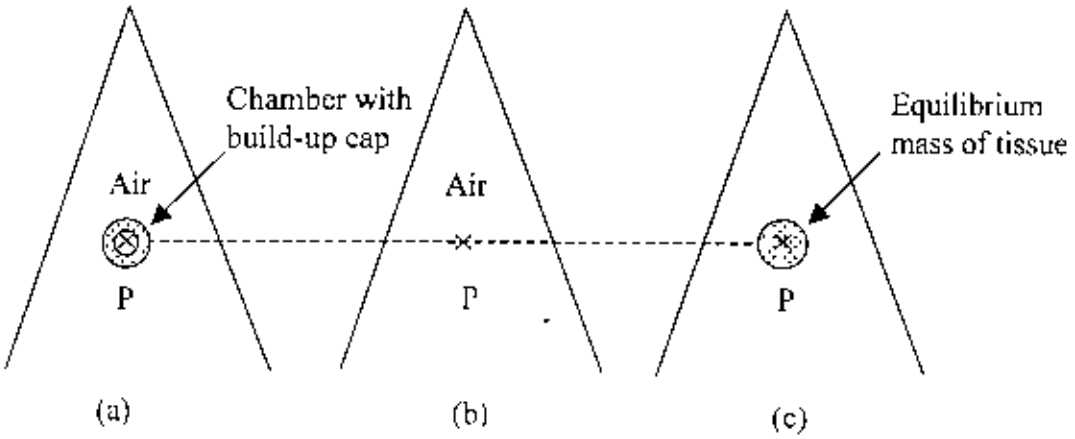

Fig.4: (a) Chamber with build up cap is placed in a radiation beam at point p in air, (b) exposure in free air at point p, (c) dose in free space at p. Courtesy of F M Khan (The Physics of Radiation Therapy, 2nd edition)

From the set up in fig.4(a) suppose the reading M is obtained after necessary corrections(correction for temperature, pressure and stem leakage etc.). The roentgen "X" is then given by

$$X=M.N_x \qquad \text{----------(21)}$$

Where N_x is the exposure calibration factor for the given chamber and for the givenbeam quality. The exposure thus obtained is the exposure at point P(center of the chamber sensitive volume) in free air in absence of the chamber fig.4(b). In other words, the perturbation influence of the chamber is cancelled out when the chamber calibration factor is applied. Again let us consider that a small amount of soft tissueat point Pis just large enough to provide electronic equilibrium at its centre fig.4(c). The dose at the center of this equivalent mass of tissue is referred to as the dose in free space. The term dose in free space was introduced by Johns and Cunninghum who related this quantity to the dose in an extended tissue medium by means of tissue air ratio[8,10,88] . In order to convert the exposure into the dose in free space, the following equation can be used:

$$D_{f,s} = f_{tissue} X.A_{eq} \qquad \text{----------(22)}$$

Where A_{eq} is the transmission factor including the ratio of the photon energy fluence at the center of the equivalent mass of tissue to that in free air at the same point i.e., $A_{eq} = \frac{\psi_{tissue}}{\psi_{freeair}}$

For ^{60}Co beam A_{eq} is close to 0.99 which approaches to 1.00 as the beam energy decreases to orthovoltage level[23,32,31]. Equations $X=M.N_x$ and $D_{f,s} = f_{tissue}. X. A_{eq}$ provide the basis for

absorbed dose calculation in any medium from exposure measurement in air. This procedure is valid when the exposure measurement is made with the chamber imbedded in a medium. Similar arrangement can be simulated in which the chamber with its build up cap is surrounded by the medium and exposed to a photon energy fluence Ψ_b as shown in fig.(a) at the center of the chamber(point p).

Chapter-II

Review

2.1 Review of the previous study

V.O. Parthiban et al. [85] performed an experiment on " *Dosimetry of blocked beams and its comparison with empirical relations*" The primary objective of this study was to find out the dose distribution of blocked beams which are routinely used in day to day practice like corner shielding. central shielding. quarter or half shielding beams, inverted-Y, mantle field, etc. In this study beams were blocked with lead shielding. Field sizes of $15\times15cm^2$, $20\times20cm^2$ were taken and above mentioned blocked beams were formed. Dose measured in water phantom at 5cm depth with 0.6cc Farmer type ionization chamber. For the calculation with Clarkson's method radii were drawn from the point of calculation to divide the field into an equal interval with sector angle of 10^0. Dose in Clarkson's method was little higher than the measured and calculated by empirical relation used in this study. The dose accuracy of empirical relation was within ± 2%.

Papanikolaou N et al. [66] carried out research on "*A study of the effect of cone shielding in intraoperative radiotherapy*" In this study they irradiate the intraoperatively determined tumour target volume with a single fraction of tumoroidal dose while minimizing the dose to all adjacent healthy tissues to found the primary goal of intraoperative radiation therapy. To reduce dose outside the treatment volume, leads sheets were often used to cover the external surface of the cone tip thus providing a shielding for the tissues out side the field. In this study the effect of the shielding on the depth dose distributions and dose profiles at different depths is studied based on experimental data. The cones varied in size havening diameters of 5cm, 7cm and 9cm, and the electron energies ranged from 6 MeV to 22 MeV. The depth dose curves and dose profiles (at two different depths in the phantom) were measured and computed with and without the lead shielding for the various combinations of cone sizes and electron energies using a water phantom to simulate the patient. It was found that the presence of lead increases on average across the treatment area the dose to the tumour from 2% up to 5%, while the dose outside the cone reduced by as much as 75%. Both measurement and calculations were found to be in agreement.

Niroomand–Rad A et al. [64] performed an experiment on "*Effect of field irregularities on the dose distribution of 4MV photon beam*". In this study they found out the strong dependence of dose distribution of the irregularly shaped fields on the shape of field

irregularities. The effect of field irregularities on the uniformity of the dose distribution of a 4MV photon beam was found significant. The uniformity index of the blocked field which is a measure of the dose uniformity of the field had been compared to its corresponding unblocked to field. The measured and computer calculated dose are compared for points with 1 and 2cm from the edge of the field irregularities at the depth of 10cm. The discrepancies between the computer calculated dose and the measured dose were in agreement.

Paliwal BR et al. [65] carried out a study on "*Evaluation and quality control of a commercial 3-D dose compensator system*". In this study a commercially available software/hardware system for automated design and fractionation of three dimensional dose compensator molds had been tested for accuracy and precision as well as for its ability to provide adequate dose compensation at depth. In 19 head and neck patients (38 compensators) the use of customized compensator resulted in an average reduction of dose variation in the target volume from 13.8% (range 7%-21%) with uncompensated parallel opposed fields to 4.5% (range 2% - 7%) with custom-compensated parallel opposed fields. A similar reduction was seen in the dose variation across lung tumor volumes. The custom compensator were also tested for accuracy of fabrication and positioning; both were found to be accurate within ±1mm of the design specifications for all compensator tested. Last, the dosimetric properties of the compensators were studied. The ratios of open-beam dose profiles to measured compensated beam dose profiles were compared with the ratio of similar profiles calculated with a treatment planning system. The ratios were equal within ±2- 9%. thus providing evidence of the fidelity of the compensator to its design and the accuracy of the treatment planning algorithm.

Harunar Rashid et al. [29] worked on the "*Investigation of doses in irregular fields usually encountered in routine radiotherapy practices*". For this purpose, 14 irregular fields were simulated in solid acrylic phantoms, of which 10 were used in the investigation of doses for photon beam from ^{60}Co teletherapy unit and the rest 4 were used in the case of 6MV photon beam from Linac-Mevatron 7445. The averaged of the mean percentage differences with 1sd between directly measured dose values at those points in open fields for ^{60}Co and for 6MV Linac-Mevatron 7445 were 6.85% ± 3.08 (range 2.59% - 11.62%) and 4.04% ± 1.50 (range

1.34% - 7.04) respectively. The mean value of the coefficients of correlation (r) between the directly measured dose values in irregular fields and the calculated dose values in the corresponding fields of ^{60}Co and 6MV Linac-Mevatron 7445 were 0.9929 ± 0 0034 and 0.949 ± 0.06 while this value was 0.935 ± 0.44 when BIF was used in place of off axis dose ratios in Day's dose calculation formula. The averaged of the mean differences with 1sd between directly measured dose values and calculated dose values by Day's method in the case of ^{60}Co were 1.39 ± 0.49 (range 0.02% - 4.16%) and 4.20%± 1.05 (range 0.02% - 12.77%) for ^{60}Co while 2.63% ± 0.75 (0.59% -5.55%) and 2.1% ± 0.23 (range 0.02% - 5.6%) for 6MV Linac respectively.

2.2 Literature Review

2.2.1 Photon Beam Dosimetry

Photons are indirectly ionizing, that is they bring about their ionization by a two-stage process. In the first stage, they interact with matter to produce electrons (and positrons) and these charged particles then produce ionization along their tracks. The energy transferred from the photon beam to the irradiated material depends first on the photon interaction coefficients of the material. These coefficients vary rapidly with photon energy, and for most interactions, with the atomic number of the material. In radiotherapy, treatment beams contain not only the relatively high-energy photons from the target but also a combination of photons and electrons scattered from the collimation system. Jaws, flatteners, monitor chambers, wedges, blocks, and even trays produce relatively low-energy photons and electrons that "contaminate" the photon beam. This scatter from the collimation system is always present, but the amount reaching the patient increases as more of the surface area of the jaws is "visible" at the patient location. Therefore, as field size increases, the scatter component of the beam increases. Since scattered photons are lower in energy than the initial photons and since the electrons produced are easily stopped in tissue, the depth of d_{max} tends to decrease somewhat as the field size increases. in fact, in a ^{60}Co beam the surface dose can be as much as 110% of the dose at d_{max} just because of this unwanted radiation from collimator scatter of very large fields[71]. The common abbreviations used in treatment planning of photon beams are discussed bellow:

Dose and distance terms

Incident dose (ID) is defined as the dose to the depth of maximum dose (d_{max}) in tissue. The depth of d_{max} depends on beam energy and field size. Generally, the greater the energy, the greater the d_{max} .Also, the larger the field size, the smaller the d_{max} . Although d_{max} for a given beam is not truly constant, in clinical usage it is considered to be constant.

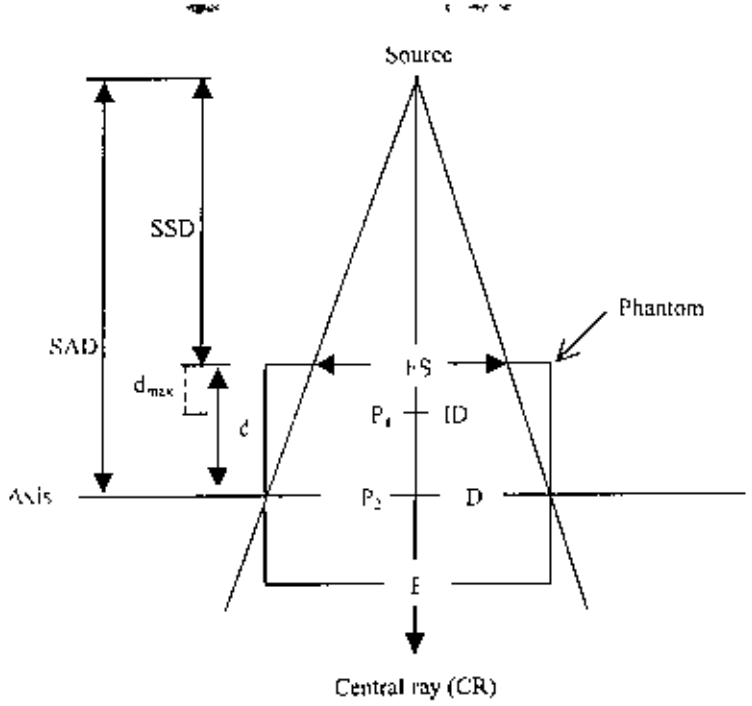

Fig.5: Depths and distances are all measured along the central ray. The field size is defined at the skin or phantom surface, at the SSD. It can also be defined at the axis when SAD or isocentric techniques are used.

The fig.5 illustrates the common abbreviations used in treatment planning and patient setup. The distance from the source to the skin of the patient (or the phantom) is called the source to skin distance (SSD). The size of the radiation field at the surface is called the field size(fs). The distance from the to the point P_2 is the source to axis distance (SAD). The two points of interest in the phantom, P_1 andP_2, are located respectively at the depths of d_{max} and the center of the tumor, d. The absorbed dose at these two points will generally be ID and D(dose at depth, d), respectively. Both of these points are on the central beam axis, called the central ray (CR). In general, simple calculations in patient dosimetry are performed for points on the central ray. Points not on the central ray are called off-axis points[71].

In fig.5 the dose at point E long the CR is called the exit dose. While it may seem inconsequential here, the exit dose is sometimes a limiting factor in the use of very high-energy photon beams. In fact, in early clinical work with betatron x-ray beams, radiation oncologists were some times surprised by skin reactions on the exit rather than entrance side of their patients. For example, a patient of 20 cm thickness irradiated to the mediastinum with a 20MV photon beam could receive a skin dose about 10-20% of the dose at d_{max}, while the exit dose at 20cm from the patient's front side surface would be about 53%. With a d_{max}

dose of 70 gray, skin at the exit point could receive a total of 37 Gy with only 7-14 Gy given to the skin at the entrance[71].

Output Factor

Output of therapy machines is measured in R/min in air (or coulomb/kg/min in SI units) for low energy X-rays and ^{60}Co beams. For linear accelerator beams, however, the output is expressed in cGy/(rads) at d_{max} in phantom per monitor unit (mu). The cgy/mu or rads/mu for a given therapy beam varies with the field size. The larger the field, the greater the output per monitor unit for linear acceleratoer beams and the output per minute for ^{60}Co machines. The reason is that as the field size increases, the amount of radiation scattered back to d_{max} by the phantom or patient also increases. There is also increased forward scattering by the jaws and change in backscattering to the monitor chamber. The factor that describes these effects is the field size correction factor (C_{fs}) and is defined as follows:

$$C_{fs} = \frac{\text{Dose at } d_{max} \text{ for a field size (fs)}}{\text{Dose at } d_{max} \text{ for a standard field size (e.g.10×10)}}$$

Where the field size is fs and 10cm ×10cm is the standard field size. C_{fs} values vary with field size for different energy of clinical photon beams. The output factors are normalized to a 10 cm × 10 cm field size (i.e., C_{fs} is 1.00 for the 10 cm × 10 cm field size). Field sizes less than 10 cm × 10 cm will have C_{fs} values greater than 1.

The shape of the C_{fs} curve varies with energy and also with manufacturer. Therefore, it must be measured for every treatment unit. For any given machine, C_{fs} is valued as a function of field size (or jaw) setting no matter what the clinical SSD[71].

Equipment Attenuation Factors

Any device that intercepts the treatment beam attenuates the beam, reducing the dose to the patient. Blocking trays and treatment tables are examples of such devices. Any calculation of time or MU to deliver prescribed doses must take this attenuation into account. The factor that corrects for this attenuation of the device is called C_{attn}:

$$C_{attn} = \frac{\text{Dose with device in radiation beam}}{\text{Dose without device in radiation beam}}$$

C_{attn} is constant for each device and beam quality is related to field size and depth of measurement to only a minor extent. For example, in a 6 MV beam, introducing a 0.6 cm thick tray reduces the beam intensity by 3%. Because the transmission factors depend to a minor on field size and depth of measurement, data should be taken at the same depth and field size, e.g., 10 cm depth and 10 cm × 10cm field.

Treatment table C_{attn} is also important in treatment calculations. Often the construction of a treatment table is non-uniform. There may be heavy bars only at the sides or only at the sides or only in the middle of the patient table. Usually these support structures should be avoided in patient treatment ; however, sometimes this is impossible. Rotational treatment requires the beam to hit the bars at some points in its motion. In these cases, treatment calculations are often performed, ignoring the presence of the bars in the isodose distribution; the bars are then accounted for using the average attenuation of the table [71].

Patient Attenuation Factor

The patient or phantom factor is a significant factor in dose calculation. Like, BSF, the factors that describe beam attenuation by the patient are dependent on beam energy, scatter, and beam geometry. The most common parameters used to quantify attenuation are depth dose (DD), tissue-air ratio (TAR) and tissue maximum ratio (TMR). As depth increases in a patient or phantom, all of these factors get smaller, because of greater attenuation; i.e., there is more tissue to absorb the radiation. Also, if the field size increases but other parameters remain unchanged, these attenuation factors all increase because of greater scatter within the patient. Even though DD, TAR, and TMR are related, their values and the way in which they are used are quite different [71].

Photon Energy and Electronic Equilibrium

The concept of exposure is confined to the photon beams in air and has an importance in radiotherapy. Its advantage in radiotherapy lies in fact that both the measurement of exposure in air and its conversion to absorbed dose in tissue is relatively easy[11,37]. A free air or standard ion chamber is an instrument used in the quantitative measurement of exposure in the unit of roentgen. According to the definition of roentgen, the electrons produced by photons in a specified volume must spent all their energies by ionization in air enclosed in the region of ion collected and the total ionic charge of either sign should be

measured. However, some electrons produced in the specified volume may deposit their energy outside the region of ion collection and thus may not be measured. On the other hand, electrons produced outside the specified volume may enter the ion collecting region and produce ionization there. Under the above circumstances, if the ionization loss is compensated by the ionization gained, a condition known as electronic equilibrium exists [23,75 76].The definition of roentgen to be effectively satisfied, electrons produced by the photon beam in the chamber air or as volume must spend all of their energy by ionization of air or gas molecules in the chamber Such a condition can exist only if the range of the electrons liberated by the incident photons is less than the distance between the collecting electrodes across the chamber gas volume. In addition, for electronic equilibrium to exist, the beam intensity (photon fluence per unit time) must remain constant across the length of specified gas volume. Accurate measurement of exposure according to the definition to its unit "Roentgen" requires a considerable care. A few corrections that are usually applied include: (a) correction for air or gas attenuation (b) corrections for recombination of ions (c) corrections for the effects of temperature, pressure and humidity on the density of air or gas and (d) correction for ionization produced by scattered photons. There are limitations on the design of a standard chamber for the measurement of exposure in roentgens for high-energy photon beams. As the photon energy increases, the range of the electrons liberated in air or gas also increases rapidly. this necessitates an increase in the separation between the collecting electrodes especially in free air ion chamber to maintain required electronic equilibrium. Too large a separation, however, creates problems of non-uniform electric field and greater ion recombination. Although the separation can be reduced by using air (gas) at high pressures, the problems still remain in regard to air attenuation, photon scatter, and reduction in the efficiency of ion collection. Because of these problems, there is an upper limit on the photon energy above which the roentgen can not be measured accurately. This limit has been observed to occur at about 3 MeV[76,41] One must realize that the exposure is not exactly appropriate for use in radiation dosimetry, since one is rarely concerned about the ionization capacity of a photon beam in air medium. However, in terms of actual measurements, electrical charge or current can easily be measured accurately with fairly simple apparatus. Therefore, the unit roentgen is still used for photon beam with energy less than 3 MeV[23,41]. Free air ion chamber satisfactorily fulfills the requirements for the measurement of exposure in roentgen according to its definition but it is too delicate and

bulky for routine use. Its main function is in the primary standard dosimetry laboratories where it is used only for calibration of secondary instruments designed for field use such as a thimble chamber.

2.2.2 Geometry of Photon Beams

2.2.2.1 Photon beam collimation and shaping

The broadened, symmetrical, and flat photon beam is collimated for treatment using a combination of two pairs continuously movable jaws in the head of LINAC or teletherapy unit, known as the upper and lower jaws. The jaws provide a rectangular opening ranging from 0×0 cm^2 to the maximum field size of 40×40 cm^2 at a distance of 80 cm from the source. The collimator is usually made of a single block of tungsten, depleted uranium, or lead, which allowed less than 5% transmission of the radiation beam. Some LINACs have more flexibly designed devices such as asymmetric (or independent) jaws. These are pairs of x-ray collimators that can move independently. That is one jaw can be moved to the midline or even across it while the other jaw is still open. Substituting for jaws, a yet more complex development is the multi-leaf collimator, which is made of many stats of metal that can move independently to shape a field much in a manner similar to custom-made blocks.

Shielding of vital organs within a radiation field is one of the major concerns of radiotherapy. Considerable time and effort are spent in shaping fields not only to protect critical organs but also to avoid unnecessary irradiation of the surrounding normal tissue. Skin sparing is an important property of megavoltage photon beams, and every effort should be directed to maintaining this effect when irradiating normal skin. The shaping of treatment fields is primarily dictated by tumor distribution –local extensions as well as regional metastases. Not only should the dose to vital organs not exceed their tolerance but the dose to normal tissue, in general should be minimized. As long as the target volume includes, with adequate margins, the demonstrated tumor as well as its presumed occult spread, significant irradiation of the normal tissue outside this volume must be avoided as much as possible.

Shielding blocks are most commonly made of lead. The thickness of lead required to provide adequate protection of the shielding areas depends on the beam quality and the

allowed transmission through the block. A primary beam transmission of 5% through the block is considered acceptable for most clinical situations. If n is the number of half-value layers to achieve this transmission,

$$\frac{1}{2^n} = 0.05$$
$$2^n = \frac{1}{0.05} = 20$$
$$n \log 2 = \log 20$$
$$n = \frac{\log 20}{\log 2} = 4.32$$

Thus a thickness of lead between 4.5 and 5.0 half-value layers would give less than 5% primary beam transmission and is, therefore, recommended for most clinical shielding.
Shielding against primary radiation for superficial and orthovoltage beams is readily accomplished by thin sheets of lead that can be placed or molded on the skin surface. However, as the beam energy increases to the megavoltage range, the thickness of lead required for shielding increases substantially. The lead blocks are then placed above the patient supported in the beam on a transparent plastic tray, called the shadow tray. Although the primary beam transmission can be reduced further by using extra thick blocks, the reduction in dose in the shielded region may not be that significant due to the predominance of scattered radiation from the adjoining open areas of the field.

The only possible field shaping through the collimators of the therapy unit is square or rectangular shapes. Most target volumes, however have more complicated shapes than that. Secondary field shaping is therefore necessary. A tray can be attached to the collimator onto which secondary beam-shaping blocks are placed. Such blocks are usually consist of lead bricks which have a thickness of 5 HVL, so that they transmit about 5% of the dose [24].

2.2.2.2 Photon Beam Shaping Blocks

The shielding blocks in radiation fields have important clinical application. Diverging blocks made with lead alloys compensate for the geometric divergence of the beam.
Ideally, the blocks should be shaped or tapered so that their sides follow the geometric divergence of the beam. This minimizes the block transmission penumbra (partial transmission of the beam at the edges of the block). However, divergent blocks offer little advantage for beams with large geometric penumbra. Divergent blocks are most suited for beams having small focal spots. Since the sides of these blocks follow beam divergence, one can reduce the lateral dimensions by designing the shields for designing the shields for smaller source-to-block distances without increasing the block transmission penumbra.

Diverging blocks can be made in an unlimited number of shapes and can match beam geometry. The blocked width on the skin surface can be determined applying the relationship

$$\frac{\text{Object size}}{\text{STD}} = \frac{\text{Image size}}{\text{SSD}}$$

Where STD = Source to Tray Distance
SSD = Source to Surface Distance

For instance, if a block obstruct a 2cm×4 cm at the blocking tray then the blocked area on the patient's skin at 100 cm SSD can be found by applying the above relation as

$$\frac{2cm}{65cmSTD} = \frac{Xcm}{100cmSSD}$$

$$X = 3.1cm$$

The projected blocked dimension of the width, 2 cm, will measure 3.1 cm on the patient, shown in fig. 6. Similarly, the length, 4 cm, will be 6.2 cm. The converse should also be true- if one knows the dimensions that require blocking on the skin surface, then the actual size of the blocks on the tray should simply be proportional to the ration of STD to SSD.

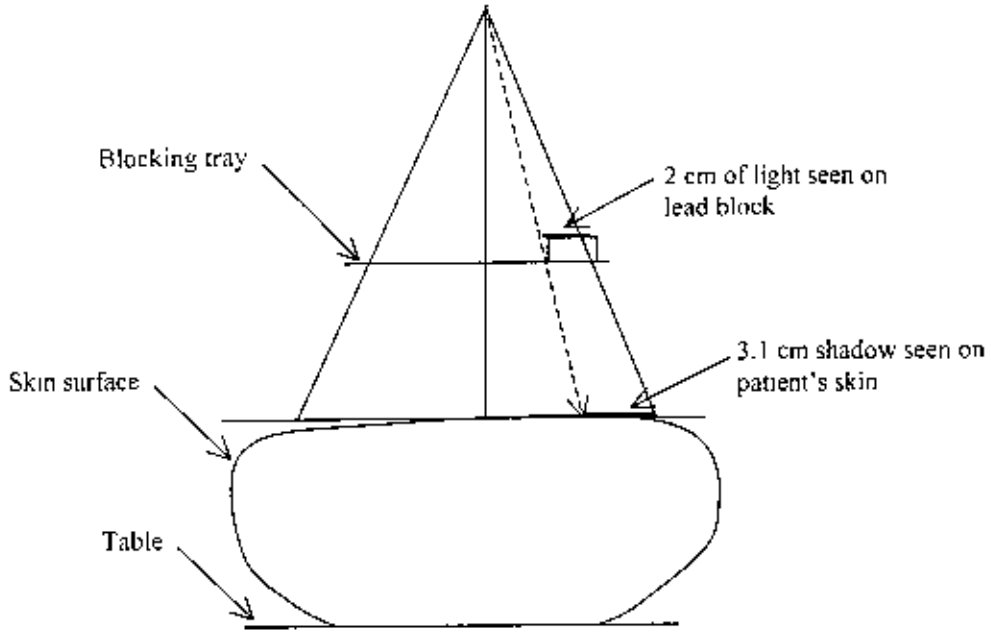

Fig.6: The width of the light field visualized on the block is directly proportional to the visualized dimension on the patient's skin.

Customized shielding using metal allows with diverging edges is a method of beam block construction where the edges of the blocks conform to the beam geometry. When oriented correctly, penumbra and the potential for partial beam transmission are greatly reduced as seen in fig. 7(a). The custom block system uses a low melting alloy,

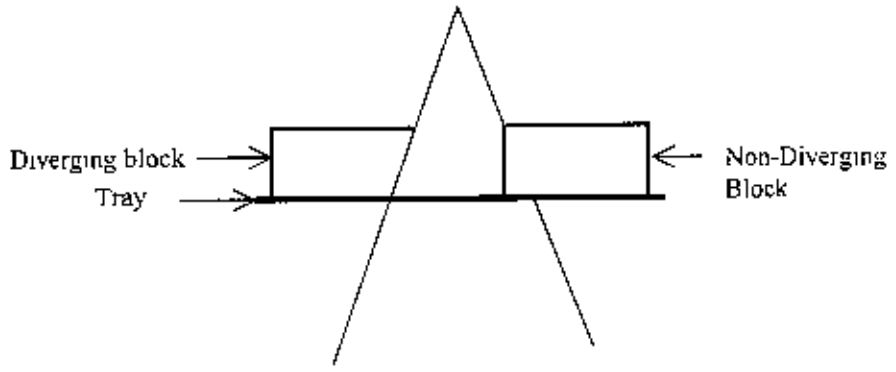

Fig. 7(a): Beam blocks The standard, non-diverging block is shown on the tray at the right. A diverging block is shown on the left. The diverging block conforms with the beam divergence and produces a crisp block shadow on the film. The standard block has partial transmission of the beam at the edge, which will result in more penumbra on the image.

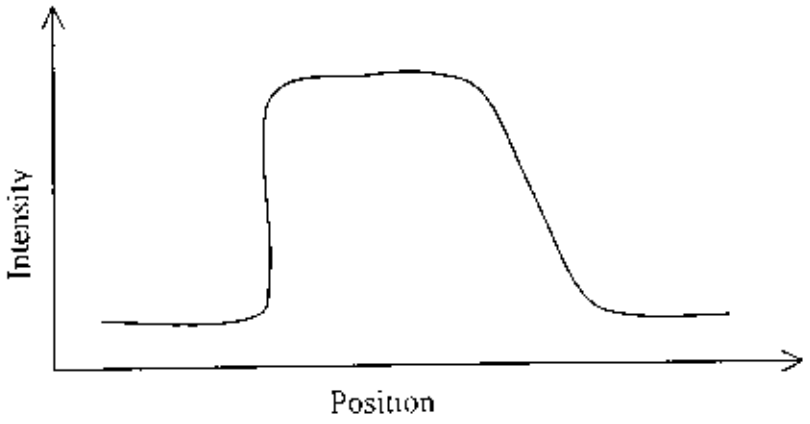

Fig. 7(b): The plot of the beam intensity demonstrates the advantage of the diverging over the non-diverging block

Lipowitz metal (brand name, Cerro bend), which has a density of 9.4 g/cm^3 at 20^{0}C (~83% of lead density). This material consists of 50.0% bismuth, 26.7% lead, 13.3% tin, and 10.0% cadmium. The main advantage of Cerro bend over lead is that it melts at about 70^{0}C (compared with 327^{0}C for lead) and, therefore, can be easily cast into any shape. At room temperature, it is harder than lead. The minimum thickness of Cerro bend blocks required for blocking is calculated using its density ratio relative to lead In the megavoltage range of photon beams, the most commonly used thickness is 7.5 cm , which is equivalent to about 6 cm of pure lead[70].

2.2.3 Exposure in Air and Medium

Exposure is a quantity expressing the amount of ionization caused in air by X- or γ-radiation. One exposure unit or X-unit is defined as that quantity of X or γ-radiation that produces ions in air carrying 1 coulombs of charge (of either sign) per kg of air (i.e. X-unit = 1 C/kg air). A roentgen (R) is an exposure of x- or gamma radiation such that the associated corpuscular emission (i.e.. ions – electrons and positive atoms or molecules) per 0.001293 gram of dry air produces, in air, ions carrying 1 electrostatic unit of charge (esu) of either sign. [In SI units: 1 roentgen = 1R = 2.58 × 10^{-4} coulomb / kg of dry air)].

Air has a density of 0.001293 g/cc and is defined very much lower than that of tissue like material. Hence the intensity or exposure rate at different distances can be calculated purely by inverse square law with out considering attenuation by the air medium. For example, 1

cm of tissue like material will absorb approximately 5% of the ^{60}Co radiation while the equivalent thickness of air will be 1/0.001293 = 775 cm. For the normal distance used in radiotherapy units, 80 cm means a little bit more than 0.5% of absorption for ^{60}Co beam. For low energy beam, say with a 1mm Al HVT, the attenuation per cm of tissue material is about 30%. With the normal operating treatment distance of 50 cm or less, the attenuation due to the air medium is in the order of 2%[6,40,70]. A low attenuation means few photon interaction in air, hence there will be very few scattered photons originated in the medium between the source and the point under consideration. At the same time, Since very few photon interactions occur within the air medium, there will be very few secondary electrons produced. Consequently, the air medium except very low energy photons and a very large distance could be considered as an empty when considering scattered photons, electron contamination and attenuation of X- or γ-ray beams[74]. However, in the case of tissue like material, the picture is quit different. All the effects mentioned above play important roles in dosimetry. When a beam of photons incident on the surface of a large tissue like phantom, placed at a distance of SSD (Source to Surface Distance) away, some of the photons will interact with the phantom material and generate high speed electrons. The absorbed dose in the medium due to the deposition of energy from these electrons along their track through the medium. An electron will deposit all its energy within its maximum range and thus the effect of an electron in a medium can be represented by a line equal to the length of its maximum range. The absorbed dose at a depth in the medium depends on how many of such tracks are crossing that level. The electron tracks at the surface of the phantom generated due to photon interactions with the phantom material can be depicted as shown in fig.8.

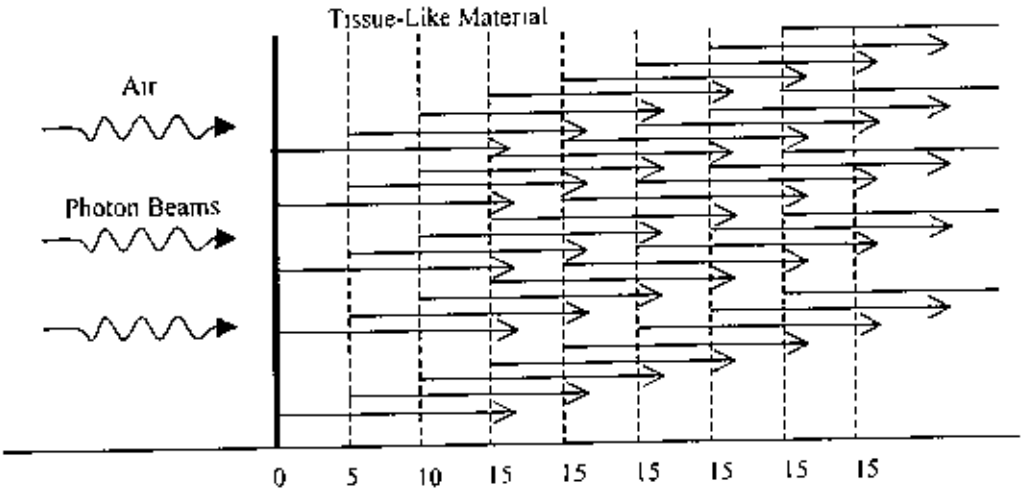

Fig.8 : Electron tracks in a medium.

For simplicity, all the tracks are shown at the direction of the radiation beam. If the number of tracks at different depths are counted, one will found that the number of tracks start off from 0 at the interface and increases with increasing depth, to a maximum at a depth equal to the electron range. The number of tracks remains constant from there on. Scattered photons are produced in the phantom; some of them will produce electrons in the backward direction[67,3 59]. The curve reaches the maximum value at about the same depth, and then starts decreasing. The decrease is due to the combined effect of inverse square law and tissue attenuation. The effect of the absorbed dose increases from a low value at the surface to a maximum at a certain depth is called the build up effect. and this region of increasing dose is called the build up region. At the position of the maximum, electronic equilibrium is said to have been achieved, which indicates to the fact at this position, the electrons entering a small volume are equal to the number of electrons leaving the volume.

2.2.4 Bragg - Gray Theory

It is already mentioned that calculation of absorbed dose is subjected to some major limitations like: it may not be used for photons above energy 3 MeV and may not be used in cases where electronic equilibrium dose not exist etc. Further to this, the term exposure applies only to x and γ radiations and for that reasons the above mentioned methods are not valid for practical dosimetry. The Bragg-Gray theory, on the other hand , may be used with such restrictions to calculate dose directly from ion chamber measurements in a medium. According to Bragg-Gray theory, the ionization produced in a gas-filled cavity placed in a medium is related to the energy absorbed in the surrounding medium. When the cavity is sufficiently small so that its introduction into the medium does not alter the number or the number or distribution of the electrons that would exist in the medium without the cavity, then the following Bragg-Gray relationship is satisfied[24,28 63].

$$D_{med} = J_g \cdot \frac{\overline{W}}{e} \cdot \left(\frac{\overline{S}}{\rho}\right)_g^{med} \qquad \text{----------(23)}$$

D_{med} is the absorbed dose in the medium(in absence of the cavity), J_g is the ionization charge of one sign produced per unit mass of the cavity gas, and $\left(\frac{\overline{S}}{\rho}\right)_g^{med}$ Is a weighted mean ratio of the mass stopping power of the medium to that of the gas for the electrons crossing the

cavity. The product of J_g(W/c) is the energy absorbed per unit mass of the cavity gas. The conditions which must be fulfilled for its validity is that the detector(chamber) should be such that the fluence of charged particles entering the chamber cavity should be the same as that present at the same position in the undisturbed medium[16]. This Bragg-Gray relationship has been modified by Spencer and Attix and uses the following relationship[32 33].

$$D_{med} = J_g \cdot \frac{\overline{W}}{e} \left(\frac{\overline{L}}{\rho}\right)_g^{med} \qquad \text{----------(24)}$$

Where $\left(\frac{\overline{L}}{\rho}\right)$ is the average restricted mass collisional stopping power of electrons

2.2.5 Tissue Equivalent Phantom

It is seldom possible to measure dose distribution directly in patients treated with radiation. Dose distribution are almost entirely derived from measurements in phantoms- tissue equivalent materials, usually large enough in volume to provide full-scatter conditions for the given beam. Tissue equivalent phantom materials are those which behave in much the same way as the body tissues when irradiated. From the analysis of the absorption processes, it is clear that a phantom material must have an effective atomic number very close to that of the tissue it simulates because of the dependence of photoelectric absorption and pair production processes on atomic number Z, an electron density close to that of the tissue simulated because of the dependence of the Compton scattering process on the number of electrons per gram, and because spatial measurements are to be made in the phantom material the density or specific gravity should be as close as possible to that of tissue simulated[87] Dose distribution are usually measured in a water phantom which closely approximates the radiation absorption and scattering properties of muscle and other soft tissues. A water phantom. however, poses some practical problems when used in conjunction with ion chambers and other detectors which are affected by water, unless they are designed to be waterproof. Since it is not always possible to put radiation detectors in water, solid dry phantoms have been developed as substitutes for water. Ideally, For a given material to be tissue or water equivalent, it must have the same effective atomic number, number of electrons per gram, and mass density. However, since the Compton effect is the

most predominant mode of interaction for megavoltage photon beams in the clinical range, the necessary condition for water equivalence for such beams is the same electron density (number of electrons per cubic centimeter) as that of water.

2.2.6 Transfer of Absorbed Dose from one Medium To another

Although water is the primary reference medium for dose calibrations, other media such as polystyrene and acrylic are frequently used for dose measurements. If a plastic phantom is used for calibration, the absorbed dose to the plastic should first be calculated and then transferred to absorbed dose to water. Further transfer of this dose to absorbed dose to tissue is considered as part of the treatment planning procedure and of the basic calibration.

The dose to any medium is related to dose to water by the following expression:

$$D_{water} = D_{med}\left(\frac{\overline{\mu_{en}}}{\rho}\right)_{med}^{water} \qquad \text{----------(25)}$$

provided the spectral distribution and energy fluence of photons at the point of measurement in the medium is the same at a comparable point in water. Because of the electron density (electrons per cubic centimeter) differences between plastic phantoms and water, additional corrections for effective depth, geometry, and scatter are sometimes necessary. In the case of polystyrene, these corrections are significant, since the electron density of polystyrene is very close to that of water. However, the electron density of acrylic is significantly higher and therefore significant corrections are required when acrylic phantoms are used for dosimetry.

Suppose $D_{plastic}(d', r, SSD)$ is the dose measured in a plastic phantom at the central axis of a beam where d' is the depth, r is the field size at the surface, and SSD is the source-surface distance. This dose can be transferred to dose in water by the following relationship:

$$D_{water}(d, r, SSD) = D_{plastic}(d', r, SSD)\cdot\left(\frac{\overline{\mu_{en}}}{\rho}\right)_{plastic}^{water}\cdot\left(\frac{SSD+d'}{SSD+d}\right)^2\cdot\frac{TAR(r_d', d)}{TAR(r_d, d)} \qquad \text{------(26)}$$

where d is given by

$$d = d' \cdot \frac{\bar{\mu}_{plastic}}{\bar{\mu}_{water}} \qquad \text{----------(27)}$$

$$r_d = r \cdot \frac{SSD + d}{SSD} \quad \text{and} \quad r'_d = \frac{r_d}{\rho_e}$$

$\bar{\mu}$ is the mean attenuation coefficient of the beam and ρ_e is the electron density of plastic relative to that of water. In the megavoltage range where Compton effect is predominant, $\frac{\bar{\mu}_{plastic}}{\bar{\mu}_{water}}$ may be approximated by ρ_e. In the range of clinically used megavoltage beams, the ratio $\frac{\bar{\mu}_{plastic}}{\bar{\mu}_{water}}$ is close to 1.01 for polystyrene and 1.14 for Lucite.

The SSD correction in equation (2) is necessitated by the shift of the point of measurement in the plastic phantom to the corresponding point in water. The term involving the ratio of TARs (or TMRs) corrects for differences in scatter between plastic and water for the same geometric field.

2.2.7 Scattering Effect in Radiotherapy Practices

The exposure at the surface of a phantom or any medium other than air is substantially greater than the exposure at the same point if no phantom or medium were present. Therefore, phantom or other media material is responsible for scattering of radiation back to the surface and this contribution is known as back scatter at the point where the beam axis centers the phantom or other medium is expressed as percentage of the contribution due to primary radiation and is termed as percentage back scatter. This percentage backscatter increases with the area of the field irradiated and with the thickness of the underlying tissues. The amount of back scatter is larger for comparatively low energy photon beam and decreases with increasing beam energy[72].

2.2.7.1 Dose Build up

At megavoltage energies, the scattered radiation is more in the following direction and gives rise to less scattered radiation outside the edges of the beam. This effect is evidenced in the isodose charts of orthovoltage and megavoltage photon beams. Analysis of Compton scattering also shows that the recoil electron is ejected more in forward direction with increasing kinetic energy and the range of recoil electron in orthovoltage is extremely small but in the case of megavoltage, the range of recoil electron is comparable and thus there is an initial build up of dose which becomes more and more pronounced as the energy is increased In the case of orthovoltage or low energy x-rays, the dose builds up to a maximum on or very close to the surface. But for higher energy beams, the point of maximum dose lies deeper into the tissue or phantom. The region between the surface and the point of maximum dose is called the dose build up region. A simple explanation to this effect is that excessive thin layer of tissue produces fast electrons, which in turn deposits their energy in several layers of tissue beyond their point of origin. Although kerma in these layers is constant, the energy deposited in each layer (absorbed dose) depends on the number of electrons passing through the layer, and the number increases as each layer adds electrons to the electron flux from the preceding layers. This increases until the electrons released only replaced those, which have come to the end of their range. The dose build up thus reaches a maximum at a depth determined by the range of the electrons and therefore by the energy of the photon beam. In practice, the kerma is not quite constant but falls as the primary radiation undergoes absorption and attenuation, with the result that the depth of the dose maximum is slightly less than the maximum range of the secondary electrons The depth of the peak in centimeters is approximately a quarter of the x-ray energy in megavolts (2 cm at 8 MV etc), ^{60}Co being approximately 5 cm higher energy beams have greater penetrating power and thus deliver a higher percentage depth dose. If the effects of inverse square law and scattering are not considered, the percentage depth dose variation with depth is governed approximately by exponential attenuation. Thus the beam quality affects the percentage depth dose by virtue of the average attenuation coefficient $\bar{\mu}$ which when decreases, the more penetrating the beam becomes, resulting in a higher percentage depth dose at any given depth beyond the build up region.

2.2.7.2 Skin Sparing Advantage

As high-energy photons enter a patient or phantom, they set electrons into motion, primarily through Compton interactions. In such interactions, the motion of the Compton electrons is predominantly in the forward direction, so there is a net flow of electrons deeper into the patient. The concurrent slowing of these electrons deposits energy in the patient. Therefore, dose begins to rise as the electrons slow down and deposit their energy. Thus, a depth related to the average distance that the Compton electrons travel is spared some of the dose of the incoming beam. The average distance traveled by electrons in a ^{60}Co beam is 0.5 cm, which is the d_{max} of ^{60}Co unit.

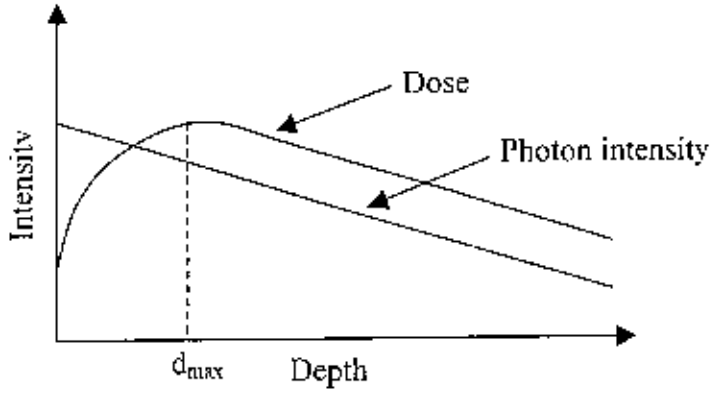

Fig.9: An illustration of the property of skin sparing. The photon intensity is maximum at the surface while the maximum dose occurs at d_{max}.

For megavoltage beam such as ^{60}Co and higher energies the surface dose is much smaller than the dose at the depth of d_{max} This dose build up effect of the higher energy beams is clinically known as the skin sparing effect and offers a distinctive advantage over the lower energy beams for which the D_{max} occurs at the skin surface. Thus, with high energy (megavoltage) photon beams, higher doses can be delivered to deep seated tumour without exceeding the tolerance of the skin. This, of course, is possible because of both the higher percent depth dose at the tumour and the lower surface dose at the skin[1]. A simple explanation to this regards is that as the higher energy photons enter a patient or phantom, they set electrons into motion, primarily through Compton interactions. In such interactions, the motion of the Compton is predominantly in the forward directions, so there is a net flow of electrons deeper into the patient. The concurrent slowing of these electrons deposits

energy in the patient. Therefore, the dose begins to rise as the electrons slow down and deposit their energy. Thus, a depth related to the average distance that the Compton electrons travel is spared some of the dose of the incoming beam[87].

2.2.8 Dose distribution in Patient or Phantom

When a beam of radiation is incident on a patient or phantom, the absorbed dose in the patient or phantom varies with depth. An essential step in the dose calculation system is to establish depth dose variation along the central axis of the beam. One way of characterizing the central axis dose distribution is to normalize the dose at depth with respect to dose at reference depth and represent the dose profile as percentage depth dose along the central axis of the incident beam. Mathematically, the percentage or percent depth dose is given by

$$P = \frac{D_d}{D_{d_0}} \times 100 \ .$$

where D_d is the dose at depth d and D_{d_0} is the dose at reference depth d_0. For orthovoltage (upto about 400 kV_p) and low energy photons the reference depth d_0 is usually the surface i.e., $d_0 = 0$. For higher energy photons beams, the reference depth is taken as the depth at which the peak absorbed dose is occured (i.e., $d_0 = d_m$). In clinical practice, this peak absorbed dose on the central axis is sometimes called the maximum dose, the dose maximum, the given dose or simply the D_{max}.

$$\text{Thus, } D_{max} = \frac{D_d}{P} \times 100 \qquad \text{----------(28)}$$

A number of parameters affect the central axis depth dose distribution. These include beam quality or energy, depth, field size and shape, source to surface distance and beam collimation. For a given beam, the dose will fall with increasing depth owing to the absorption in the successive layer of the medium and the increasing distance from the target following inverse square law. Superimposed on this radiation from the target will be the scattered radiation which results from the Compton scattering processes within the beam penetrating medium. The magnitude of these effects depends on the beam quality, its size and shape and the nature of the medium itself. Fig.10 shows the central axis depth dose curve for a ^{60}Co beam along with the contribution from scatter plotted separately.

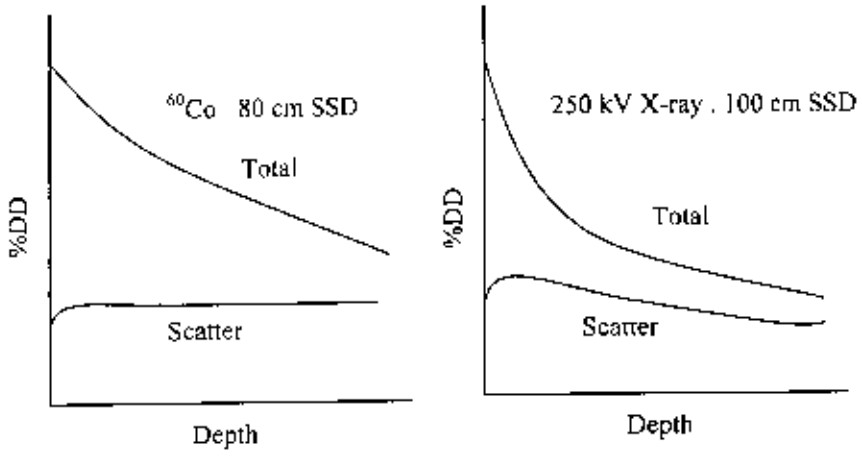

Fig.10: Percentage depth dose curve for A ^{60}Co & B. 250 kV beam showing the relative magnitude of dose contributed by the scattered radiation

At orthovoltage energies, the exposure to the surface (zero depth) is significantly affected by scattered radiation while radiation in the case of megavoltage energies, the surface dose is less and builds up to a maximum at some distance below the surface. This build up is a physical phenomenon, which explains the skin sparing effect of megavoltage radiations and is one of the principal advantages of these higher energy beams in radiotherapy. The exposure at the surface of the phantom is substantially greater than the exposure at the same point if no phantom were present. This is because the phantom material is scattering block to the surface a considerable amount of as backscatter. The percentage of backscatter increases with the area of the field irradiated and with the thickness of the underlying phantom material. The amount of back scatter at the surface of an irradiated phantom varies in a complicated way with beam quality. It is larger for a beam quality of 0.8 mm Cu-HVT the deep therapy region and falls as the beam quality increases, i.e., as the Compton scatter becomes increasing in the forward direction as well as decreasing in magnitude. It also falls with softer quality beams where Compton interactions are swamped by photoelectric interactions are absorbed. At its maximum, the percentage backscatter can reach 50% and is, therefore, very important[49.53].

The percentage depth dose (beyond the depth of maximum dose) increases with beam energy. Higher energy beam have greater penetrating power and thus deliver a higher percentage depth dose fig.11 the effects of the inverse square law and scattering are not considered, the percentage variation of depth dose with depth is governed approximately by

exponential attenuation. Thus, the beam quality affects the percentage depth dose by virtue of the average attenuation coefficient $\bar{\mu}$ of the medium.

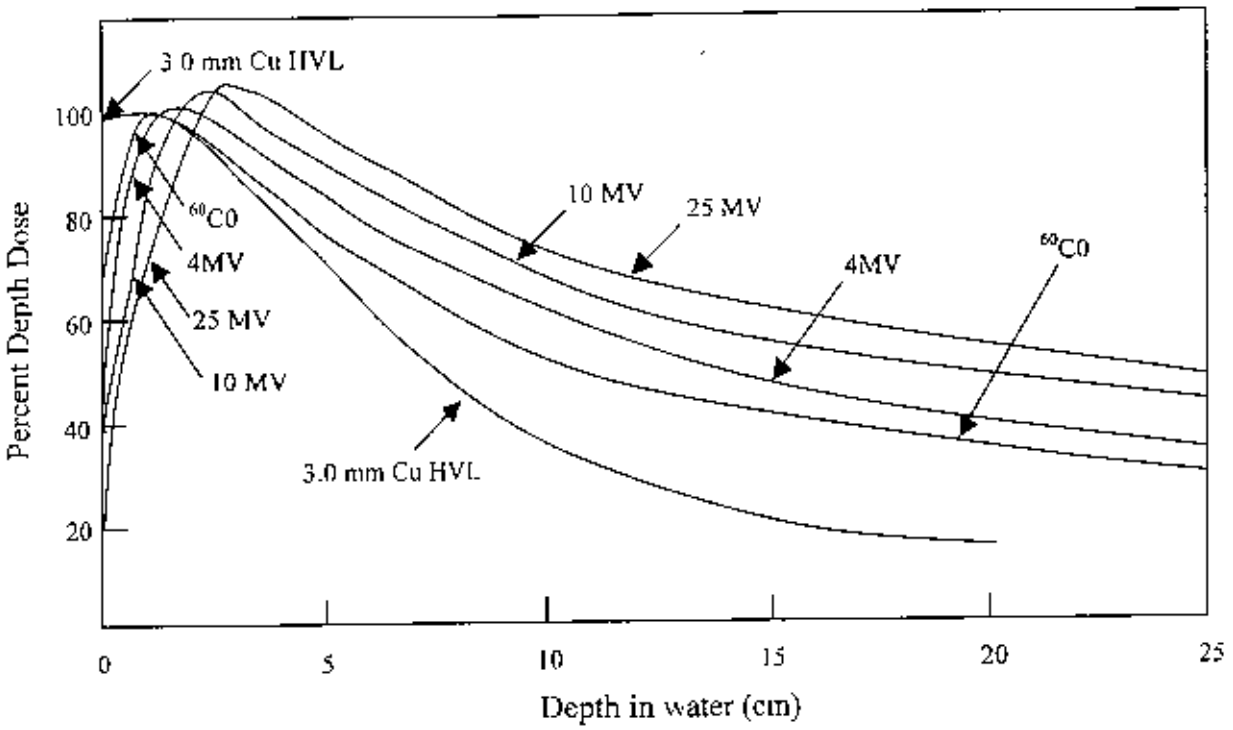

Fig.11: Central axis depth dose for different quality photon beams. Field size 10x10 cm, SSD = 100 cm for all beams except for 3.0 mm Cu HVL, SSD = 50 cm.

The percentage depth at all points other than the central point is less than 100%. The beam intensity at any point p (say) off the axis of the field will be dropped to a value following inverse square law such as intensity at p which if 5 cm (say) off the axis will be

$$\frac{SSD^2}{SSD^2 + 5^2} \qquad \text{----------(29)}$$

If SSD = 80 cm, then intensity at p will be 0.996. Thus using beam intensity factor the doses at different points in the field can also be approximately calculated.

2.2.8.1 Effect of Field Size and Shape on Depth Dose

Field size may be specified either geometrically or dosimetrically. The geometrical field size is defined as the "projection" on a plane perpendicular to the beam axis, of the distal end of the collimator as seen from the front centre of the source[37,56]. This definition corresponds to the field defined by the light localizer, arranged as if a point source of light were located at the centre of the front surface of the radiation source. The dosimetric or physical size is

defined as the distance intercepted by an isodose curve (usually 50% isodose) on a plane perpendicular to the beam axis at a stated distance from the source.

For a significantly small field, the depth dose at a point is effectively the result of the primary radiation because in such a small field, the scatter contribution negligibly small or zero. But as the field size increases, the contribution of the scattered radiation to the absorbed dose increases. Since this increase in scattered dose is greater at larger depths than at depth of D_{max}, the percent depth dose increases with increasing field. The increase in percent depth dose causes by increase in field size depends no beam quality. Since the scattering probability or cross-section decreases with energy increase and the higher energy photons are scattered more predominantly in the forward direction, the field size dependence of percent depth dose is less pronounced for the higher energy than for the lower energy beam.

2.2.8.2 Dependence on Source - Surface Distance (SSD)

Photon fluence emitted from a point source of radiation varies inversely as a square of the distance from the source. Corresponding the source as a point one even in the case of clinical source, the exposure or dose rate in free space varies inversely as the square of the distance between the source and point of interest. The percent depth dose increases with SSD because of the effects of inverse square law. Although the actual dose rate at a point decreases with increase in distance from the source, the percent depth dose, which is a relative dose with respect to a reference point, increases with SSD. This is illustrated in fig. 12 in which relative dose rate from a point source of radiation is plotted as a function of distance from the source, following the inverse square law.

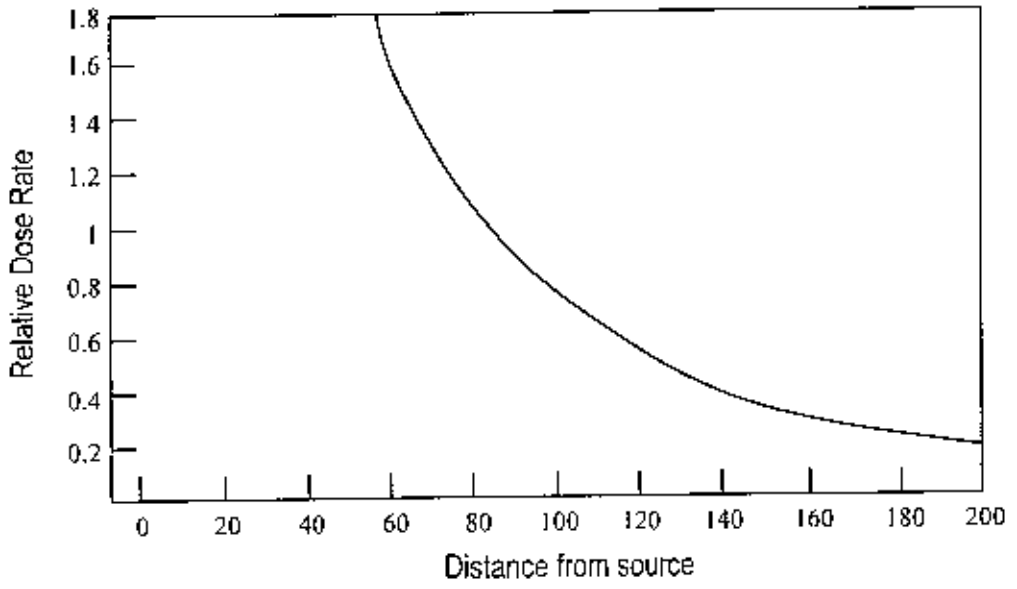

Fig.12: Plot of relative dose rate as inverse square law as a function of distance from a point source with reference distance = 80 cm.

The plot shows that the percent depth dose, which represents depth dose relative to a reference point, decreases more rapidly near the source than far away from the source. In clinical radiotherapy, SSD is a very important parameter, since percent depth dose determines how much dose can be delivered at depth relative to the surface dose or D_{max}, the SSD needs to be as large as possible. However, since dose rate decreases with distance, the SSD, in practice, is set at a distance which provides a compromise between dose rate and percent depth dose. For the treatment of deep-seated lesions with megavoltage beams, the minimum recommended SSD is 80 cm[75,77].

2.2.9 DOSE CALCULATION PARAMETERS

2.2.9.1 Tissue -Air Ratio (TAR) and Scatter - Air -Ratio (SAR)

There are several methods for calculation of doses in patient or any other medium. Two of these use percent depth dose and TAR. However, there are certain limitations to these methods. The dependence of source to surface distance (SSD) makes this quantity unsuitable for isocentric techniques. Although, tissue-air ratio (TAR) and scatter-ratio(SAR) eliminates that problem, their application to the beams of energy higher than those of ^{60}Co has limitations as they require measurement of dose in free space[36,37]. As the beam energy increases, the size of the chamber build up cap for in -air measurements has to be increased

and thus it becomes increasingly difficult to calculate the dose in free space from such measurements. To overcome these limitations of TAR another quantity, tissue phantom ratio (TPR) is introduced which remains the properties of TAR but limits the measurements to the phantom rather than air[87]. A few years later, another quantity tissue maximum ratio (TMR) is being introduced which also limits the measurements to the phantom[54,36,55].

Scatter-air ratios are used for the purpose of calculating scattered dose in the medium. The computation of the primary and the scattered dose separately is particularly useful in the dosimetry of irregular fields.

Scatter-air ratio may be defined as the ratio of the scattered dose at a given point in the phantom to the dose in free space at the same point. The scatter-air ratio like the tissue-air ratio is independent of the source-surface distance but depends on the beam energy, depth, and field size

Since the scattered dose at a point in the phantom is equal to the total dose minus the primary dose at that point, scatter-air ratio is mathematically given by the difference between the TAR for the given field and the TAR for the 0×0 field.

$$SAR(d,r_d) = TAR\ (d,r_d) - TAR\ (d,0)$$

Here TAR(d,0) represents the primary component of the beam.

Since. SARs are tabulated as functions of depth and radius of a circular field at that depth.

2.2.9.2 Collimator Scatter Factor and Phantom Scatter Factor

The dose to a point in a medium may be considered to be composed of primary and scattered components. The primary dose is contributed by the initial or original photons emitted from the source and the scattered dose is the result of the scattered photons. The scattered dose may further be analyzed into collimator and phantom components, since the two can be varied independently by blocking. Blocking a portion of the field does not significantly change the output or exposure in the open portion of the beam but may substantially reduce the phantom scatter[13,49]. Determination of primary dose in a phantom which excludes both collimator and phantom scatter is in fact very difficult. However, for megavoltage photon beams, it is reasonably accurate to consider collimator scatter as part of the primary beam so that the phantom scatter could be determined separately. Thus, an effective dose is defined as the dose due to the primary photons as well as those scattered from the collimating

system. The effective primary dose in a phantom may be thought as the dose at depth minus the phantom scatter. Alternately, the effective primary dose may be defined as the depth dose expected in the field when scattering volume is reduced to zero while keeping the collimator opening constant. Representation of primary dose by the dose in a 0×0 field poses conceptual problems because of the absence of lateral electronic equilibrium in narrow fields in megavoltage photon beams This tissue has not yet received any practical solution and the concept of 0×0 field to represent primary beams with the implicit assumption that lateral electronic equilibrium exists at all points will continue to be used for routine dosimetry [61,9 62]. Collimator scatter factor (S_c) may be determined with an chamber having a build up cap of a size large enough to provide maximum dose build up for the given energy beam. In the measurement of S_c the field must fully cover the build up cap for all field sizes if measurements are to reflect photon fluences. Normally, the collimator scatter factors are measured at the source-axis distance (SAD). However, larger distances can be used provided the field sizes are all defined at the SAD. This phantom scatter factor (S_p) takes into account the changes in scatter radiation originating in the phantom at a reference depth as the field size is changed. this S_p can be determined by using a large field incident on phantoms of various cross-sectional sizes. The photon beams for which backscatter factors can be accurately measured (e.g., ^{60}Co and 4 MV), S_p factor at the depth of maximum dose may be defined simply as the ratio of the backscatter factor (BSF) for the given field to that for the reference field. Mathematically

$$S_p(r) = \frac{BSF(r)}{BSF(r_0)} \qquad \text{----------(30)}$$

where r_0 is the size of the reference field (10×10 cm^2)

A more practical method of measuring S_p, which can be used for all beam energies consists of indirect determination from the following equation

$$S_p(r) = \frac{S_{c,p}(r)}{S_c(r)} \qquad \text{----------(31)}$$

where $S_{c,p}(r)$ is the total scatter factor at a reference depth for field size r divided by the dose at the same point and depth for the reference field size (10×10 cm^2). Thus $S_{c,p}$ contains both the collimator and phantom scatter and when divided by $S_c(r)$yields S_p and S_c are defined at

the reference depth D_{max}, actual measurement of these factors at these depth may create problems because of the possible influence of electron contamination incident on the phantom. This can be divided by making measurements at a greater depth (e.g., 10 cm) and converting the readings to the reference depth of D_{max} by using percent depth dose data. presumably measured with a small- diameter chamber. The rationale for this procedure is the same as for the recommended depths of calibration[60,34].For megavoltage beams in the range of 20 to 45 MV, the depth of maximum dose D_{max} has been found to depend significant on field size as well as on SSD[21,78].

In order that the calculative functions be independent of machine parameters. they should not involve measurements in the build up region. Hence, the reference depth must be equal or greater than the largest d_m. Since dm tends to decrease with field size[48] and increase with SSD[10] one should choose d_m for the smallest field and the largest SSD.

2.2.9.10 DOSIMETRIC CALCULATION SYSTEM

2.2.10.1 SSD Technique in Accelerator

Percent depth dose (PDD) is a suitable quantity for calculation of doses involving SSD techniques. Machines are usually calibrated to deliver 1 rad per monitor unit (MU) at the reference depth t_0, for a reference field size 10×10 cm and a source to calibration point distance of SCD. Assuming that S_c factors relate to collimator field size defined at SAD, the monitor units necessary to deliver a certain tumor dose (TD)at depth d for a field size r at the surface at any SSD are given by

$$MU = \frac{(TD \times 100)}{\left[K \times (\%DD)_d \times S_c(r_c) \times S_p(r) \times (SSDfactor)\right]} \qquad \text{----------(32)}$$

where K is 1 rad per MU, r_c is the collimator field size, given by

$$r_c = r.\frac{SAD}{SSD}$$

$$\text{And SSD factor} = \left[\frac{SCD}{(SSD + t_0)}\right]^2 \qquad \text{----------(33)}$$

2.2.10.2 Isocentric or SAD Technique

Tissue-Maximum-Ratio (TMR) is the quantity of choice for dosimetric calculations involving isocentric technique. Since the unit is calibrated to give 1 rad /MU at the reference depth t_0, source calibration distance SCD, and for the reference field (10×10 cm^2), then the monitor units necessary to deliver isocenter dose (ID) at depth d are given by

$$MU = ID / [K\times TMR\ (d, r_d)\times S_c(r_c) \times S_p\ (r_d)\times(SAD\ factor)]$$

$$\text{Where SAD factor} = (SCD / SAD)^2$$

2.2.10.3 Dose Calculation in ^{60}Co Unit

In the case of ^{60}Co, the machine can be calibrated either in air or in phantom to deliver dose as rad/min. provided the following information is available:(a) dose rate D_0 (t_0,r_0,f_0) in phantom at depth t_0 of maximum dose for a reference field size r_0 and standard SSD f_0 ; (b) S_c; (c)S_p; (d) percent depth doses; and (e) TMR values. In addition, the SSD used in these calculations should be confined to a range for which the out put in air obeys an inverse square law for a constant collimator opening. In teletherapy, the dose is usually delivered to the patient with respect to time, i e., how long the beam should remain "ON" to deliver a certain prescribed dose to the patient while in the case of accelerator MU is used to serve the purpose. The necessary treatment time is given by

$$Time = \frac{(TD\times100)}{[D_0(t_0,r_0,f_0)\times\%DD(t,r,f)\times S_c(r)\times S_p(r)\times(SSD-factor)]} \qquad \text{----------(34)}$$

where SSD-factor = $(SSD1/SSD2)^2$

2.2.10.4 Dose in Asymmetric Field

Most of the modern accelerators are now equipped with x-ray collimators (or jaws) that can be moved independently to allow asymmetric fields with field centers positioned away from the true central axis of the beam. When a field is collimated asymmetrically, it is needed to take into account the changes in the collimator scatter, phantom scatter, and off axis-beam quality[51]. The use of beam flattering filter (thicker in the middle and thinner in the periphery) results in greater beam hardening close to the central axis compared with the

periphery of the beam[53,77]. For a point at the center of an asymmetric field and a lateral distance 'x' away from the beam central axis, the collimator scatter factor may be approximated to a symmetric field of the same collimator opening as that of the given asymmetric field. This approximation is reasonable as long as the point of the dose calculation is centrally located i.e., away from the field edge. Since beam flatness within the central 80% of the maximum field size is specified within ± 3% at a 10 cm depth, ignoring off-axis dose correction in asymmetric fields will introduce errors of that magnitude. Thus off-axis dose correction will follow changes in the beam flatness as a function of depth and distance from central axis. The following equations are proposed for the calculation of monitor units for asymmetric fields[57].

For SSD type of treatment

$$MU = \frac{(TD \times 100)}{\left[K \times (\%DD)_d \times S_c(r_c) \times S_p(r) \times (SSD - factor) \times OAR_d(x)\right]} \quad \text{----------(35)}$$

Where OAR_d is the off-axis ratio at depth d.

Similarly for isocentric treatment

$$MU = \frac{ID}{\left[K \times TMR(d, r_d) \times S_c(r_c) \times S_p(r_d) \times (SAD - factor) \times OAR_d(x)\right]} \quad \text{----------(36)}$$

The above formalism is general and can be used for calculation of an off -axis point dose in symmetric fields generated by blocks or collimators, including multileaf collimators. For irregularly shaped fields the parameter r_d is the equivalent field size determined by Clarkson's technique or geometric approximation and r_c is the collimator opening size projected at the standard SSD.

2.2.10.5 Dose Distribution in Irregular Field

Any fields other than the square, rectangular or circular fields may be termed irregular fields . These irregularly shaped fields are frequently encountered in radiotherapy practices. Irregularly shaped fields, in fact, appear when radiation sensitive structures are shielded from the primary beam or when the field extends beyond the irregularly shaped patient's body contour. Since basic standard dosimetric data are available for rectangular or square fields only, special methods including several correction factors are necessary to use these

basic data for calculation of doses in irregularly shaped fields. For certain specific irregular fields, some special methods are in general use. However, irregular fields are not universal rather, it can be different for different clinical situations. Therefore, several approaches are in progress for making generally applicable methods for calculation of doses in individual irregular fields.

2.2.10.6 Dose Calculation in Irregular Field

Although rectangular or square fields are usually used as clinical fields, but these fields are often shaped irregularly to protect critical or normal regions of the body. Hence, a dose calculation system must be generally applicable to the above practices, with acceptable accuracy and simplicity for routine use. The computation of the primary and scatter dose separately is important for calculation of dose in irregular fields and to do this, a quantity known as scatter-air ratio (SAR) is introduced which is defined as the ratio of the dose at a given point in the phantom to the dose at the same point in air. Like TAR, SAR is also independent of the source-surface distance but depends on the beam energy, depth, and the field size. Mathematically it is defined as the difference between the TAR for the given field and the TAR for the 0×0 field i.e.,

$$SAR(d, r_d) = TAR(d, r_d) - TAR(d, 0) \qquad \text{----------(37)}$$

where TAR(d,0) represents the primary components of the beams.

Any field other than square, circular or rectangular field may be termed as irregular field. These irregularly shaped fields are very often encountered in radiotherapy practices. Dose calculation method in such irregular fields, originally proposed by Clarkson and later developed by cunninghum has proved to be the most general in its application[20.12].

Clarkson's method is based on the principle that the scattered component of the depth dose, which depends on the size and shape of the field, can be calculated separately from the primary component which is independent of the field size and shape and as such the quantity SAR is used to calculate the scattered dose. In this method, for calculation of dose at any point in the irregular field like Mantle field, radii are drawn from that point to divide the field into a number of elementary sectors in which each sector is being characterized by its radius and be considered as of the circular field of that radius. Using an SAR table for circular fields, the SAR values for the sectors are being calculated and then summed to have

the average scatter-air ratio $\overline{(SAR)}$ for the irregular field at that point. For sectors passing through a blocked area the net SAR is determined by subtracting the scatter contribution by the blocked part of the sector. The computed $\overline{(SAR)}$ is converted to average tissue-air ratio $\overline{(TAR)}$ by equation

$$\overline{(TAR)} = TAR(0) + \overline{(SAR)} \qquad \text{----------(38)}$$

where TAR(0) is the tissue air ratio for 0×0 field.

The percent depth dose (%DD) at any point can be calculated relative to D_{max} on the central axis as

$$\%DD = 100 \times \frac{\left[\frac{\{f + d_m\}}{\{f + d\}}\right]^2}{BSF} \qquad \text{----------(39)}$$

where BSF is the backscatter factor for the irregular field which can be calculated by Clarkson method[42]. This Clarkson's method is a general technique of dose calculation in irregular field but it is not practical for routine manual calculations which is very important for necessary cross check of the results between computer and manual calculations and further to this, even when computerized, it is time consuming since a considerable input data is required by the computer program which is not practical in routine radiotherapy practices. With the exception of mantle, inverted-Y and a few other complex fields, reasonably accurate calculation can be made for most blocked fields by using relatively simple approximation method. In the blocked fields, approximate rectangles can be drawn containing the point of calculation. In drawing rectangles, certain blocked area may be included in the rectangle, provided this area is small and remotely located relative to that point. The rectangles thus formed may be called effective field, while the unblocked field defined by the collimator, may be called the collimator field[23]. Once the effective field has been determined one can proceed with the usual calculation method for dose determination in that field. It is also be noted that, calculation of depth dose distribution at any point within the field or out of the field is possible by using Clarkson's technique , however, as it is not practical for manual calculation, some other simple methods proposed by Day and Wrede are used for calculation of doses in irregular fields. Both the methods are basically same and

based on approximation of rectangular or square fields in the irregular (blocked) fields and thereafter use of perimeter formula for determination of equivalent square fields. If once equivalent square fields could be determined, then usual dose calculation methods are used for calculation of doses at any point in the irregular (blocked) fields. Another method, known as negative field method may be used for dose calculation in irregular fields[79,51]. In this method, the dose at any point is equal to the dose from the overall (unblocked) field minus dose expected if the entire field were blocked, leaving the shielded volume open. In other words, the blocked portion of the field is considered a negative field and its contribution is subtracted from overall field dose distribution. A computerized negative field method not only is a fast method of calculating isodose distribution in blocked fields but is very convenient for manual point dose calculation[53,90 68].

2.2.10.6.1 Depth Dose Calculation Formulism used in Irregular Field

Dosimetry of irregular fields using TMRs and SMRs is analogous to the method using TARs and SARs. An irregular field at depth d may be divided into n elementary sectors with radii emanating from any point Q (say). A Clarkson type integration my be performed to have averaged scatter maximum ratio $\overline{SMR}(d,r_d)$ for the irregular field r_d

$$\overline{SMR}(d,r_d)=\frac{1}{n}\sum_{i=1}^{n}SMR(d,r_i) \qquad \text{----------(40)}$$

where r_i is the radius of the ith sector at depth d and n is the total number of sectors $n = 2\pi/\Delta\theta$ is the sector angle.

The computed $\overline{SMR}(d,r_d)$ is then converted to $\overline{TMR}(d,r_d)$ by using the equation

$$TMR(d,r_d)=\left[K_p TMR(d,0)+\overline{SMR}(d,r_d)\right]\times\frac{S_p(0)}{\overline{S_p}(r_d)} \qquad \text{----------(41)}$$

where K_p is the off axis ratio representing primary dose at Q relative to that at the central axis. $\overline{TMR}(d,r_d)$ may be converted to the percent depth dose P(d,r,f) by using equation

$$P(d,r,f)=100\left[K_p.TMR(d,0)+\overline{SMR}(d,r_d)\right]\times\frac{S_p(0)}{\overline{S_p}(r_d)}\times\frac{\overline{S_p}(r_d)}{\overline{S_p}(r_{i0})}\times\left[\frac{(f+t_0)}{(f+d)}\right]^2 \qquad \text{----------(42)}$$

The final expression takes the form

$$P(d,r,f)=100\left[K_p TMR(d,0)+\overline{SMR}(d,r_d)\right]\times\frac{1}{\left(1+\overline{SMR}(t_0,r_{t0})\right)}\times\left[\frac{(f+t_0)}{(f+d)}\right]^2 \quad \text{----------(43)}$$

2.2.10.6.2 Depth Dose data for Irregular Field

Percent depth dose data are usually tabulated for square fields. But majority of the treatment fields encountered in radiotherapy practices are rectangular and irregularly shaped (blocked) fields and hence a system of equating square fields to different field shapes is required. Semi empirical formulas have been developed to relate central axis depth dose data for square, rectangular, circular and irregular shaped fields. Although general methods, based on Clarkson's principle are available, similar methods have been developed specially for interrelating square, rectangular, and circular field data. Day and others [17,28,10] have shown that, for central axis depth dose distribution, a rectangular field may be approximated by an equivalent square or by an equivalent circle. A simple rule of thumb method is used for equating rectangular and square fields according to which a rectangular field is equivalent to a square field if they have the same area/ perimeter (A/P) [76,77].The following formulas are useful for quick calculation of the equivalent field parameters. For rectangular fields

$$\frac{A}{P}=\frac{a\times b}{2(a+b)} \quad \text{----------(44)}$$

where a is the field width and b is the field length. For square fields, a = b

and so $\frac{A}{P}=\frac{a}{4}$, where 'a' is the side of the square.

From the above two equations it is clear that the side of an equivalent square of a rectangular field is: side of an square = 4 A/P

This perimeter formula is widely used in clinical practices and has been extended as a field parameter to apply to other quantities such as backscatter factor, tissue air ratios, and even beam output in air or phantom. The radii of equivalent circles may be obtained by the relationship:

$$r=\frac{4}{\sqrt{\pi\left(\frac{A}{P}\right)}} \quad \text{----------(45)}$$

This has been derived by assuming that the equivalent circle is the one that has the same area as the equivalent square.

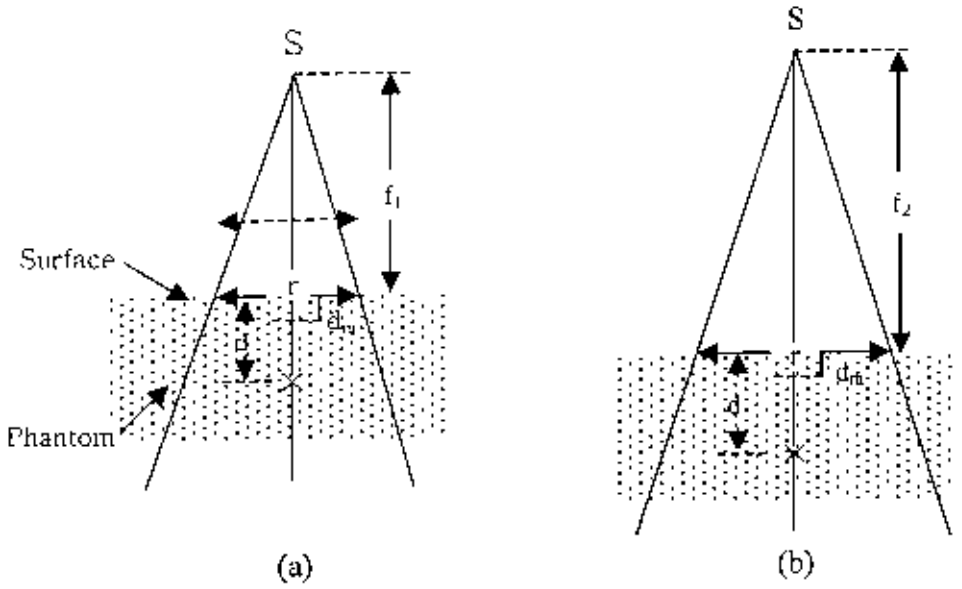

Fig.13: Change of percent depth dose with SSD. (a) has SSD = f1 and condition (b) has SSD = f2. For both conditions, field size on the phantom surface, r× r and depth d are the same.

Percent depth dose for clinical use are usually measured at a standard SSD (80 or 100 cm for megavoltage units). In a given clinical situation, however, the SSD set on a patient may be different from the standard SSD. Larger SSDs may be required for treatment techniques that involves field sizes larger than the ones available at the standard SSD. Thus, the percent depth doses for a standard SSD must be converted to those applicable to the actual treatment SSD. As a simple approximation method to solve this inconsistency, a factor known as Mayneord F factor[87,88] is in use which is based on a strict application of the inverse square law, without considering changes in scattering, as the SSD is changed. The irradiation condition is depicted as follows.

The percent depth dose at depth d for SSD = f_1 and for SSD = f_2 is given by

$$\frac{P\{d,r,f_2\}}{P\{d,r,f_1\}} = \left[\frac{\{f_2+d_m\}}{\{f_1+d_m\}}\right]^2 \cdot \left[\frac{\{f_1+d\}}{f_2+d}\right]^2 \qquad \text{----------(46)}$$

The term on the right hand side of this equation is called the Mayneord F factor.

Thus
$$F = \left[\frac{\{f_2+d_m\}}{f_1+d_m}\right]^2 \cdot \left[\frac{\{f_1+d\}}{\{f_2+d\}}\right]^2 \qquad \text{----------(47)}$$

This Mayneord F factor method, works reasonably well for small fields since the scattering is minimal under these conditions, however, it overestimates the increase in percent depth dose with increase in SSD for relatively larger fields. Since the percent depth dose depends

on SSD, so SSD correction to the percent depth dose is to be applied to be applied to correct for the varying SSD- a procedure which becomes cumbersome to apply routinely in clinical practice. A simpler quantity, namely TAR (Tissue air ratio) is introduced to remove the SSD dependence which is defined as the ratio of the dose D_d at a given point in the phantom to the dose in free space (D_{fs}) at the same point. This TAR depends on depth and the field size r_d at that depth .

$$TAR(d, r_d) = \frac{D_d}{D_{fs}} \qquad \text{----------(48)}$$

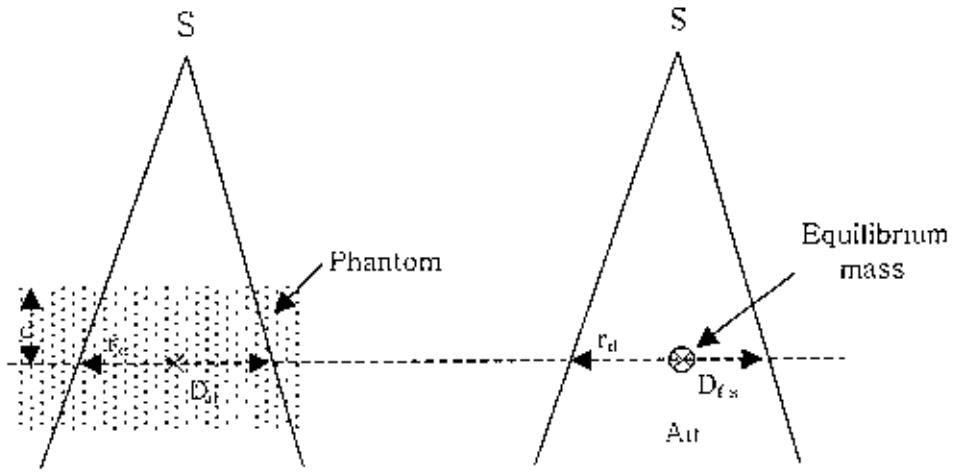

Fig.14: Illustration of the definition of $TAR(d,r_d) = D_d/D_{fs}$

It has been shown that the fractional scatter contribution to the depth dose is almost independent of the divergence of the beam and depends only on depth and the field size at that depth[17]. Hence tissue air ratio, which involves both the primary and the scatter component of the depth dose is independent of the source distance. This TAR varies with the energy, depth and field size very much like the percent depth dose. For megavoltage beams, the tissue air ratio builds up to a maximum at the depth of maximum dose (d_m) and then decreases with depth more or less exponentially. For a narrow beam or a 0×0 field size, in which the scatter contribution to the depth dose is neglected, the TAR beyond d_m varies approximately exponentially with depth i.e.,

$$TAR(d,0) = e^{-\bar{\mu}(d-d_m)} \qquad \text{----------(49)}$$

Where $\bar{\mu}$ is the average attenuation coefficient of the beam for the given phantom. As the field size is increased, the scatter component of the dose increases and the variation of TAR with depth becomes more complex. However, for megavoltage beams, for which the scatter is minimal and is directed more or less in the forward direction, the TAR variation with depth can still be approximated by an exponential function, provided an effective attenuation coefficient (μ_{eff}) for the given field size is used. Another term Backscatter factor (BSF) which is simply the TAR determined at the depth of maximum dose on central axis of the beam. It is defined as the ratio of the dose on central axis at the depth of maximum dose to the dose at the same point in free space Mathematically it is defined as

$$BSF = \frac{D_{max}}{D_{fs}} \qquad \text{----------(50)}$$

$$\text{or,} \quad BSF = TAR(d_m, r_{dm}) \qquad \text{----------(51)}$$

where r_{dm} is the field size at d_m of maximum dose.

This backscatter factor, like TAR, is independent of distance from the source and depends on the beam quality and the field size. For orthovoltage beams with usual filtration, the BSF can be as high as 1.5 for large field sizes. This amounts to a 50% increase in dose near the surface compared with the dose in free space or in terms of exposure, 50% increase in exposure on the skin compared with the exposure in air. While for megavoltage beams (^{60}Co and higher energies) the backscatter factor is much smaller. For example BSF for a 10×10 cm field for ^{60}Co is 1.036. This means that the D_{max} will be 3 6% higher than the dose in free space. This increase in dose is the result of radiation scatter reaching the point of D_{max} from the overlying and underlying tissues. As the beam energy is increased, the scatter is further reduced and so is the BSF. Above about 8 Mv, the scatter at the depth of D_{max} becomes negligibly small and the BSF approaches its minimum value of unity.

Chapter-III

Treatment Planning

3.1 Aims of Treatment Planning

Treatment planning is a process of determining the best method of treating a tumor with radiation. The major objectives of treatment planning are to ensure that the tumor receives a uniform radiation dose while healthy tissue and critical structures are protected Other important objectives of treatment planning are to develop reproducible setups and maintain patient comfort. Treatment planning includes determining the volume to be treated and then designing appropriate radiation fields to treat that volume. It begins before the first radiation treatment and continues throughout a course of therapy to ensure that the intended plan is being implemented. A treatment plan may some times be changed during a course of therapy to compensate for changes in a patient's condition

Treatment planning is often a challenging process during which teamwork is required to achieve optimal and reproducible radiation treatments.

There are three aims of treatment planning

- To develop a plan that treats the tumor volume. This plan would give as homogeneous a dose distribution as possible throughout the clinical target volume.
- To minimize a radiation dose to healthy structures. Areas outside the target volume should receive as little radiation as possible. Limiting dose to healthy tissues requires knowledge of how much radiation the tissues in the treatment field can tolerate. Dose levels to critical structures such as the spinal cord, kidneys, and the lens of the eyes must be minimized.
- To provide a permanent record of dose calculations and distributions so that others may, in the future, understand the treatment plan. This record may become important if the patient needs to receive more radiation in the future.

The treatment planning includes visualization, localization, field selection and placement, and verification[7].

Visualization

Visualization is the determination of the location and extent of the tumor, particularly with respect to anatomical landmarks. This process uses every reasonable method of examination, including palpation.

Simulation or Localization

Localization, or simulation, is the determination, radiographically, of the field borders required to encompass the clinical target volume. Ideally localization is ferformed using a **simulator**- radiographic (imaging) unit that simulates all the movements of the linear accelerator or Cobalt-60 treatment unit and matches its geometry, distances (SSD, SDD, etc), beam divergence, and field size. A simulator produces high-quality images of the treatment field.

Field lights

Field lights are the most essential beam alignment devices to achieve accurate alignment of the radiation fields on the patient, because the **light field** on a therapy machine corresponds to the radiation fields to an accuracy ±3 mm.

body contour

A body contour is a precise outline of a patient, usually in a transverse plane that includes the region of the tumor. A contour is required both for computing and for displaying the dose distribution in the treatment volume. Frequently done at the time of localization, a contour is usually taken at the central axis plane of the fields but may be taken at other levels as well to evaluate the dose distribution[71].

3.2 Dose Profiles

Measurement of dose made by passing a dosimeter (ionization chamber or diode) across the beam produces what is called a **dose profile.** The fig.15(a) shows that the dose within the field is fairly constant (depending on the beam flatness) and that beyond the field edge the dose is low.

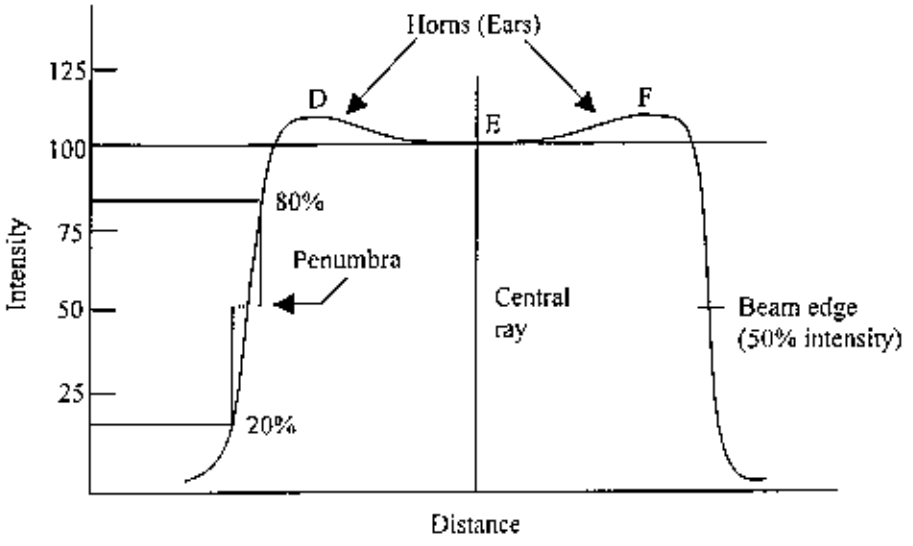

Fig.15(a): Beam profile vocabulary. The central ray, beam horns, and beam edge are shown. The beam edge is defined as the 50% intensity location on each side of the beam. The penumbra is the width of the field between 20% and 80% of the central ray intensity.

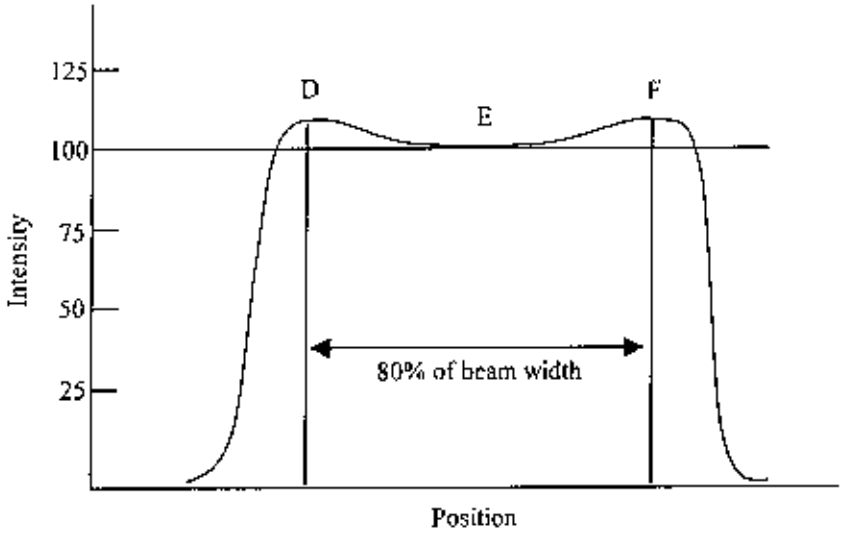

Fig.15(b): Beam profile and regions of interest in the definition of flatness and symmetry. The central 80% of the scan is the region in which flatness (the difference between the maximum and minimum intensity) and symmetry (the difference between intensity at the 80% edges) are measured.

The area of transition at the edge of the beam is the penumbra . The **penumbra** is marked as the width between the 20% and 80% values on the beam profile, shown in fig.15(a). The central 80% of the scan is the region of symmetry (the difference between intensity at the 80% edges). The **symmetry** is a measure of the side to side equality of the beam. The ratio of intensity at D and F in fig.15(b) measures the symmetry of the beam. Usually the symmetry

is required to be ±1-2% from one side of the beam to the other. The central 80% of the scan is the region of flatness (the difference between the maximum and minimum intensity). The definition of **flatness** varies with manufacturer of the treatment machine but is generally the maximum variation of beam intensity in the central 80% of the beam. In figure 15(b), points D and F are the highest intensity points on each side of the beam, and point E the lowest intensity point in this central region. The ratio of intensity at F and E measures the flatness of the beam, the maximum variation of intensity in the central 80% of the beam. Flatness is required to be ±2-3% across the beam[71].

Depth and field size are both critical to beam symmetry and flatness. The deeper we go in the phantom, the more uniform and symmetric the beam becomes due to increased scatter in the phantom. In general, the smaller the beam, the poorer the flatness. The factor used in dosimetry that describes this effect is the ratio of the dose at any point on a profile divided by the dose at the central ray on that profile. It is referred to as the off-center ratio (OCR), or off-axis ratio (OAR). The OCR at point F is the dose ratio of F to E. The beam's edge is defined as the point where the OCR is 50% or 0.50.

The horns or ears are the high intensity regions beneath the thin edges of the beam flattering filter. The lower the energy of the megavoltage beam, the larger the value of the OCR in the horn region. This is because the beams are specified to be flat at a depth of 10 cm. Radiation at the edges of the beam can scatter out of the beam, leaving the edges without sufficient intensity. Therefore, added intensity is put in the beam edges at shallow depths so that enough will be left at a 10 cm depth to provide a flat beam for treating the tumor[71].

3.3 Tissue Inhomogeneties

Tissue inhomogeneities are volumes within the patient that have non-uniform tissue densities. For example, while the density of most soft tissue is about 1, that of lung is much lower, bone somewhat above 1, and mental plates used in bone repair much greater than 1. Tissue inhomogeneties alter the dose distribution from the standard curves due to attenuation and scatter. One method for correcting tissue inhomogeneties is the **effective TAR method.** It is a point by point calculation technique instead of a line-by line technique. For each point in the patient (actually each point of interest) the equivalent water path length or depth is calculated using electron densities of overlying tissues. If we imagine that the

patient contour is filled with a matrix of calculation points and that the computer calculates doses at each of the matrix points, shown in figure16.

The fig.16 illustrates effective TAR computation process using only three points. The three points on the rights of the phantom (P_1, P_2 and P_3) are traversed by the photon beam from the left. To reach the three points, however, the radiation beam has to travel through three different materials – air, water, and bone.

In order to calculate the appropriate TAR for each material, the water equivalent path length must be determined. This is the thickness of water that will provide the identical attenuation of the actual beam path.

The calculation for point P_1 is as follows :

Path length P_1 = 5 cm water + 6 cm air ÷ 5 cm water
= 10 cm water + 6 cm air
= 10 cm water

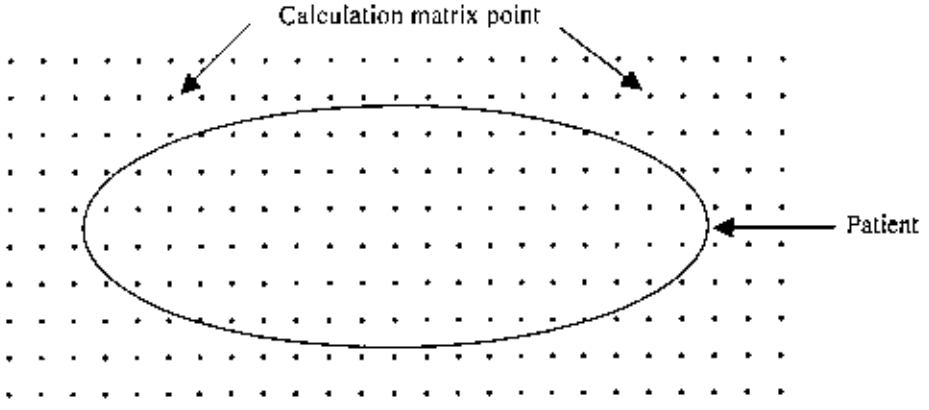

Fig.16: Computer view of a patient is actually a set of points in space surrounded by attenuating material. Each point lies in a rectangular array of points, a matrix of calculation points at which individually computed doses are produced

Because of its low density, 6 cm of air is equivalent to less than 1 mm of water and is ignored. Therefore, the equivalent length is just 10 cm.

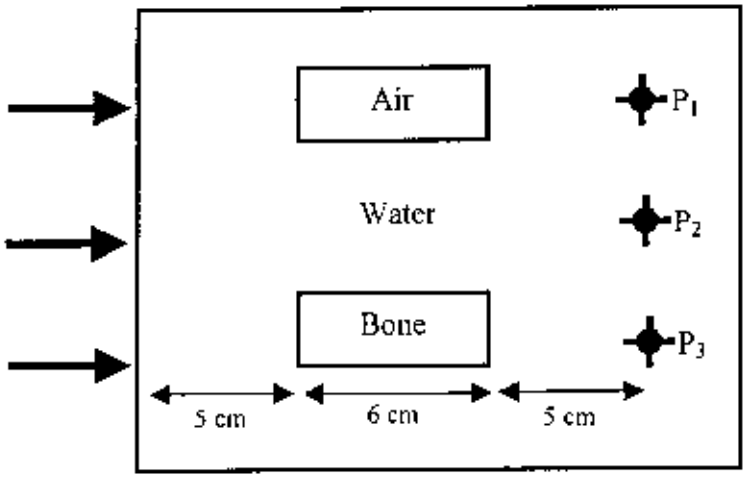

Fig.17: This figure illustrates the TAR computation process involved, using only three points P_1, P_2, P_3 are behind three materials – air, water, and bone. The air supplies less attenuation than the water, while the bone supplies more.

The calculation for P_2 is handled similarly :

$$\text{Path length } P_2 = 5 \text{ cm water} + 6 \text{ cm water} + 5 \text{ cm water}$$
$$= 16 \text{ cm water}$$

and for P_3,

$$\text{Path length } P_3 = 5 \text{ cm water} + 6 \text{ cm bone} + 5 \text{ cm water}$$
$$= 10 \text{ cm water} + 6 \text{ cm bone} \left(\frac{\text{Bone density}}{\text{Water density}}\right)$$
$$= 10 \text{ cm water} + 6 \text{ cm bone} \left(\frac{1.5 \text{ g/cm}^3}{1.0 \text{ g/cm}^3}\right)$$
$$= 19 \text{ cm water}$$

Thus the dose at point P_1 > dose at P_2 > dose at P_3 .Once the path length for a point is calculated, it is used as the depth to determine the TAR for the point in equation[71].

3.4 Tissue Compensator

The missing tissue missing from the beam incident on an irregular or sloping surface changes the desired uniform dose distribution pattern in the target volume. The degree of heterogeneity varies with the amount of missing tissue along the incident beam. In certain clinical situations, surface irregularity gives rise to unacceptable dose heterogeneity in the target volume or causes excessive irradiation of sensitive structures such as spinal cord.

Many techniques are in use to overcome this problem, including the use of wedge fields, multiple fields and the addition of bolus material or compensators. Bolus is a tissue equivalent material placed directly on the skin with a view to fill up the air gap (the region having missing tissue) and thus to even out the irregular contours of a patient to present a flat surface normal to the beam so that one is treating a surface as if there is no missing tissue present. Placing bolus directly on the skin surface is satisfactory for treatment with low energy orthovoltage radiation, but for high energy megavoltage beams, this bolus technique results in the loss of its inherent skin sparing advantage. For such radiations, a compensating filter is used, which approximates the effect of the bolus as well as preserves the skin – sparing effect. Therefore, a compensator is simply an absorber inserted into the radiation beam. The thickness of the compensator at different points of the beam is such that it will attenuate the primary radiation just enough to compensate the increase in dose due to the missing tissue at that point. To preserve the skin – sparing properties of the megavoltage photon beams, the position of the compensator should be such that electron contamination from it is minimal. For ^{60}Co and other megavoltage radiation beams, the compensator should be placed at a suitable distance usually 15 – 20 cm away from the patient[23].

3.5 Treatment volume concept in Radiotherapy

Determination of treatment volume plays a vital role in medical radiotherapy treatment in regard to complete irradication of the malignant cells. A target volume consists of the demonstrable tumors (s), if present and any other tissue with presumed tumor is to be determined as 1st step for commencing radiotherapy treatment. This is the volume which

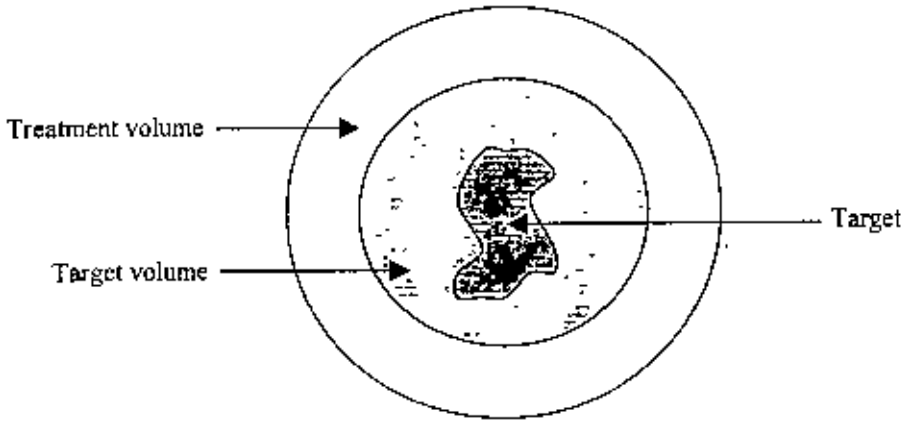

Fig.18: Target, targetvolume and treatment volume etc.

needs to be irradiated to a specified or prescribed absorbed dose with optimum uniformity. In delineating the target volume, comprehensive attention must be paid to consider the local invasive capacity of the malignant tumor and its potential spread to the regional lymph nodes. Therefore, determination of target volume is crucial one, which should include sufficient margins around the tumor to allow for the uncertainty in anatomic location of this volume. Further to this, additional margins must be provided around the above mentioned target volume to allow for limitations of the treatment technique (fig-14). Thus, the minimum target dose should be presented by an isodose surface which adequately covers the target volume in order to provide that margin. The volume enclosed by this isodose surface is called the treatment volume and depends on particular treatment technique and concerned target[4].

3.6 Simulation in Radiotherapy

Simulation refers to the procedure for combined trial set up and verification of the designed treatment plan using a simulator. Before commencing actual treatment for a patient, the treatment plan should be checked through trial set up whether the feasibilities of the plan are practically executable and reproducible as well. A trial set up is usually involved taking a film under treatment conditions as per treatment plan with the therapy unit or the simulator. Simulation refers to the procedure for combined trial setup and verification of the designed treatment plan using a simulator. A simulator is an apparatus that uses a diagnostic X-ray tube but duplicates a radiation treatment unit in terms of its geometrical, mechanical and optical properties. The main function of a simulator is to display the treatment fields so that the target volume may be accurately encompassed without delivering excessive irradiation to surrounding normal tissues. By radiographic visualization of internal organs, correct positioning of fields and shielding blocks can be obtained in relation to external landmarks. Most commercial simulators have fluoroscopic capability by dynamic visualization before a hard copy is obtained in terms of the simulator radiography. The need for a simulator arises from four factors : (a) Geometrical relationship between the radiation beam and the internal and external anatomy of the patient (b) Although field localization can be achieved by taking a port film, the radiographic quality of the image is poor, particularly in megavoltage high energy photons and for ^{60}Co a large source size as well (c) Field localization is a time

consuming process which, if carried out in the treatment room, could engage the therapy machine for a prohibitive length of time (d) Unexpected problems with a patient set up or a treatment technique can be solved during simulation thus conserving the time within the treatment room. Besides, localizing treatment volume and setting up the fields, other necessary data like : contours and thickness, including those related to compensator or bulus design can also be obtained during simulation as the simulator's table resembles the treatment table. Fabrication and testing of individualized shielding blocks can also be accomplished with a simulator provided the simulator should be equipped with accessories like laser lights, contour marker and shadow tray.

3.6.1 Portal Film in Radiotherapy

Portal films are radiographic film. The purpose of port filming is to verify the treatment volume under actual conditions of treatment. Although portal films are poorer overall image quality than other radiographic images, they contain sufficient information to determine the accuracy of beam placement. A diagnostic or simulator based port film is considered mandatory not only as a treatment record, a port film must be of sufficiently good quality so that the field boundaries can clearly be described anatomically. Radiographic technique significantly influences the image quality of a port film. The choice of film and screen as well as the exposure time is very important in this regards. The major limitations of sample port films are (a) relatively long processing time to view the image (b) it is impractical to do port film before each treatment (c) Film images are of poor quality specially for photon energies greater than 6 MV. Electronic portal imaging system overcomes the problems stated in a and b by making it possible to view portal images instantaneously i.e., images can be displayed on computer screen before initiating a treatment or in real time during the treatment. Verification films are often repeated on a weekly basis during each patient's treatment course to ensure continued correct field placement.

Chapter-IV

Experimental Method and Facility

4.1 Irradiation facility

The irradiation facility of high energy photon beams from ^{60}Co teletherapy unit of model: Alcyon II#90106, available at Delta Medical Centre, Mirpur, Dhaka were used for necessary investigation of doses in different irregular fields. The energies of the photon beams of ^{60}Co are 1.17 and 1.33 MeV having average energy of 1.25 MeV. ^{60}Co teletherapy unit has been supplied by Alcyon, France. The calibration of the ion chamber and electrometer was performed by output (cGy) of this ^{60}Co teletherapy unit. Photograph of the teletherapy machine is shown in fig.19. The other associated equipment and materials used were: ion chamber, electrometer, thermometer, barometer etc., which were the property of Delta Medical Centre. Slab phantom of solid perspex sheets, available at Delta Medical Center were used to simulate necessary irregular fields as we usually encountered in routine radiotherapy practices.

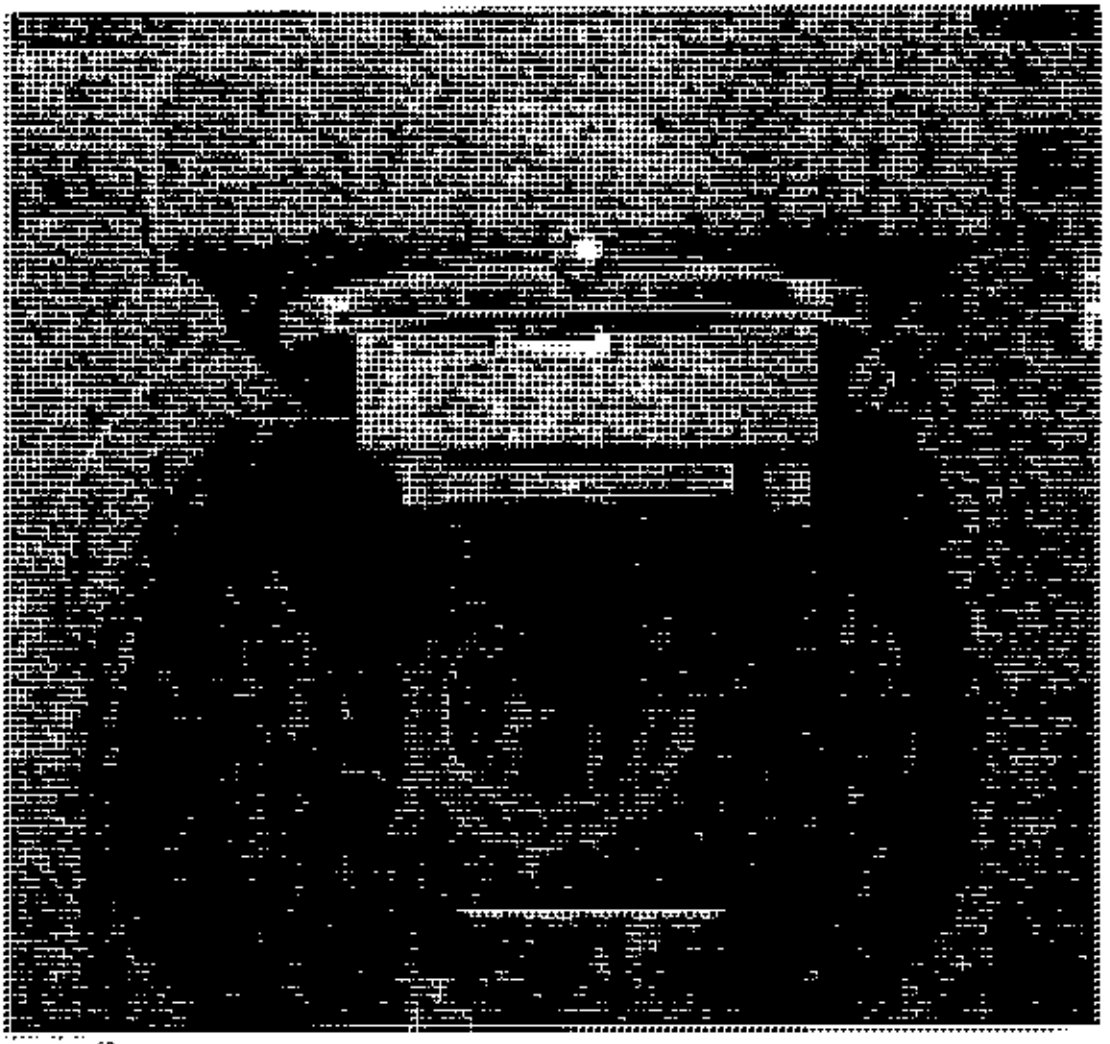

Fig.19: ^{60}C teletherapy unit (Alcyon II#90106) of Delta medical center Ltd.

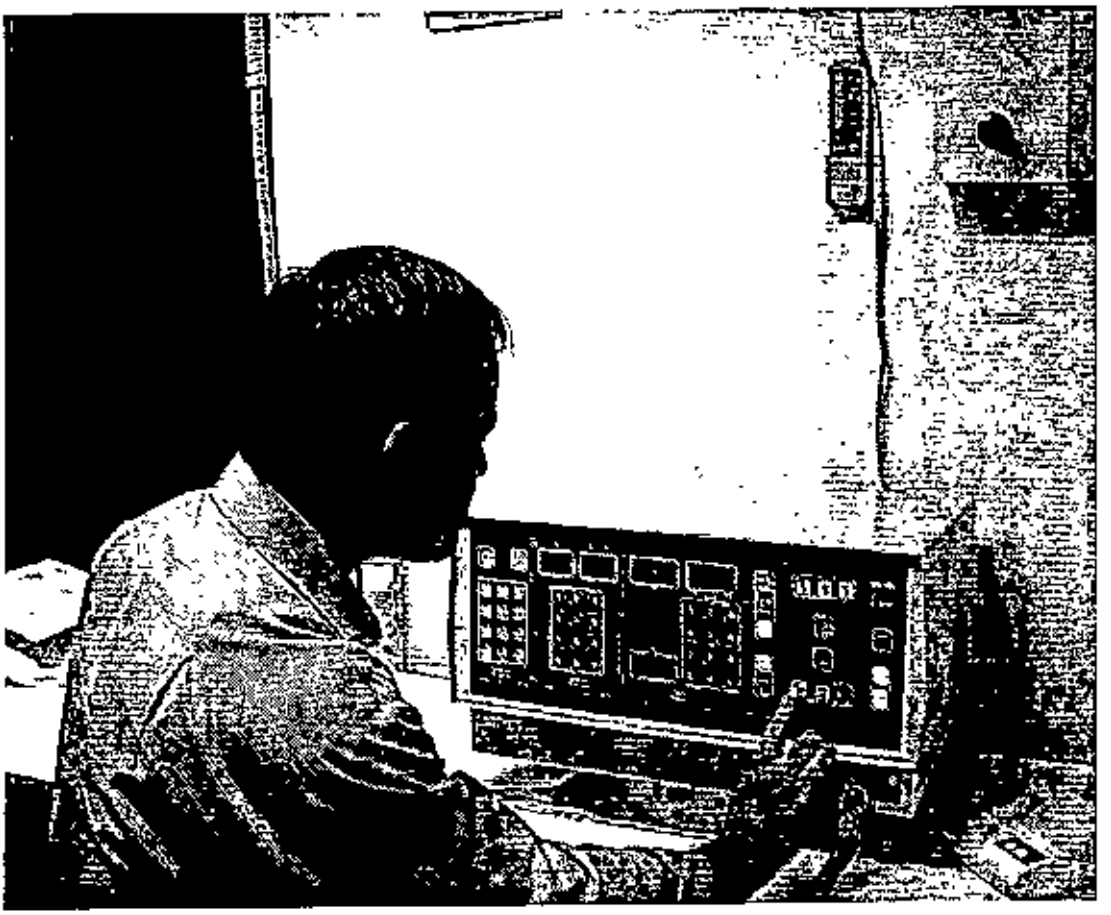

Fig.20: Control panel of the ^{60}Co teletherapy unit of Delta medical center Ltd.

4.2 Working Principles of Alcyon II Co-60 Unit

The source holder of Alcyon II#90106 teletherapy unit, containing the radioactive cobalt-60 source is inserted into a drum, Fig. 21, the rotation of which moves the source from the storage position into the treatment position The ^{60}Co source is assembled into a cylinder type drum. A motor drives it from the "Beam OFF" to "ON" position by rotation through an angle of 115 degree in less than 2.5 seconds. The source is held in the "BEAM ON" position by the motor reducer drive remaining energized [15]. At the end of irradiation, the power is switched OFF automatically and a powerful spring brings it back to the "BEAM OFF" or storage position. A mechanical device locks it in this position to ensure precise positioning of the field light system. However, as one must always think of the possibility of a situation in which the source becomes jammed in the irradiation position, the source holder has been fitted at the back with a wheel which can be used manually to retract the source to its storage position. if the source does not return to the storage position automatically. Two colored

sectors "Green and Red" located sideways on the radiation head cover, indicate the source position.

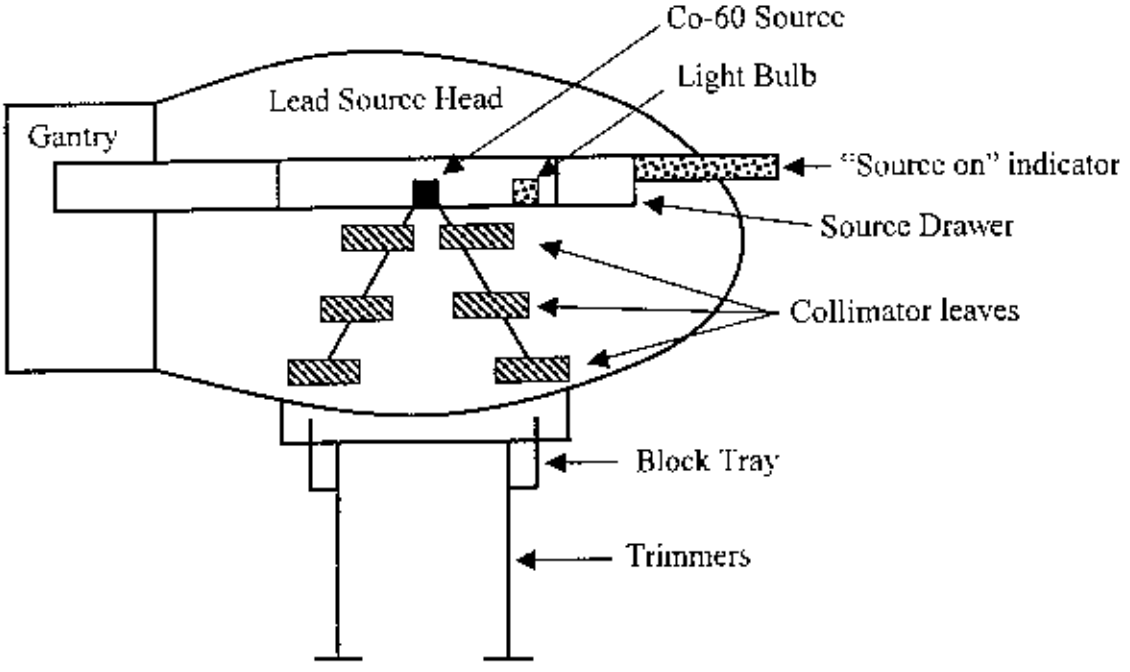

Fig.21: Cross sectional view of Cobalt-60 teletherapy head.

The ^{60}Co source decays to ^{60}Ni with the emission of beta particles (E_{max} =0.32 MeV) and two photons per disintegration of energies 1.17 and 1.33 MeV with average energy of 1.25 MeV, fig.22.

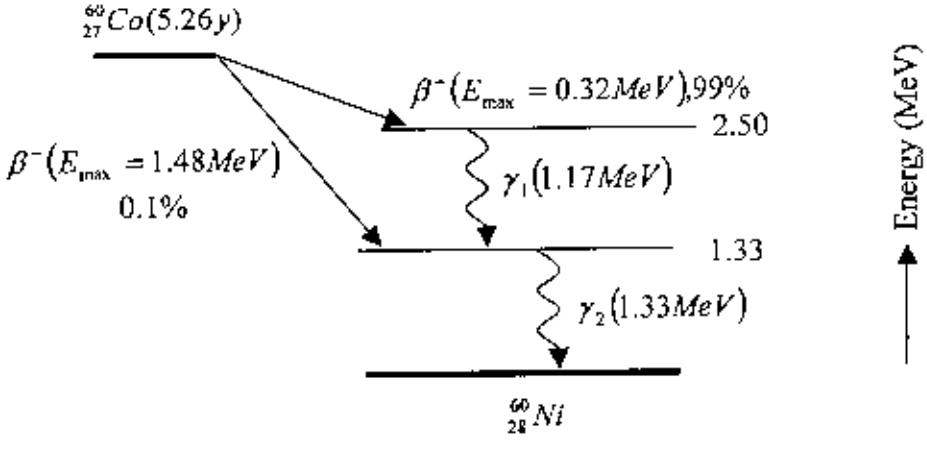

Fig.22: Energy level diagram for the decay of the ^{60}Co nucleus.

These γ- rays constitute the useful treatment beam in radiotherapy practices. The β- particles are absorbed in the cobalt metal itself and in its shielding house resulting in the emission of

bremsstrahlung x-rays along with a small amount of characteristic x-rays. However, these x-rays of average energy around 0.1 MeV do not contribute appreciably to the dose in the patient because they are strongly attenuated in the material of the source and source housing. The other contaminants to the treatment beam are the lower energy γ-rays produced by the interaction of the primary γ-photons with the source itself, the surrounding source housing materials and the collimator system. The scattered components of the beam contribute significantly (~10%) to the total intensity of the beam[1]. All these secondary interactions, thus to some extent, result in heterogeneity of the beam. In addition, electrons are also produced by these interactions and constitute what is usually referred to as the electron contamination of the photon beam. ^{60}Co source is a cylinder of 20mm diameter and is typically positioned in the cobalt unit with its circular end facing the patient. The fact that the radiation source is not a point source complicates the beam geometry and gives rise to what is known as geometric penumbra. The penumbra (DE) at depth 'd' is shown in fig.23.

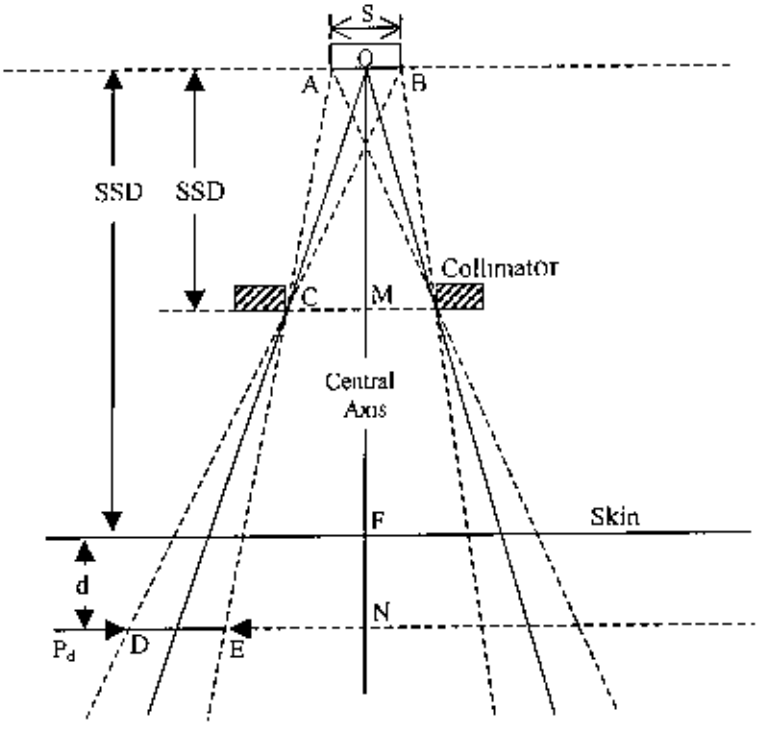

Fig.23: Diagram for calculating geometric penumra. Penumra is related to the size of the source. The larger the source size the larger the penumra (if SSD are fixed)

The collimator system is designed to vary the size and shape of the treatment beam to meet the individual requirements. However, the conventional collimator system can shape the beam either squire or rectangular only. The simplest form of a continually adjustable

collimator (diaphragm) consists of two pairs of heavy metal blocks. Each pair can be moved independently to obtain a squire or rectangular shaped field. Some collimator system, however, contains multiple blocks to control the size of the beam. If the inner surface of the blocks is made parallel to the central axis of the beam, the radiation will pass through the edges of the collimating blocks resulting in what is known as the transmission penumbra. The extent of this penumbra will be more pronounced for larger collimator openings because of greater obliquity of the rays at the edges of the blocks. This penumbra can be minimized but can not be completely removed. The term "penumbra" in several senses, means the region, at the edge of a radiation beam over which the dose rate changes rapidly as a function of distance from the beam axis. the transmission penumbra is the region irradiated by the photons, which are transmitted through the edge of the collimator block. The other penumbra "geometric penumbra" is defined as the geometric with of the penumbra at any depth from the surface of a patient which can be determined by considering similar triangles ABC and DEC, fig-23. From geometry, we have DE/AB=CE/CA=CD/CB=MN/OM=(OF+FN-OM)/OM if AB=s (source diameter). OM=SDD (source to diaphragm distance) OF=SSD (source to skin or surface distance) then, from the above equation, the geometric penumbra DE at depth d is given by

$P_d = s(SSD + d\text{-}SDD)/SDD.$

The penumbra at the surface can be calculated by putting d = 0.

The penumbra width increases with increase in source diameter, SSD and depth but decreases with an increase with an increase in SDD. The geometric penumbra is however, independent of the field size as long as the movement of the diaphragm is in one plane i.e. SSD stays constant with increase in field size.

4.3 Ion Chamber and Dosimetry

Farmer ion-chamber of volume 0.6cc type 31005 along with an electrometer PTW UNIDOS. A thermometer and a barometer were used as a dosimetry system for the necessary air pressure and temperature.

The characteristics of the used ion chambers were as follows:

Volume	0.6 cc
Useful range	30KeV - 50 MeV
Response Leakage	1×10^{-8} C/Gy
Leakage	$\pm 4.10^{-15}$ A
Polarizing voltage	Max. 500 V
Cable leakage	1×10^{-12} C/Gy-cm
Wall material	PMMA [(C_5,H_8O_2)+ Graphite]
Wall thickness	0.55 mm PMMA +0.15 mm C
Wall material's density	1.19 g/cc [PMMA] and 0.82 g/cc C.
Area density	78 mg/cm^2
Electrode	Aluminium, Graphite coated
Width	1.5 mm
Long	14.25 mm
Range of temp.	+10 - +40 degree Celsius
In collection time	0.06 ms at 500 V biasing
Relative Humidity	10% - 80%

They were calibrated in German SSDL which were traceable to PSDL. The calibration was performed at the ambient conditions of **20** degree Celsius and pressure **1008** mbar[43].

4.4 Physical Characteristics of Dosimetry System

The PTW UNIDOS with plug system "BNT" is a microprocessor controlled universal field class dosimeter for measurement of dose and dose rate in radiation therapy, diagnostic x-ray and radiation protection purposes. This UNIDOS is internationally familiarly classified as class1, type B equipment in the field of radiation dose measurement. The UNIDOS provide several measuring modes like measurement of current and charge in electrical units (Amp C), measurement of radiological quantities as exposure in R, photon equivalent dose H_x in S_v, air kerma K_a and absorbed dose to water D_w in G_y. This UNIDOS can measure radiation doses in radiation therapy up to 3 MG_y as well as the dose of very short x-ray exposures in the range of millisecond. It is prepared for measuring radiation doses with ionization chambers, semiconductor probes and other solid state probes (e.g. diamond detector). This

UNIDOS stores the type and serial number for each ion chamber in a non volatile memory, together with the individual calibration factors and other factors specific for the chamber and the user can not change calibration factors in the case of officially calibrated chambers. In dose rate mode, dose measurement is performed by numerical integration of the current. The maximum integration time is 18 hrs and the maximum measuring value is 3 MGy. The offset current of UNIDOS without a chamber and or detector is less than $\pm 10^{-15}$ A. In the case of charge measurement, the drift is less than $\pm 6.10^{-14}$C with in the measuring time of 1 min.

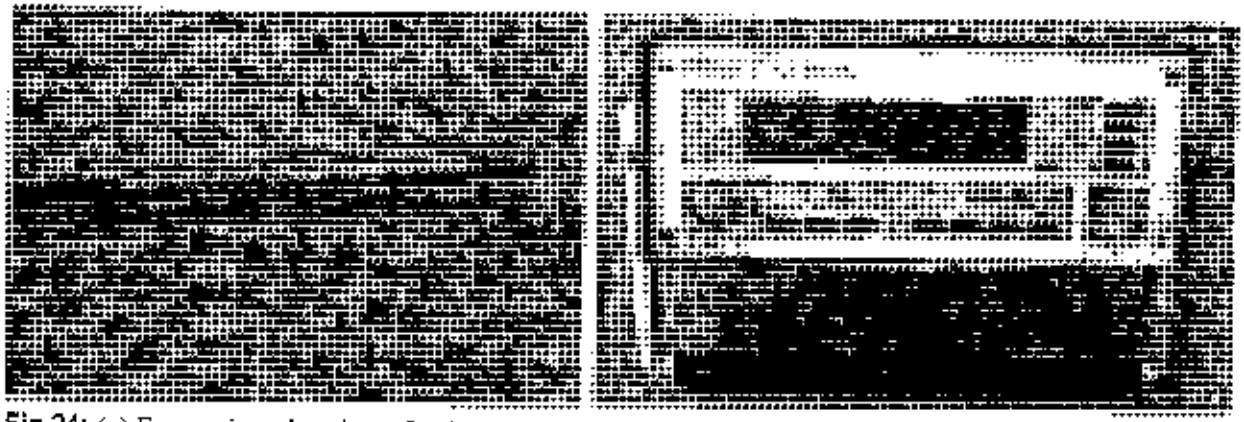

Fig.24: (a) Farmer ion-chamber of volume 0.6cc (b) PTW UNIDOS Electrometer

4.5 Experimental Method

For investigation of photon doses in different irregular fields, which are often encountered in daily radiotherapy practices, a tissue equivalent solid phantom in slab form of dimension 40cm×40cm×10cm was used. The phantom is made of Perspex ($C_5H_8O_2$; ρ=1.190g/cm^3) sheets with average thickness of 2.0 cm, which is also known as Acrylic sheet. Routine therapy application procedures which were traceable to international norms for radiotherapy practices were followed during dose determination in solid phantoms for ^{60}Co teletherapy unit. Photon doses were investigated at 0.5 cm depth of the phantom at different interested points with 0.6cc Farmer type ionization chamber integrated with PTW UNIDOS dosimeter. The simulated irregular fields with interested points of dose investigations have shown in appendix-2. In each field, the interested points of dose investigations were labeled with numericals 1,2,3,4,5 ---- etc.

During dose investigation, the field was modified according to the simulated irregular fields with beam modifying blocks and under this conditions doses were measured at different interested points and then blocks were removed very carefully making the fields open and doses were investigated in those points to see, if there was any difference between the two measurements (Modified & open fields). For the calculation of dose at a point 'p' (say) in Clarkson's method radii were drawn from point 'p' (say) to divide the field into an equal interval of sector angle10^0. In this study we calculated the dose of blocked beams with two correction factors C'_{psk} and CF_t by using Empirical relation

$$D_{W(Irregular)} = (OFD) \times C'_{psk} \times CF_t \times K_{IF}$$

Where *(OFD) =Open Field Dose rate*

4.6 Investigation of Beam Profile for Reference Data

To check the beam profile and thereby establishing the dose symmetry and uniformity, doses were measured in open field of size 5×5cm^2, 10×10cm^2, 15×15cm^2, 20×20cm^2, 25×25cm^2, 30×30cm^2 at depth 0.5 cm and SSD at 80 cm across the major axes (x,y-axis). The field sizes and dimensions of the solid phantom were made with a margin of 10 cm in all sides having a margin of 5.0 cm beyond the dose measurement surface. The doses were

measured at 1.0 cm increments from centre of the field to either edges extending 5 cm beyond different specified field sizes with a view to observe the penumbra regions on each axis. The dose at the centre of the field is termed as the central axis dose and doses in other points were expressed as percentage to this central axis dose. Beam alignment and positions like rotation axis, geometric axis, radiation axis and light beam axis were carefully checked and apparently coincided and corrected where needed during dose investigations. The beam profile data are shown in Table: 1&2. Their graphical presentations are shown in fig.25&26. This open field dosimetric scan-data were being preserved and considered as reference data during dosimetry for all irregular fields.

Table 1: Data for beam profile of open field along lateral axis (X-axis) of 10×10 cm^2 field size at d_{max}.

Locations X+	cGy/min	% to central axis dose	Locations X-	cGy/min	% to central axis dose
0	61.36	100			
1	61.31	99.9	1	61.31	99.9
2	61.20	99.7	2	61.10	99.6
3	60.95	99.3	3	60.75	99.0
4	59.19	96 5	4	56.76	92.5
5	32.78	53.4	5	24.26	39.5
6	4 75	7.74	6	3.24	5.28
7	1.78	2.90	7	1.66	2.71
8	1.09	1.77	8	1.09	1.78
9	0.81	1.32	9	0.83	1.36
10	0.64	1.04	10	0.66	1.07
11	0.53	0.86	11	0.53	0.87
12	0.45	0.73	12	0.45	0.74
13	0.39	0.64	13	0.39	0.64
14	0.37	0.60	14	0.37	0.59
15	0.37	0.59	15	0.35	0.57

Table 2: Data for beam profile of open field along vertical axis (Y-axis) of 10×10 cm^2 field size at d_{max}.

Locations Y+	cGy/min	% to central axis dose	Locations Y-	cGy/min	% to central axis dose
0	61.66	100			
1	61.60	99.9	1	61.54	99.80
2	61.48	99.7	2	61.41	99.60
3	61.23	99.3	3	61.11	99.10
4	59.56	96.6	4	59.38	96.30
5	33.05	53.6	5	32.99	53.50
6	4.90	7.94	6	4.80	7.78
7	1.90	3.08	7	1.81	2.94
8	1.09	1.77	8	0.99	1.62
9	0.81	1.32	9	0.76	1.23
10	0.64	1.04	10	0.62	1.00
11	0.53	0.86	11	0.50	0.80
12	0.45	0.73	12	0.44	0.71
13	0.39	0.64	13	0.35	0.56
14	0.37	0.60	14	0.36	0.59
15	0.36	0.59	15	0.36	0.58

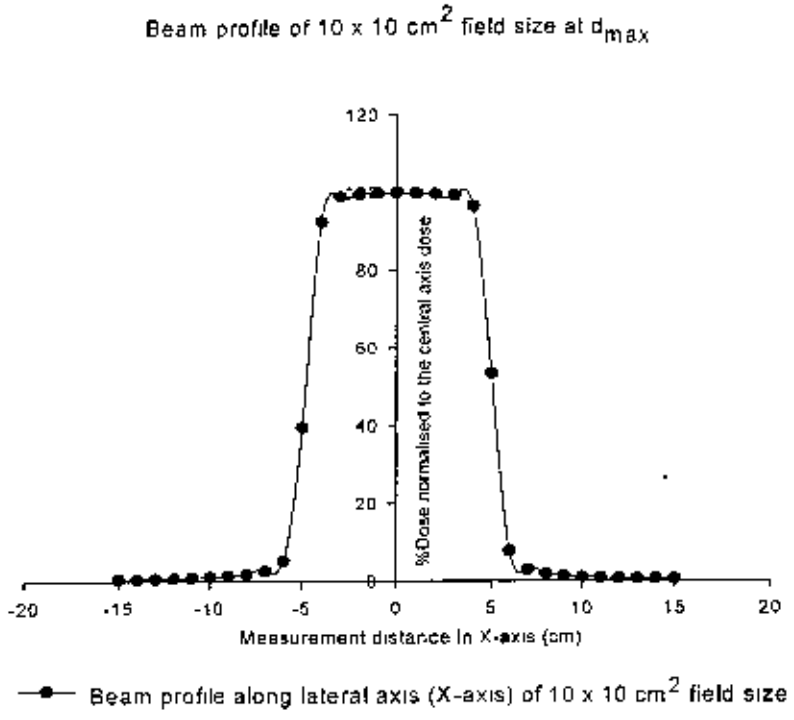

Fig.25: Beam profile along X-axis of ^{60}Co unit.

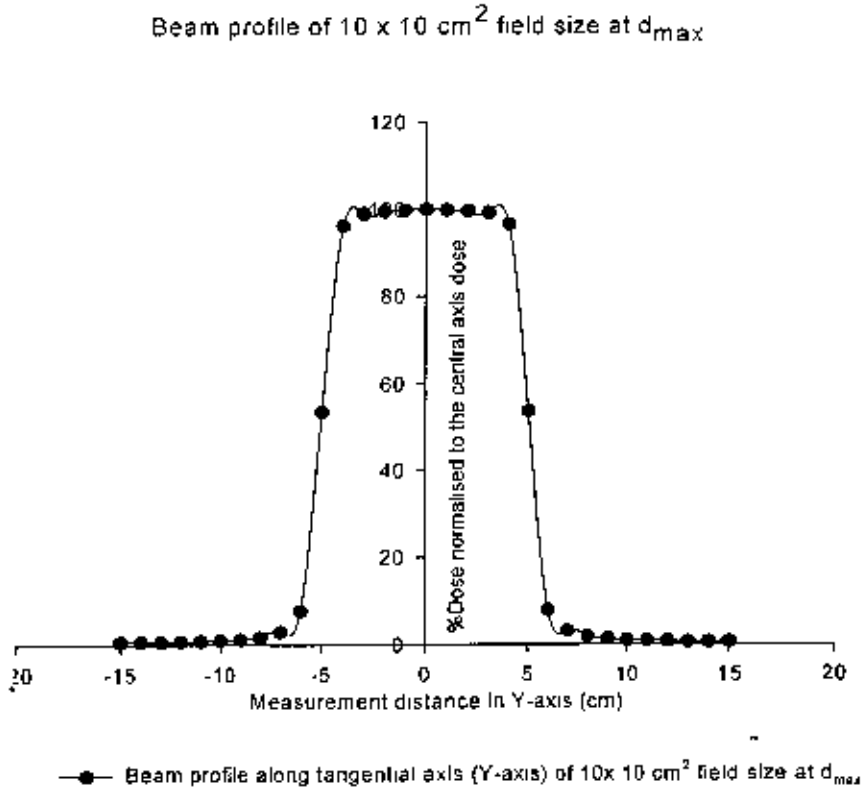

Fig.26: Beam profile along Y-axis of ^{60}Co unit.

4.7 Dose Investigation Technique

The beam modifying lead blocks were of 5 cm thick and most of these were comparatively heavier . These blocks were very narrowly fit into the available shadow tray of ^{60}C0 unit (Alcyon II#90106, France). During dose measurement, ion chamber was aligned in such way that the radiation fluence is assumed to be uniform over the cross-section of the chamber and beam was perpendicular to the chamber's axis. The Dosimeter connected with this ion chamber was PTW UNIDOS, which was very sensitive and was calibrated with ion chamber as its integral part. Block supporting tray was kept in the same position during dose measurement both in open and modified fields so that no correction factor regarding tray was needed in data presentation.

In each simulated irregular fields on solid phantoms, different interested points were designated as 1, 2, 3, 4, 5... etc. for investigation of doses at those points. Similar geometry was maintained during investigation of doses in both open and modified irregular fields. The open fields of the corresponding irregular fields were of the same dimensions. The beam modifying blocks were placed very carefully so that it clearly blocks the photon beam to the area supposed to be shielded in the simulated irregular fields in the phantoms. The doses were investigated at 0.5 cm depth with source to surface distance (SSD) 80 cm and the ion chamber was placed perpendicularly to the central axis of the photon beam. Doses at the interested points in the irregular fields (blocked beams) were investigated 1st and recorded. The beam modifying blocks were then carefully removed from supporting tray making the fields open and doses were again measured at the same corresponding points keeping all measurement conditions symmetrical in both open and blocked fields and recorded for comparison. The doses were relative and have been presented as directly measured values in cGy/min for ^{60}Co and finally comparison with other calculation techniques were made.

4.8 Dose Investigation for Photon Beam of ^{60}co Unit

The doses were measured at 0.5 depth of the solid phantom on which the irregular fields were simulated. Different interested points were being designated by numericals 1,2,3,4,5.. .....etc. along long axis for the investigation of doses at those points Ion chamber was placed at those points in such a way that the radiation fluence is assumed to be uniform

over the cross section of the chamber and ion chamber's axis remains always perpendicular to the photon beam. Similar geometry was maintained during investigation of doses in both open and modified irregular fields. The open fields of the corresponding irregular fields were of same dimensions. The beam modifying blocks were placed very carefully so that it clearly blocks the photon beam to the area supposed to be shielded in the simulated irregular fields in the phantoms. The doses were investigated at 0.5 cm depth with source to surface distance (SSD) 80 cm and the ion chamber was placed perpendicularly to the central axis of the photon beam. Doses at the interested points in the interested points in the irregular fields (blocked fields) were investigated 1st and recorded. The beam modifying blocks were then carefully removed from the supporting tray making the fields open and doses were again measured at the same corresponding points keeping all measurement conditions symmetrical in both open and blocked fields and recorded for comparison were relative and have been presented as directly measured values in mGy/min later converted into cGy/min for ^{60}Co and finally comparison with other calculation technique(Clarkson's method) was made. The Dosimeter connected with this chamber was PTW UNIDOS which were very sensitive and was calibrated with ion chamber as its integral part. Block supporting tray was kept in the same position during dose measurement in open field so correction factor regarding tray was needed in data presentation. The beam modifying blocks were placed at 60 cm above the phantom surface using a block supporting tray made of acrylic sheet having thickness of 1.5 cm. The dose measurements were carried out with the following settings: For ^{60}Co, SSD was 80 cm. focus to diaphragm distance(FDD) = 45 cm, Diaphragm-phantom surface distance = 35 cm, focus to shadow tray distance (FSTD) = 52 cm, shadow tray to surface distance (STSD) = 28 cm, shadow tray thickness = 1.5 cm. block thickness = 5.1 cm. Doses were measured at 0.5 cm with 0.6 cc ion chamber integrated with PTW UNIDOS.

The exposure Roentgen (X) were obtained by using the formula

$$X = M.N_x.C_{t,p}.C_s.C_{st} \qquad \text{----------(52)}$$

where M is the monitor reading and N_x is the chamber calibration factor. $C_{t,p}$ is the correction factor for temperature and pressure, C_s is the correction factor for ion recombination and C_{st} is the stem leakage correction factor However, in our present work, $C_{t,p}$ were considered but for the sake of simplicity C_s and C_{st} were ignored considering very

little variation. The exposure roentgens (X) were obtained as R(X) min in the case of ^{60}Co. Finally the doses were converted to absorbed dose in Medium as mGy/min for ^{60}Co by using the formula

$$D_{med} = f_{med} X(R) \qquad \text{----------(53)}$$

where the quantity $f_{med} = 0.875 \left[\frac{\left(\frac{\overline{\mu}_{en}}{\rho} \right)_{med}}{\left(\frac{\overline{\mu}_{en}}{\rho} \right)_{air}} \right]$ is the factor which is sometimes called the roentgen to rad conversion factor. The experimental arrangement for investigation of doses at different interested points both in open (regular) and blocked (irregular) fields are shown in fig. 27. The procedure of lead block setting into the block supporting tray is shown in fig.28.

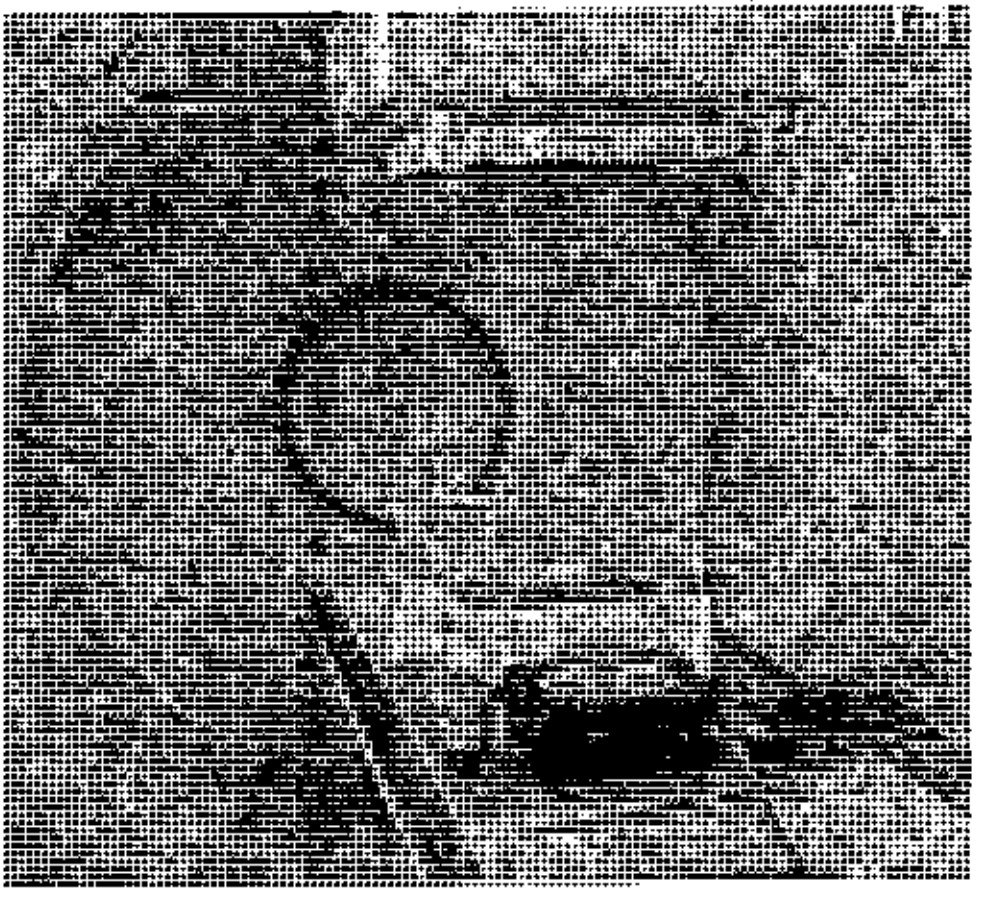

Fig.27: Experimental arrangement for dose measurement of ^{60}Co unit

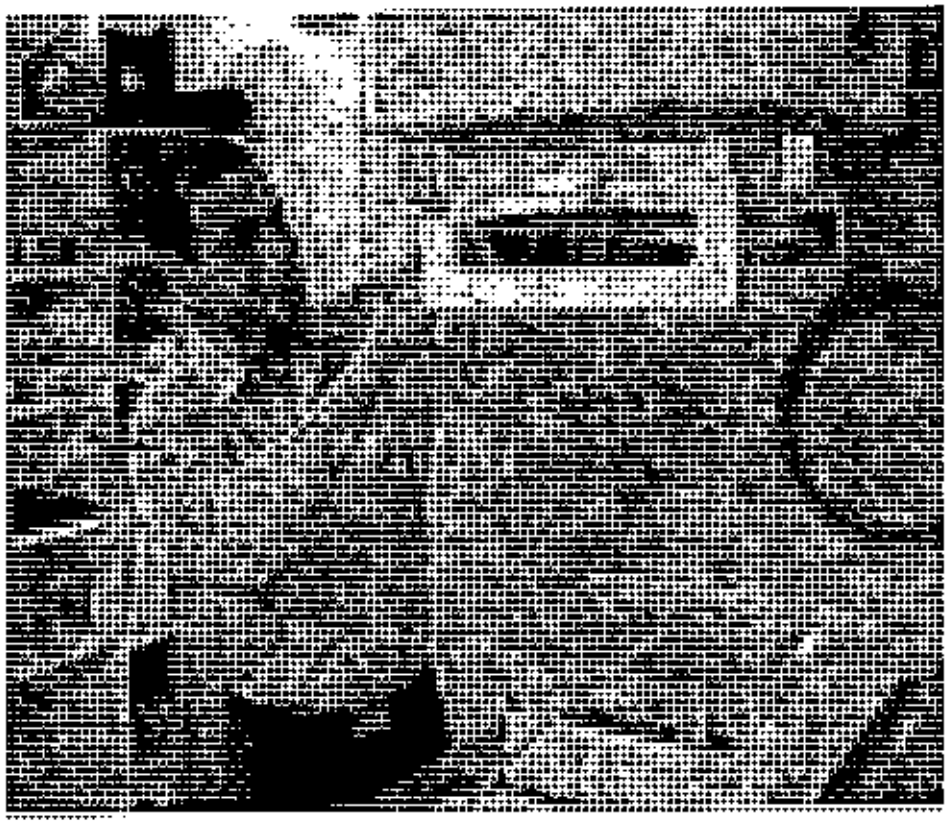

Fig.28: ^{60}Co teletherapy head with mantle block into block supporting tray

These dosimetric arrangements were easily reproducible and kept constant throughout the entire dose measurements both in open (regular) and blocked (irregular) fields. The observed doses in different open (regular) and blocked (irregular) fields are presented in Table-3(I-XI) along with the corresponding fields and graphical representations.

Cornea Block

Table 3(i) : ^{60}Co-beam: Field type- Square, Field size: 5x5 cm^2,SSD = 80cm,Depth=0.5cm

Points along X-axis	Dose measured with 0.6 cc Farmer type ion chamber in cGy/min				Calculated dose in cGy/min (Clarckson's method)		Calculated dose in cGy/min (Empirical relation)		Correction Factor C'_{jrk}	Correction Factor CF_r
	Blocked beam's dose D_{Bw}	%to central axis dose in open beam	Open beam's dose, D_{ow}	%difference between blocked & open beam	Calculated dose, D_{Calw}	%difference between D_{Calw} &D_{Bw}	Calculated dose, D_{Emw}	%difference between D_{Calw} & D_{Emw}		
1	36.439	65.719	55.446	34.280	36.419	0.055	36.439	0.055	0.69598462	1.00055885
2	51.947	93.689	55.414	6.257	51.469	0.920	51.948	0.920	0.98415610	1.00927739
3	44.969	81.104	48.468	7.254	44.520	0.998	44.969	0.998	0.97328199	1.01007257

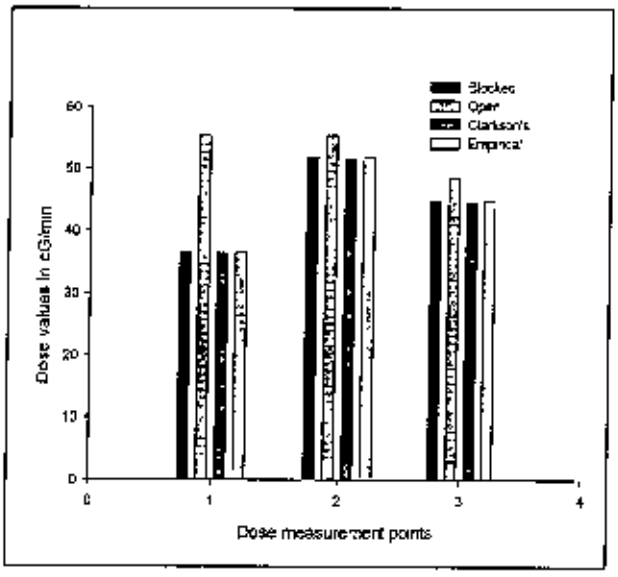

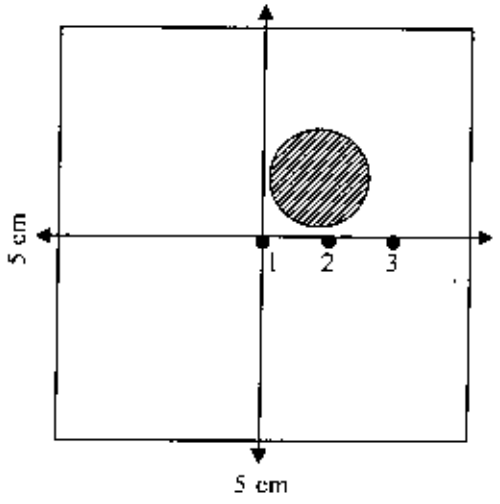

3 (i) : Cornea Block

Double Cornea Block

Table 3(II) : ^{60}Co-beam: Field type. Square, Field size: 5x5 cm^2,SSD = 80 cm, Depth= 0.5 cm

Points along X-axis	Dose measured with 0.6 cc Farmer type ion chamber in cGy/min				Calculated dose in cGy/min (Clarkson's method)		Calculated dose in cGy/min (Empirical relation)		Correction Factor $C'_{\mu\nu k}$	Correction Factor CF_r
	Blocked beam's dose, $D_{B,W}$	%to central axis dose in open beam	Open beam's dose, $D_{o,w}$	%difference between blocked & open beam	Calculated dose, $D_{Cal\,W}$	%difference between $D_{Cal\,W}$ &$D_{F\,W}$	Calculated dose, $D_{Em\,W}$	%difference between $D_{Cal\,W}$ & $D_{F\,W}$		
1	36.472	65.779	55.446	34.220	36.382	0.25	36.464	0.22	0.69526888	1.00248202
2	50.502	91.083	55.414	8.864	50.014	0.97	50.502	0.97	0.95632437	1.00976612
3	45.472	82.011	48.469	6.183	45.009	1.02	45.472	1.03	0.983977401	1.01027107

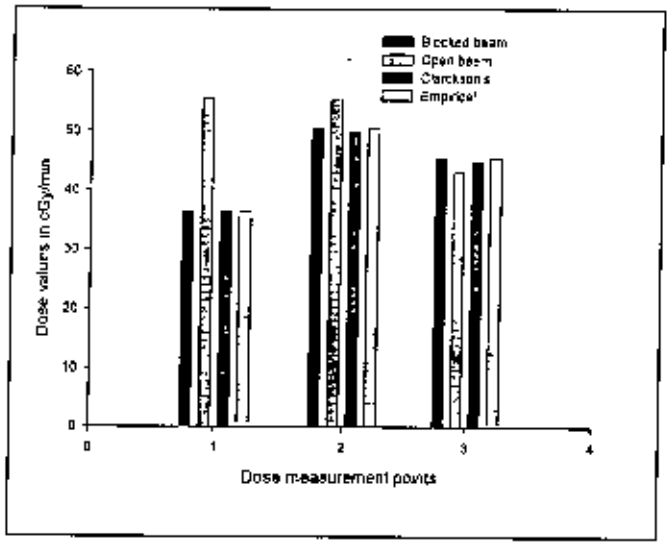

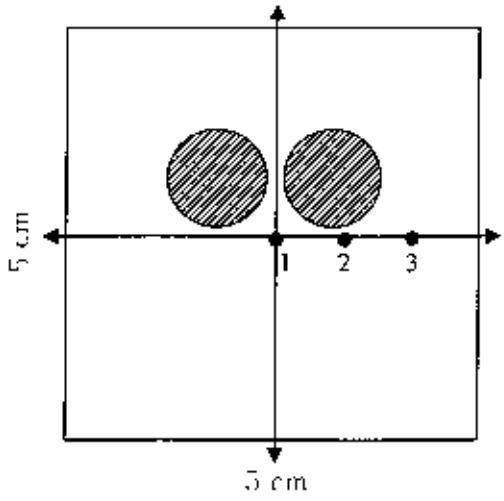

3 (ii) : Double Cornea Block

Corner Block

Table 3(III) : ^{60}Co-beam: Field type: Square, Field size: 10x10 cm^2,SSD = 80cm,Depth=0.5cm

Points along X-axis	Dose measured with 0 6 cc Farmer type ion chamber in cGy/min				Calculated dose in cGy/min (Clarekson's method)		Calculated dose in cGy/min (Empirical relation)		Correction Factor C_{yrk}	Correction Factor CF_i
	Blocked beam's dose, D_{BW}	%to central axis dose in open beam	Open beam's dose, D_{OW}	%difference between blocked & open beam	Calculated dose D_{CalW}	%difference between D_{CalW} &D_{BW}	Calculated dose, D_{EmW}	%difference between D_{CalW} & D_{EmW}		
1	56 203	91 597	61.364	8 410	57 864	2 87	56.203	2 87	1 01652719	0 97128459
2	56 192	91.572	61 309	8 346	57 712	2 63	56 192	2 63	1 01475415	0 97365784
3	56 181	91 554	61 290	8 201	57.763	2 74	56 181	2 74	1 01745024	0.97261559
4	55 942	91 164	60 949	8.209	57.452	2 63	55.942	2 63	1 01613887	0 97370340
5	54 298	88 485	59 186	8 259	55 765	2 63	54 298	2.63	1 01568387	0 97368871
6	23 855	38 875	32 783	27.234	24 723	3.51	23 855	3 51	0 81295332	0 96490567

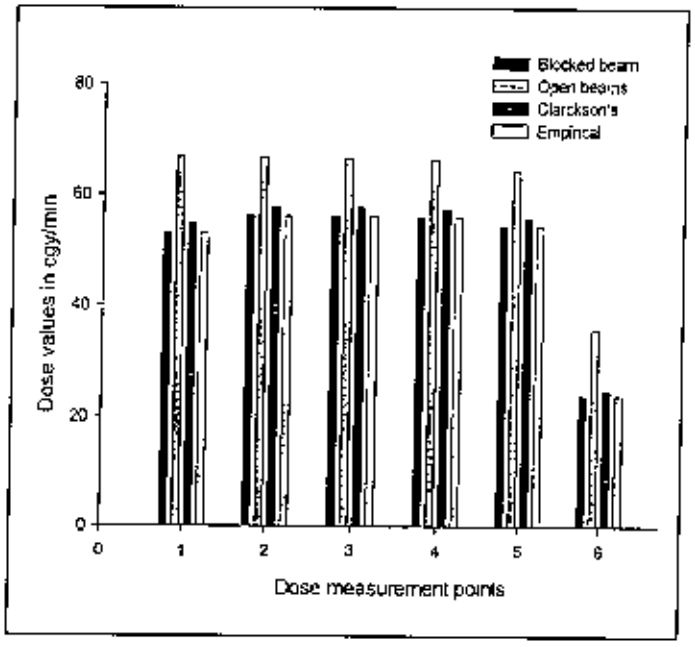

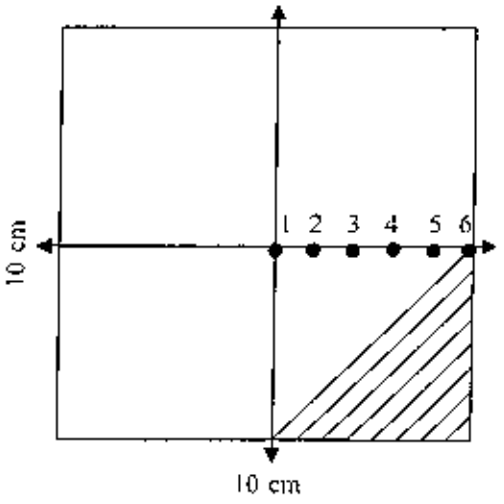

3 (iii) : Corner Block

Half Beam Device

Table 3(IV) : ^{60}Co-beam: Field type: Square. Field size: 15x15 cm^2,SSD=80 cm, Depth=0.5 cm

Points along X-axis	Dose measured with 0.6 cc Farmer type ion chamber in cGy/min				Calculated dose in cGy/min (Clarekson's method)		Calculated dose in cGy/min (Empirical relation)		Correction Factor C'_{fsk}	Correction Factor CF_i
	Blocked beam's dose, $D_{B,w}$	%to central axis dose in open beam	Open beam's dose, $D_{o,w}$	%difference between blocked & open beam	Calculated dose $D_{Cal\,w}$	%difference between $D_{Cal\,w}$ &$D_{B,w}$	Calculated dose, $D_{Em,w}$	%difference between $D_{Cal\,w}$ & $D_{Em,w}$		
1	32.356	50.441	64.146	49.56	33.571	3.62	32.356	3.62	0.58159567	0.96381409
2	32.575	50.783	64.135	49.21	33.936	4.02	32.572	4.01	0.58802277	0.95982685
3	32.529	50.711	64.022	49.19	34.145	4.74	32.527	4.74	0.59278553	0.95263673
4	32.494	50.656	63.831	49.09	34.174	4.91	32.494	4.92	0.59496501	0.95083397
5	32.391	50.496	63.798	49.23	31.219	5.37	32.382	5.37	0.59605358	0.94631559
6	32.218	50.226	63.079	48.92	34.142	5.63	32.218	5.64	0.60148879	0.94364663

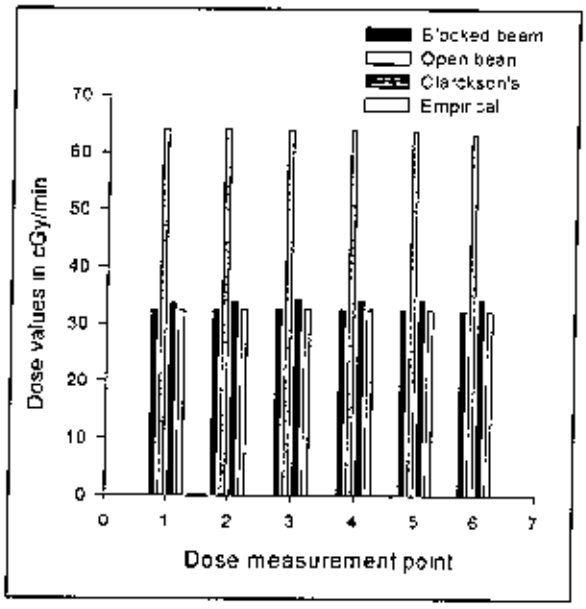

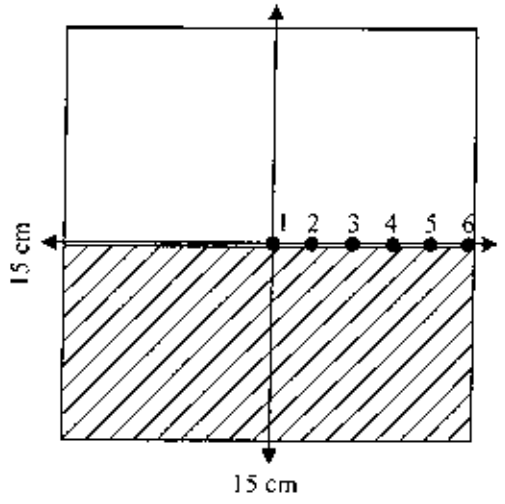

3 (iv) : Half Beam Device

Corner Block

Table 3 (V) : ^{60}Co-beam:Field type: Square, Field size:15x15cm^2, SSD=80cm, Depth=0.5 cm

Points along X-axis	Dose measured with 0.6 cc Farmer type ion chamber in cGy/min				Calculated dose in cGy/min (Clarckson's method)		Calculated dose in cGy/min (Empirical relation)		Correction Factor $C'_{\mu,w}$	Correction Factor CF_r
	Blocked beam's dose $D_{F,w}$	%to central axis dose in open beam	Open beam's dose, $D_{o,w}$	%difference between blocked & open beam	Calculated dose $D_{Cal,w}$	%difference between $D_{Cal,w}$ &$D_{F,w}$	Calculated dose, $D_{Em,w}$	%difference between $D_{Cal,w}$ & $D_{Em,w}$		
1	61.643	96.098	61.146	2.50	63.369	2.72	61.643	2.72	1.21190144	0.97276064
2	61.699	96.185	64.135	2.44	63.370	2.74	61.632	2.74	1.09980556	0.97256203
3	61.609	96.045	64.022	2.41	63.372	2.78	61.609	2.78	1.10020951	0.97217558
4	61.429	95.764	63.831	2.40	63.063	2.59	61.429	2.59	1.09791065	0.97410373
5	61.138	95.311	63.798	2.66	62.675	2.45	61.138	2.45	1.09174404	0.97546701
6	60.801	94.785	63.079	2.28	62.172	2.20	60.801	2.21	1.09530558	0.97795242

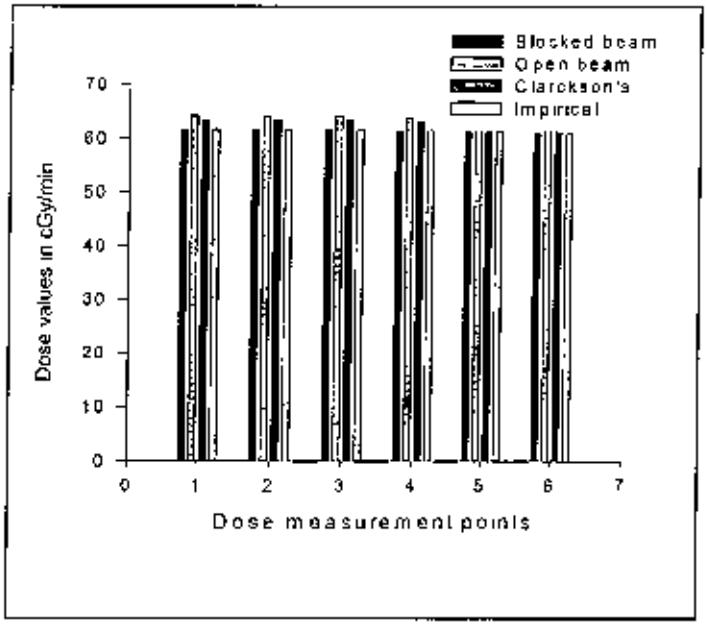

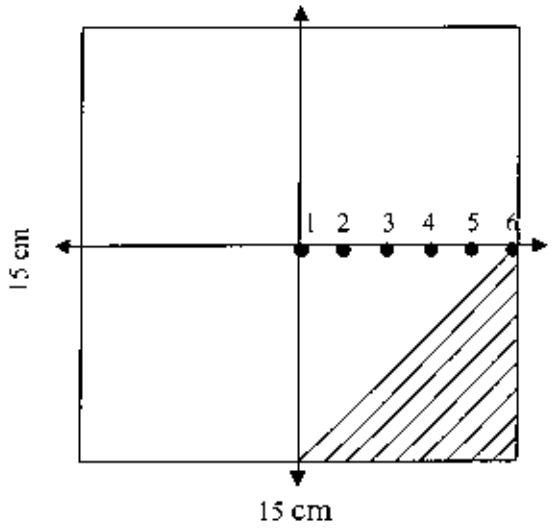

3 (v) : Corner Block

Rectangular Block

Table 3 (VI) : ^{60}Co-beam: Field type : Square, Field size: 15x15 cm^2 SSD=80cm, Depth=0.5cm

Points along X-axis	Dose measured with 0 6 cc Farmer type ion chamber in cGy/min %difference between blocked & open beam				Calculated dose in cGy/min (Clarckson s method) Calculated dose $D_{Cal\,w}$		Calculated dose in cGy/min (Empirical relation)		Correction Factor C'_{jck}	Correction Factor CF_r
	Blocked beam's dose, D_{Bw}	%to central axis dose in open beam	Open beam s dose, D_{ow}	%difference between blocked & open beam	Calculated dose, $D_{Cal\,w}$	%difference between $D_{Cal\,w}$ &D_{Bw}	Calculated dose $D_{Em\,w}$	%difference between $D_{Cal\,w}$ & $D_{Em\,w}$		
1	61 126	95 292	64 146	3 02	62 286	1 86	61 127	1 861	1 079081858	0 98138741
2	61 362	95 659	64 135	2 77	62 559	1 91	61 362	1.913	1 083991981	0 98087083
3	61 328	95 607	64,022	2 69	62 459	1 81	61 329	1.809	1 084351347	0 98190165
4	61 205	95 415	63 831	2 63	62 312	1 78	61 205	1 777	1.084840952	0 98223665
5	60 969	95 047	63 798	2 85	62 082	1 79	60 969	1 793	1 081408216	0 98207893
6	60 520	94 347	63 079	2 56	61,423	1 47	60 520	1 470	1 082118437	0 98530135

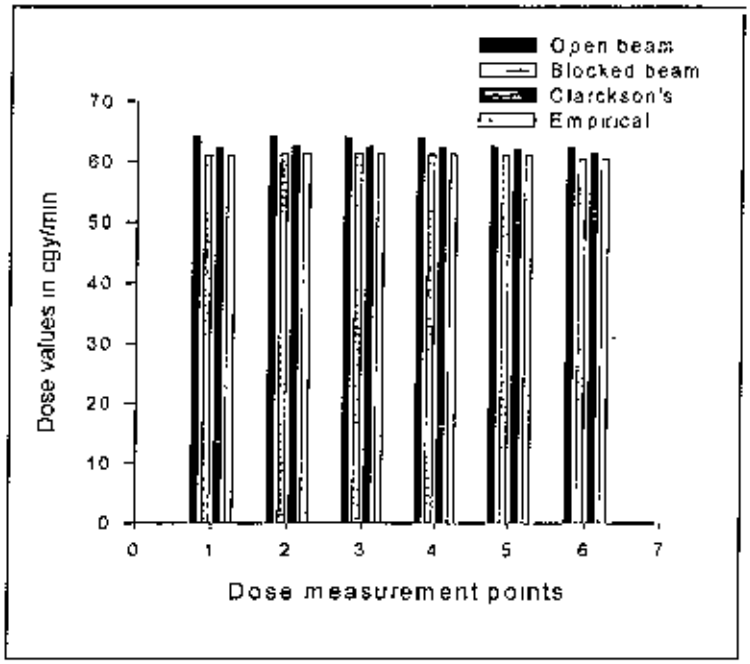

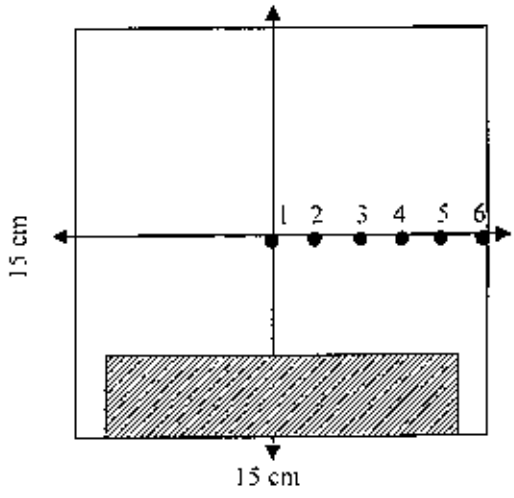

3 (vi) : Rectangular block

Irregular Shaped Block

Table 3 (VII) : ^{60}Co-beam:Field type: Square, Field size:15x15cm^2, SSD=80cm, Depth=0.5 cm

Points along X-axis	Dose measured with 0.6 cc Farmer type ion chamber in cGy/min				Calculated dose in cGy/min (Clarekson's method)		Calculated dose in cGy/min (Empirical relation)		Correction Factor C_{pq}	Correction Factor CF_i
	Blocked beam's dose, D_{Bw}	%to central axis dose in open beam	Open beam's dose, D_{ow}	%difference between blocked & open beam	Calculated dose, $D_{Cal\,w}$	%difference between $D_{Cal\,w}$ & D_{Bw}	Calculated dose $D_{Em\,w}$	%difference between $D_{Cal\,w}$ & $D_{Em\,w}$		
1	58.534	91.251	64.146	8.75	58.827	0.49	58.534	0.49	1.01914843	0.99501758
2	58.567	91.303	64.135	8.68	58.842	0.47	58.567	0.47	1.01959424	0.99532988
3	58.422	91.077	64.022	8.75	58.697	0.47	58.421	0.47	1.01903079	0.99531411
4	58.242	90.796	63.831	8.76	58.516	0.47	58.242	0.47	1.01876362	0.99531358
5	57.973	90.377	63.798	9.13	58.252	0.48	57.973	0.48	1.01469552	0.99520172
6	57.445	89.554	63.079	8.93	57.719	0.47	57.445	0.47	1.01685429	0.99525630

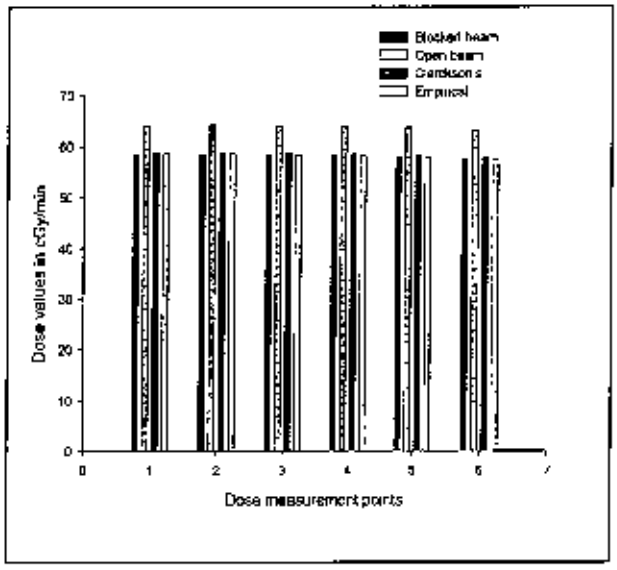

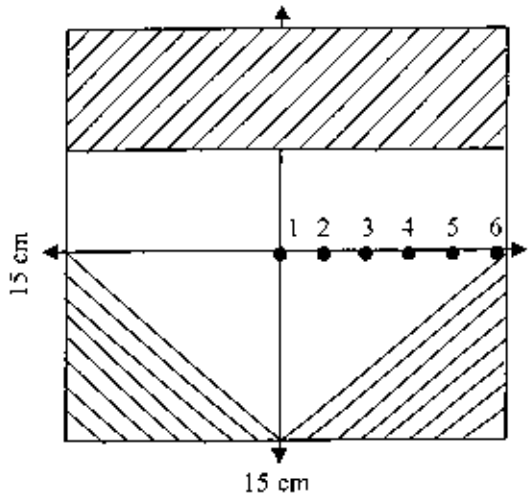

3 (vii) : Irregular shaped Block (Rectangular + Double Corner Block)

Double Corner Block

Table 3 (VIII) : ^{60}Co-beam Field type: Square, Field size: 20x20 cm^2,SSD=80cm, Depth=0.5cm

Points along X-axis	Dose measured with 0.6 cc Farmer type ion chamber in cGy/min				Calculated dose in cGy/min (Clarkson's method)		Calculated dose in cGy/min (Empirical relation)		Correction Factor $C'_{\mu l}$	Correction Factor CF_t
	Blocked beam's dose, D_{Ew}	%to central axis dose in open beam	Open beam's dose, D_{ow}	%difference between blocked & open beam	Calculated dose $D_{Cal\,w}$	%difference between $D_{Cal\,w}$ &D_{Ew}	Calculated dose, $D_{Em\,w}$	%difference between $D_{Cal\,w}$ & $D_{Em\,w}$		
1	61.982	91.078	68.054	8.92	63.983	3.13	61.982	3.13	1.05459794	0.96872360
2	61.993	91.094	68.020	8.86	63.993	3.13	61.993	3.13	1.05528721	0.96875229
3	61.971	91.062	67.998	8.86	63.969	3.12	61.971	3.12	1.05525447	0.96875094
4	61.778	90.778	67.805	8.88	63.772	3.13	61.778	3.13	1.05497531	0.96873865
5	61.586	90.496	67.522	8.79	63.569	3.12	61.586	3.12	1.05604968	0.96878419
6	61.167	89.880	67.182	8.95	63.142	3.13	61.166	3.13	1.05424817	0.96870921

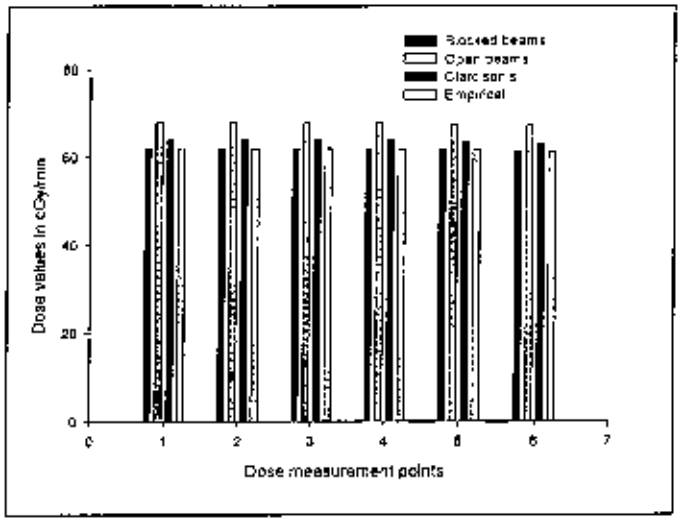

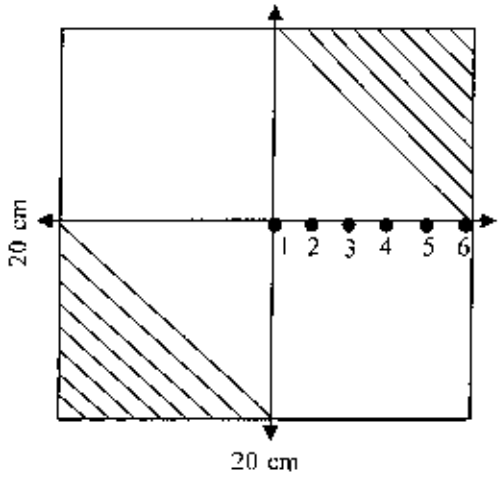

3 (viii) : Double Corner Block

Irregular Shaped Block

Table 3 (IX) : ^{60}Co-beam: Field type: Square, Field size: 25x25 cm^2,SSD=80cm, Depth=0.5cm

Points along X-axis	Dose measured with 0.6 cc Farmer type ion chamber in cGy/min				Calculated dose in cGy/min (Clarkson's method)		Calculated dose in cGy/min (Empirical relation)		Correction Factor C_{rck}	Correction Factor CF_r
	Blocked beam's dose, D_{Bw}	%to central axis dose in open beam	Open beam's dose, D_{ow}	%difference between blocked & open beam	Calculated dose D_{Clw}	%difference between D_{Clw} & D_{Bw}	Calculated dose D_{Emw}	%difference between D_{Clw} & D_{Emw}		
1	63.787	91.140	69.682	8.45	65.596	2.76	63.787	2.76	1.06277919	0.97242511
2	63.764	91.507	69.682	8.49	65.629	2.76	63.821	2.75	1.06332511	0.97244639
3	63.776	91.524	69.602	8.37	65.582	2.75	63.776	2.75	1.06376438	0.97246413
4	63.684	91.392	69.454	8.31	65.486	2.75	63.684	2.75	1.06447853	0.97249175
5	63.491	91.115	69.249	8.31	65.287	2.75	63.491	2.75	1.06438783	0.97248904
6	63.251	90.771	68.998	8.33	65.041	2.75	63.251	2.75	1.06423541	0.97248238

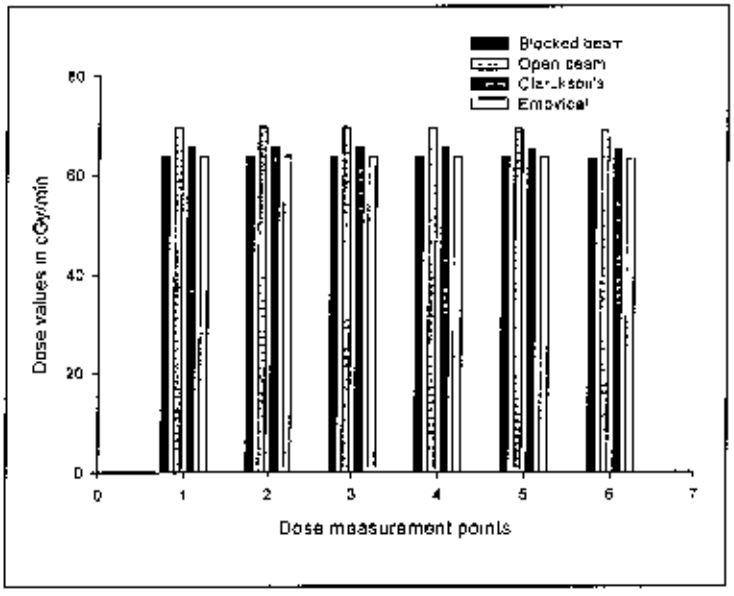

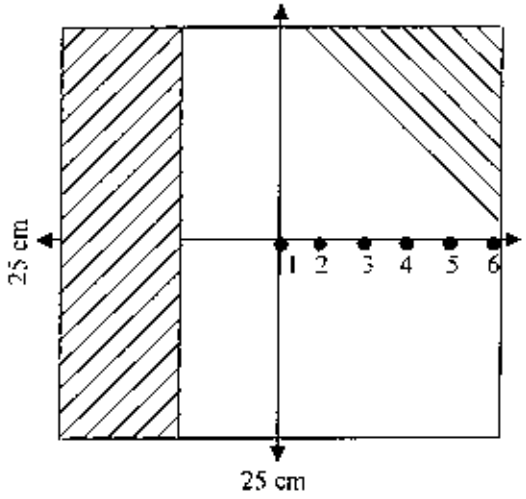

3 (ix) : Irregular shaped Block (Rectangular + Corner Block)

Inverted-Y Block

Table 3 (X) : ^{60}Co-beam: Field type. Square, Field size. 25x25 cm^2,SSD=80cm, Depth=0.5cm

Points along X-axis	Dose measured with 0 6 cc Farmer type ion chamber in cGy/min				Calculated dose in cGy/min (Clarekson's method)		Calculated dose in cGy/min (Empirical relation)		Correction Factor $C'_{,ch}$	Correction Factor CF_r
	Blocked beam's dose, $D_{L,w}$	%to central axis dose in open beam	Open beam's dose, $D_{o,w}$	%difference between blocked & open beam	Calculated dose, $D_{Cal,w}$	%difference between $D_{cal,w}$ &$D_{F,w}$	Calculated dose, $D_{Em,w}$	%difference between $D_{Cal,w}$ & $D_{Em,w}$		
1	57 185	82 066	69.682	17.934	59 833	4 43	57 185	4 43	0 96940299	0 95574752
2	52 419	75 226	69.682	24 774	54 819	4 38	52 419	4 38	0 88818314	0 95619997
3	42 475	60 955	69 602	38 974	44 909	5 42	42 454	5 42	0 72809956	0 94579345
4	30 890	44 329	69 454	55 525	33 336	7 31	30 890	7 34	0 54187912	0 92663165
5	22 692	32 565	68 998	67 112	24.458	7 22	22.692	7 22	0 40019511	0 92777704
6	12 828	18 409	68 998	81 408	13 824	7 20	12 828	7 20	0 22619399	0 92796534

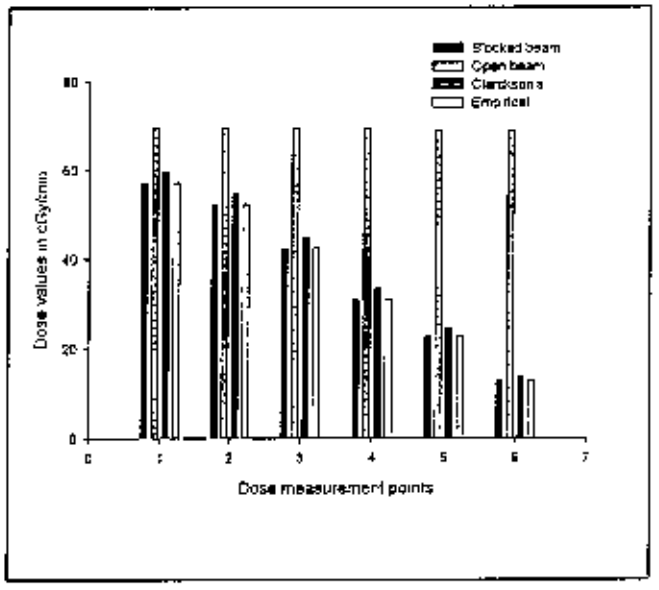

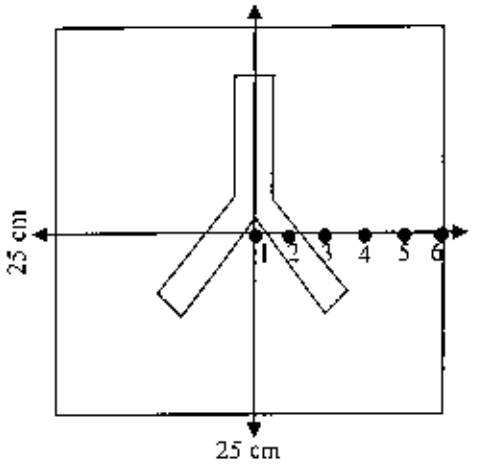

3 (x) : Inverted –Y Block

Mantle Block

Table 3 (XI) : ^{60}Co-beam:Field type: Square, Field size:30x30cm^2, SSD=80cm, Depth=0.5 cm

Points along X-axis	Dose measured with 0.6 cc Farmer type ion chamber in cGy/min				Calculated dose in cGy/min (Clarckson s method)		Calculated dose in cGy/min (Empirical relation)		Correction Factor C'_{jnk}	Correction Factor CF_j
	Blocked beam's dose, $D_{E,w}$	%to central axis dose in open beam	Open beam's dose, $D_{in,w}$	%difference between blocked & open beam	Calculated dose, $D_{Cal,w}$	%difference between $D_{Cal,w}$ & $D_{E,w}$	Calculated dose $D_{Em,w}$	%difference between $D_{Cal,w}$ & $D_{Em,w}$		
1	62.855	90.807	69.218	9.19	64.121	1.97	62.855	1.97	1.05022275	0.98025678
2	55.381	80.009	69.195	19.96	56.776	2.46	55.381	2.46	0.92977678	0.97542982
3	56.331	81.138	69.195	18.59	57.714	2.39	56.331	2.39	0.94512885	0.97604411
4	60.875	87.947	69.149	11.96	62.197	2.13	60.875	2.13	1.01921112	0.97875119
5	63.095	91.154	69.012	8.57	64.384	2.00	63.095	2.00	1.05714862	0.97999006
6	64.263	92.841	68.772	6.56	65.528	1.93	64.263	1.93	1.07970427	0.98068556

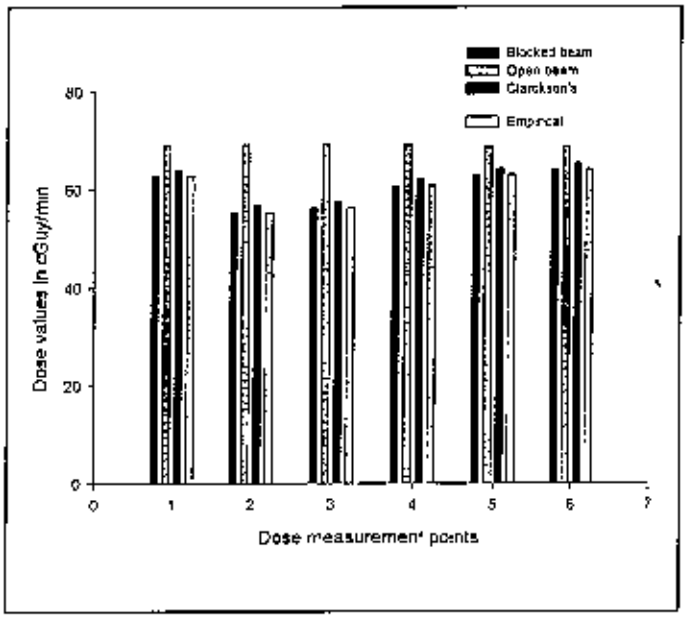

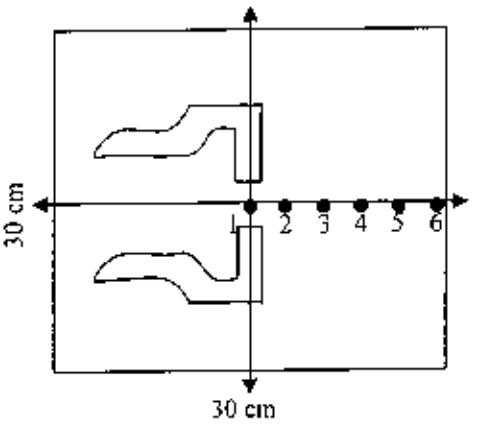

3 (xi) : Mantle Block

Chapter-V

Data Analysis

5.0 DATA ANALYSIS

In direct measurements the observed dosimeter (electrometer) reading from the ion chamber positioned at different interested points in irregular and open fields were corrected for obtaining the doses as roentgen/min for ^{60}Co by using the formula

$$X = M.N_x.C_{t,p}.C_r.C_{st} \qquad \text{--------- (54)}$$

Where M = Dosimeter reading

N_x = Chamber calibration factor for temperature and pressure

$C_{t,p}$ = Correction factor for temperature and pressure

C_r = Ion recombination correction factor and

C_{st} = Stem leakage correction factor

Since we were interested in relative dosimetry rather than absolute one, the observed data were corrected for temperature and pressure only while the other two correction factors were neglected for simplicity and assuming minor variations in the case of relative dosimetry system. The observed readings thus converted to roentgen (X)/min were again converted to absorbed dose in medium by using the following relationship:

$$D_{med} = X.f_{med}.A_{eq} \qquad \text{----------(55)}$$

Where X = Roentgen/min for ^{60}Co

f_{med} = f-factor or roentgen to rad conversion factor

$$= 0.876\left[\left(\frac{\overline{\mu_{en}}}{\rho}\right)_{med}\right] \Big/ \left[\left(\frac{\overline{\mu_{en}}}{\rho}\right)_{air}\right]$$

A_{eq} = Ratio of the energy fluence at the center of the equilibrium mass of tissue to that in free air at the same point.

However, the factor A_{eq}, which is very small, particularly in the case of ^{60}Co were ignored again for simplicity of data calculation. During data analysis, it was also assumed that these correction factors would have very small impact on the final data sets which would be propagated through out the entire data calculation system. In addition, since the final data sets were presented as percentage differences in all cases, so it was assumed that this

propagation errors in data sets would not hamper our prime objectives of dose investigation and assessment of its accuracy in irregular fields on the basis of relative dosimetry concept. The final dose values in different irregular fields were presented in Tables-3(I - XI). These directly measured dose values in irregular (blocked) fields were being compared with calculated dose values derived by using Clarkson's method of dose calculation in rectangular fields. This Clarkson's method can be applied for calculation of dose at any point in any irregular fields. For application of this method to the present work the irregular (blocked) fields were divided into a number of elementary sectors by drawing radii from the point of calculation in the plane of the field cross-section at any depth d. Each sector was characterized by its radius and could be considered as part of a circular field of that radius. In the present study the sector angle was 10^0, then the scatter contribution from this sector would be $10^0/360^0 = 1/36$ of that contributed by a circular field of that radius and centered at the point of calculation. Thus the scatter contribution from all the sectors was calculated and summed by considering each sector to be a part of its own circle. The SAR values for the sectors were calculated and then summed to give the average scatter air ratio $\left(\overline{SAR}\right)$ for the irregular field at the point of calculation for sectors passing through a blocked area, the net SAR was determined by subtracting the scatter contribution by the blocked part of sector. The computed $\left(\overline{SAR}\right)$ is converted to average tissue –air ratio $\left(\overline{TAR}\right)$ by the equation

$$\overline{TAR} = TAR(0) + \overline{SAR} \qquad \text{---------(56)}$$

Where $TAR(0)$ is the tissue – air ratio for 0×0 field i.e. $TAR(0) = e^{-\bar{\mu}(t-d_m)}$ where $\bar{\mu}$ is the average linear attenuation coefficient for the beam and d is the depth of dose calculation point

In our study dosimetry of irregular fields was performed by the method using TARs and SARs. The irregular field at depth d can be divided into n elementary sectors with radii emanating from any point P (say). A Clarkson type integration my be performed to have averaged Scatter Air Ratio $\overline{SAR}(d, d_a)$ for the irregular field r_a

$$\overline{SAR}(d,r_d)=\frac{1}{n}\sum_{i=1}^{n}SAR(d,r_i) \qquad \text{----------(57)}$$

where r_i is the radius of the ith sector at depth d and n is the total number of sectors $n = 2\pi/\Delta\theta$ is the sector angle.

The computed $\overline{SAR}(d,r_d)$ is then converted to $\overline{TAR}(d,r_d)$ by using the equation

$$TAR(d,r_d)=\left[K_p TAR(d,0)+\overline{SAR}(d,r_d)\right]\times\frac{S_p(0)}{\overline{S_p}(r_d)} \qquad \text{----------(58)}$$

Where K_p is the off axis dose ratio representing primary dose at P relative to that at the central axis. $\overline{TAR}(d,r_d)$ may be converted to the percent depth dose P(d,r,f) by using equation

$$P(d,r,f)=100\left[K_p TAR(d,0)+\overline{SAR}(d,r_d)\right]\times\frac{S_p(0)}{\overline{S_p}(r_d)}\times\frac{\overline{S_p}(r_d)}{\overline{S_p}(r_{t0})}\times\left[\frac{(f+t_0)}{(f+d)}\right]^2 \text{---(59)}$$

The final expression takes the form

$$P(d,r,f)=100\left[K_p TAR(d,0)+\overline{SAR}(d,r_d)\right]\times\frac{1}{\left(1+\overline{SAR}(t_0,r_{t0})\right)}\times\left[\frac{(f+t_0)}{(f+d)}\right]^2 \text{---(60)}$$

This is the basis of Clarkson's method. In the case of an irregular (blocked) field, the dose at any point P (say) can be calculated by the following mathematical formula based on Clarkson's method:

$$DD=(OFD)(PEF)\left(\frac{SSD+d_{max}}{SSD+d}\right)^2\left(\frac{\overline{TAR}}{BSF}\right)\left(\frac{1}{TF}\right) \quad \text{at depth } d_{max} \qquad \text{----------(61)}$$

Where OFD = Open Field Dose rate

PEF = Phantom Exposure Factor

SSD = Source to Surface Distance

d_{max} = Depth of maximum dose

d = Dose calculation depth

$\overline{TAR}$ = Average value of Tissue Air Ratio

BSF = Back Scatter Factor

TF = Tray Factor

In the present work, we have calculated the doses in irregular fields at different points using the above formula (61). The direct measurement dose values in irregular fields at different points were compared with the calculated dose values at the corresponding points in respective fields obtained by using the above formula (61).

The direct measurement of doses was made for both blocked (irregular) and open fields for each interested points in the respective fields. The observed dose values in both fields were compared and percentage difference between these values was determined. The direct measurement dose values at different points were normalized to the central axis dose values in open fields. These direct measurement values in the blocked field were also compared with the calculated values obtained by using Clarkson's method based on equation (61). A percentage difference between the direct measurement values and the corresponding calculated values obtained by using the above equation were also presented in Table-3(I – XI).

Chapter-VI

Results and Discussion

6.1 RESULTS AND DISCUSSION

The dosimetric scan of beam profile to check the performance status of Alcyon II#90106 ^{60}Co teletherapy unit was done using 10×10cm^2 field size with 80 cm SSD at 0.5 cm depth in solid phantom along the major axes (x. y-axes). The performances were found satisfactory which are presented in Tables 1 and 2 and graphically in figs.25 and 26.

In this thesis work we have investigated the accuracy of dose measurement in irregular photon fields usually encountered in routine radiotherapy practices through comparison of directly measured dose values with the calculated dose values of Clarkson's method and developed an Empirical relation for the accuracy of dose prescription in radiotherapy treatment procedure. In order to serve the purpose, eleven (11) irregular fields were simulated in solid perspex phantom. It was expected that these fields would almost cover the different irregular fields usually encountered in daily radiotherapy practices of different therapy establishments. The direct measurement of dose values in these irregular fields were presented in Tables 3(I - XI) of ^{60}Co unit. The direct measurement dose values in irregular fields were compared with calculated dose values obtained by the use of Clarkson's method of dose calculation in irregular photon field and newly developed Empirical relation. The Tables 3(I-XI) contain, directly measured dose values at various interested points in different irregular fields, the directly measured dose values at those points in the corresponding open fields, percentage difference of dose values between irregular (blocked) and open fields, calculated dose values at respective points in irregular fields (Clarkson's method), percentage difference of dose values between directly measured and calculated values dose (Clarkson's method), calculated dose values at respective points in irregular fields (Empirical relation), percentage difference of dose values between calculated dose values of Clarkson's method and Empirical relation, the numerical values of correction factors $C'_{fs,i}$ and CF_r

The directly measured dose values at different points in irregular fields were normalized to the central axis dose values in the respective open fields. In this study, since directly measured dose values are in good agreement with calculated dose values of Empirical relation, so that, the dose calculated by Empirical relation could be presented as normalized to the central axis dose values in the respective open fields for dose estimation in irregular

fields. It is thus, expected that dose estimation in irregular fields could be approximated with reasonable accuracy from the calculated dose values of empirical relation normalized to central axis beam dose data in respective open fields.

The observed mean percentage difference with 1sd (standard deviation) between directly measured dose values at different points in irregular (blocked) fields and the corresponding dose values at those points in open fields of Tables 3(I - XI) for ^{60}Co were found to be 15.93% ±12.98 (range 6.26% – 34.28%), 16.42% ± 12.63 (range 6.18% – 34.22%), 11.44% ± 7.06 (range 8.20% – 27.23%), 49.20% ± 0.19 (range 49.09% - 49.56%), 2.45% ± 0.12 (range 2.28% – 2.66%), 2.75% ± 0.15 (range 2.56% – 3.02%), 8.83% ± 0.15 (range 8.68% – 9.13%). 8.88% ±0.05 (range 8.79% – 8.95%), 8.38% ± 0.07 (range 8.31% – 8.49%), 47.62% ± 22.59 (range 17.93% ± 81 41) and 12.47% ± 5.07 (range 6.56% – 19.96%).

The averaged value of these mean differences with 1sd was found to be 16.76% ± 9.12 (range 2.45% – 49.20%)

The mean percentage differences with 1sd between directly measured dose values and calculated dose values by Clarkson's method at the corresponding irregular fields of Tables 3(I - XI) were found to be–

0.658% ± 0.427 (range 0.055% – 0.998%), 0.747% ± 0.352 (range 0.250% – 1.020%), 2.835% ± 0.314 (range 2.63% – 3.51%), 4.715% ± 0.706 (range 3.62% – 5.63%), 2.580% ± 0.202 (range 2.20% – 2.78%), 1.770% ± 0.141 (range 1.47% – 1.91%), 0.475% ± 0.008 (range 0.47% – 0.49%), 3.127% ± 0.005 (range 3.12% – 3.13%), 2.753% ± 0.005 (range 2.75% – 2.76%), 5.998% ± 1.301 (range 4.43% – 7.34%), 2.147% ± 0.207 (range 1.93% – 2.46%).

The coefficients of correlation between the directly measured dose values in irregular fields and the calculated (Clarkson's method) dose values in the corresponding fields of Tables 3(I - XI) for ^{60}Co were found to be 0.999, 0.999. 0.999, 0.999, 0.999, 0.999, 0.999, 0.999, 0.999, 0.999 and 0.999. The mean value of these coefficients of correlation was found to be 0.999.

The observed average value of uncertainty between the directly measured dose values and the calculated dose values (Clarkson's method) in the corresponding fields of Tables 3(I - XI) for ^{60}Co unit were found to be– ±0.330%, ±0.374%, ±1.430%, ±2.420%, ±1.310%, ±0.894%, ±0.239%, ±01.587%, ±1.39%, ±3.090%, 1.086% respectively.

The corresponding values between calculated dose values of Clarkson's method and newly developed Empirical relation in the corresponding fields of Tables 3(I - XI) for ^{60}Co were found to be –

0.658% ± 0.427 (range 0.055% - 0.998%), 0.740% ± 0.369 (range 0.220% – 1.030%), 2.835% ± 0.314 (range 2.830% – 3.510%). 4.717% ± 0.709 (range 3.620% – 5.640%), 2.582% ± 0.199 (range 2.210% – 2.780%), 1.770%± 0.142 (range 1.470% – 1.913%), 0.475% ± 0.008 (range 0.470% – 0.490%), 3.127% ± 0.005 (range 3.120% – 3.130%), 2.752% ± 0.004 (range 2.750% – 2.760%), 5.998% ± 1.301 (range 4.380% – 7.340%), 2.147% ± 0.207 (range 1.930% – 2.460%).

The coefficients of correlation between the directly measured dose values in irregular fields and the calculated (Empirical relation) dose values in the corresponding fields of Tables 3(I - XI) for ^{60}Co were found to be 0.999. 0.999, 0.999, 0.999, 1, 0.999, 0.999, 0.999, 0.999, 0.999 and 1 respectively. The mean value of these coefficients of correlation was found to be 0.999. This means that the directly measured dose values are in good agreement with both Clarkson's method (0.999) and newly developed empirical relation (0.999) for ^{60}Co unit.

The observed average value of uncertainty between the calculated dose values of Empirical relation and Clarkson's method in the corresponding fields of Tables 3(I - XI) for ^{60}Co unit were found to be– ±0.330%, ±0.374%, ±1.430%, ±2.420%, ±1.310%, ±0.894%, ±0.239%, ±1.587%, ±1.390%, ±3.090%, 1.086% respectively.

The averaged value of these mean values (i.e. Direct method & Clarkson's method and Clarkson's method & empirical relation) were found to be–

2.528% ± 1.622 (range 0.475% – 5.998%) and 2.527% ± 1.623 (range 0.475% – 5.998%) for ^{60}Co unit.

The mean differences with 1sd between directly measured dose values in irregular fields and calculated dose values at the corresponding fields by Clarkson's method are approximately equal to that of the Clarkson's method and newly developed Empirical relation. This is due to the good agreement between the directly measured dose values and the calculated dose values of Empirical relation.

The averaged mean percentage difference 16.76 % ± 9.12 (range 2.45 %– 49.2%) between directly measured dose values at different points in irregular (blocked) fields and the corresponding points in respective open fields could be considered statistically significant in case of dose prescription for a patient receiving radiotherapy treatment with irregularly shaped photon fields.

The averaged value of uncertainty between directly measured dose values (blocked) & calculated dose values (Clarkson's method) was ±1.291% and the corresponding value between Clarkson's method and newly developed Empirical relation was ±1.291% which is statistically satisfactory because according to the International Commission on Radiation Units and measurements (ICRU) the dose delivered to the target volume should be at least within ±5%[40].

The other information which were expected to be useful in routine radiotherapy with irregularly shaped fields is that, since in our study, directly measured dose values in irregular fields are in good agreement with calculated dose values by Empirical relation, so that, the dose calculated by Empirical relation could be presented as normalized to the central axis dose values in respective open fields. It is thus, expected that dose estimation in irregular fields could be approximated with reasonable accuracy from the calculated dose values of Empirical relation normalized to central axis beam dose data in respective open fields.

For any particular irregular field, the directly measured dose values at different points as normalized to the central axis dose values of corresponding open field could to be used to find the desired dosimetry information available of that irregular field in routine radiotherapy practices. But, since the direct dose measurement procedure is time consuming, so that, the Empirical relation could be useful for the dosimetry of different irregular fields following the dosimetry protocol of radiotherapy to maintain the accuracy of treatment

procedure. To sustain the accuracy of dosimetry in irregular fields the correction factors of Empirical relation was determined relative to the dose values of direct measurement and Clarkson's method.

As the primary aim of our present work was intended to investigate the accuracy of the doses in irregular photon fields by direct dose measurement method based on the use of ion chamber, in comparison with Clarkson's method and newly developed Empirical relation, we calculated the doses by the Clarkson's method and the Empirical relation. Dose calculated by the Empirical relation using the correction factors C'_{fsk} and CF_i is found approximately equal to the directly measured dose values.

It was observed that if the points of measurement were closer to the centre of the photon-field, the dose values were close enough in comparison to the direct measurement values as well as the calculated values obtained by Clarkson's method and newly developed empirical relation.

It was observed that if the points of measurement were closer to the central axis of the field, the calculated dose values (Clarkson's method) were close in comparison to the direct measurement dose values, on the other hand, for points lying on the peripheral zone of the field i.e. away from the central axis of the field, the results were over estimation of doses in comparison to the direct measurement dose values. Table 3(VI&XI). Theoretically, we know that the use of shielding for beam modification would reduce certain dose values, because of lowering scattered radiation especially from phantom or patient i.e. lowering BSF. In our study we observed that for corner shielding block of field size $10\times10cm^2$ and $15\times15cm^2$ the mean percentage difference of dose reduction values were 11.44%±7.06 and 2.45%±0.12 respectively. Although the dose reduction value in $10\times10cm^2$ field size was greater than that the field size of $15\times15cm^2$, the blocked beam doses in $15\times15cm^2$ was greater than that of $10\times10cm^2$ as a result of larger field size, Table 3(III & V). This means that the total dose values at any point in the field is dependent on the field size, beam quality and above all how many portion of the field was blocked.

The important finding of this study is the remarkable reduction of dose values expressed in percentage difference between directly measured dose values at different points in the irregular (blocked) fields and the dose values at the corresponding points in the respective open fields, which is statistically significant. In this study, the observed averaged value of mean percentage difference with 1sd (standard deviation) between directly measured dose values at different points in irregular (blocked) fields and the corresponding dose values at those points in open fields was found to be 16.76% ± 9.12 (range 2.45 %- 49.2%) This dose reduction in blocked fields can reasonably be considered significant in routine radiotherapy practices with ^{60}C teletherapy units where irregular fields are very common during treatment of a patient. For a single dose application, the dose reduction 16.76% ± 9.12 might not be significant but if a patient is planned to provide 80Gray dose in 40 fractions (say) with a view to complete eradication of his or her tumor, this dose reduction becomes significant, because, in that case, the patient would receive a dose about 13.4Gray less than the prescribed dose which might result in under dose treatment with consequence of lowering the probability of tumor destruction and is not totally desired in a radial radiotherapy practices

In our country as Medical physicist is not available in most of the therapy units so, as a common practice, when beam modification is needed to protect certain critical organs from unnecessary radiation burden, required portion of the field is usually blocked to serve the protection purpose but dosimetry requirements in that case is very often ignored and thus providing a dose that is lower than that expected which might result in under dose treatment and the entire treatment does not come out with desired results. The newly developed empirical relation in our study could be useful for the dosimetry of irregular fields following dosimetric protocol to avoid under dose treatment problem.

6.2 Conclusion

From this study we can conclude that the newly developed Empirical relation could be useful for the dosimetry of irregular fields in daily radiotherapy treatment procedure. Also, this study provides us quantitative information about dose reduction in irregular (blocked) fields in comparison with the open fields of corresponding size thus it can be concluded that, to sustain the accuracy in radiotherapy treatment procedure for the proper treatment of cancer patients with irregular fields, either the radiation oncologist should be meticulous to provide extra dose after doing proper dosimetry of irregular fields by the newly developed Empirical relation or must be taken into account about 17 – 18% dose reduction in irregular (blocked) fields for respective ^{60}Co unit.

Beam modification with appropriate shielding block is important in day-to-day radiotherapy treatment procedure, with paying due attention in making dosimetry information available for the blocked beam, so that, critical organs could properly be saved with prescribing adequate dose for the accuracy of dose delivery in treatment of malignant diseases. In this regard the newly developed Empirical relation could play a vital role so that adequate dose could be prescribed to have desired treatment results.

In our study we have simulated eleven (11) irregular fields which would cover the most useful irregular shaped fields required in routine radiotherapy practices and since directly measured dose values in irregular fields are presented as normalized to the central axis dose values in open fields which are in good agreement with calculated dose values by Empirical relation, so it is expected that dose estimation in irregular fields could be approximated with reasonable accuracy from the dose values calculated by Empirical relation normalized to the central axis dose values in respective open fields. Thus, the calculated dose values of Empirical relation normalized to central axis dose values in respective open fields could be approximated with reasonable accuracy as the estimated dose of irregular fields in respective open fields. More required dosimetry data in daily radiotherapy treatment procedure with irregular fields could be found by using the empirical relation with appropriate correction factors.

Appendix

APPENDIX-1:

(a) Example of dose calculation in Clarkson's method:

Block: Rectangular shielding block
Block material: Lead
Block Length: 13.1 cm
Height: 5.15 cm
Width: 5.0 cm
Sector angle: 10^0 (ten degree)

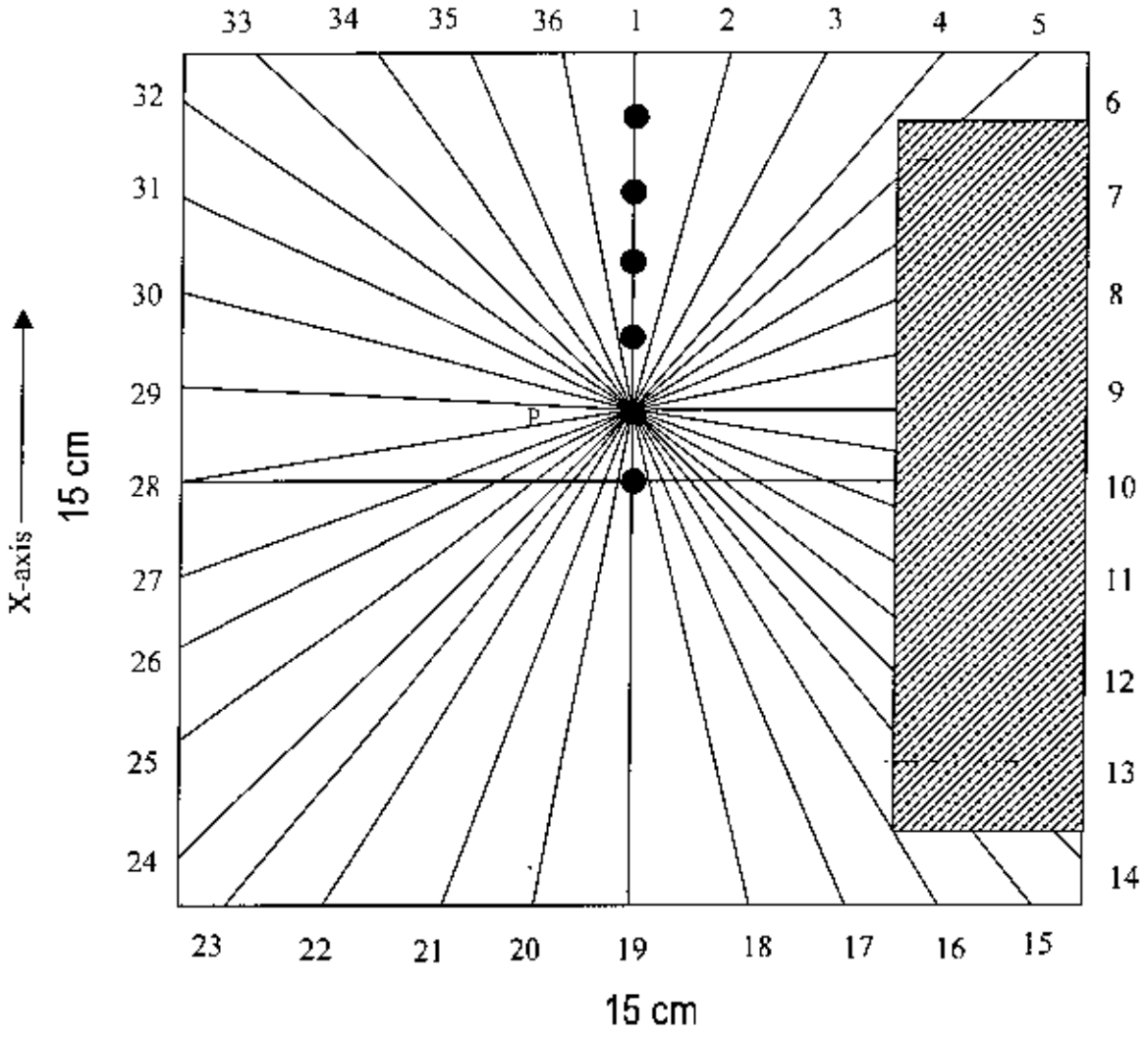

Fig. 29: Example of dose calculation (say at point P) in Clarkson's method of irregular field

(a) Example of dose measurement in irregular field:

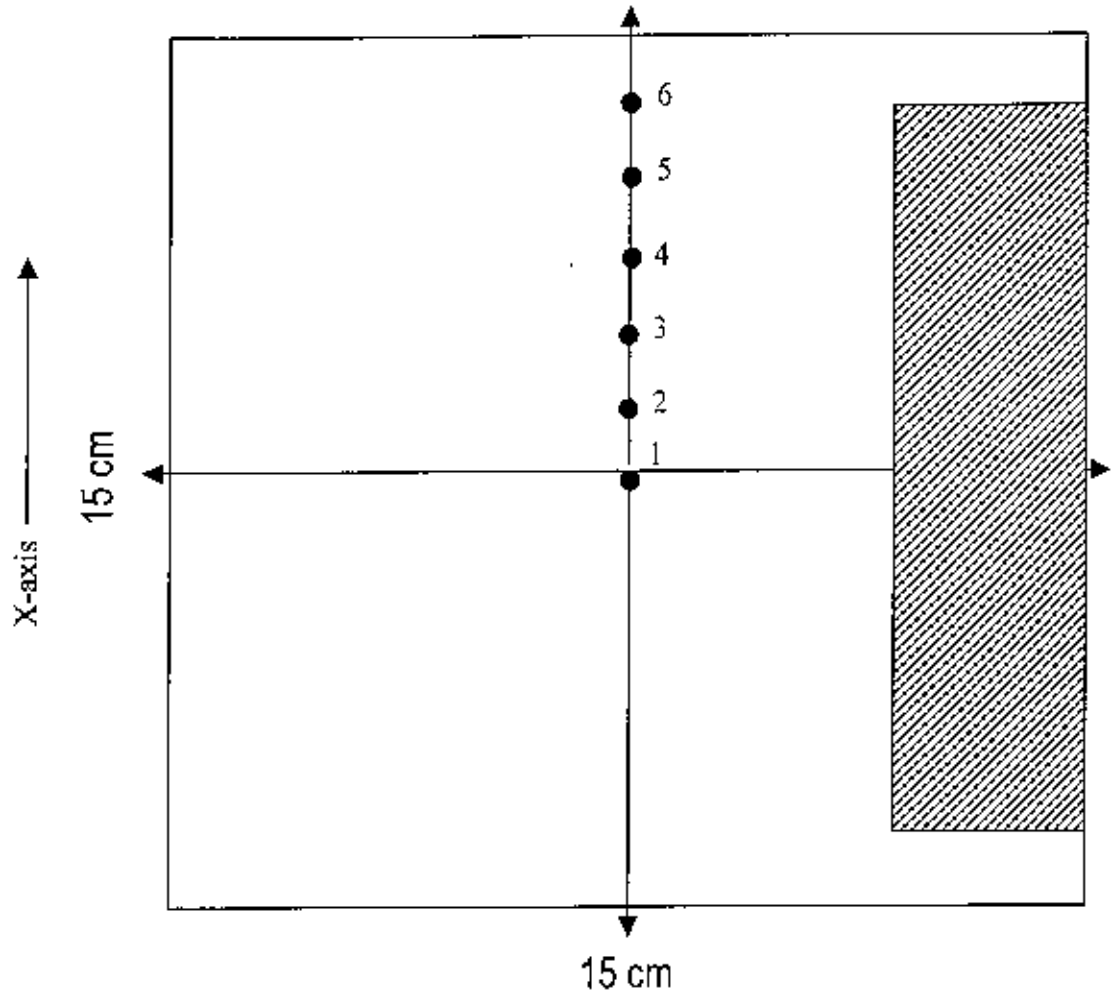

Fig.30: Examples of dose measurement in experimental method

APPENDIX-2:

Different simulated irregular fields with interested points of dose investigation of the experimental work.

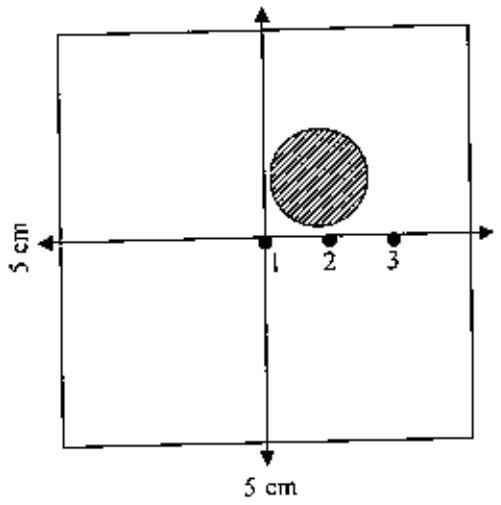

3 (i) : Cornea Block

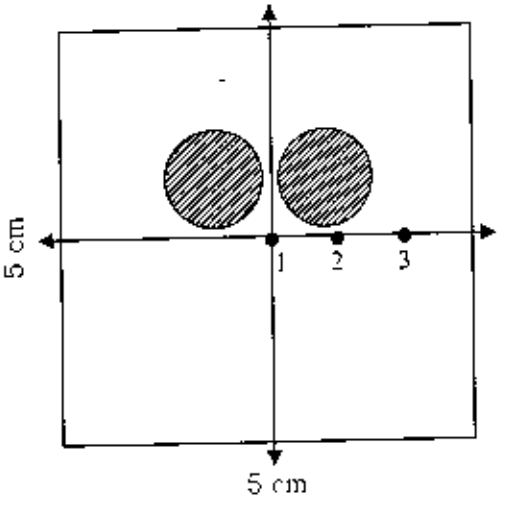

3 (ii) : Double Cornea Block

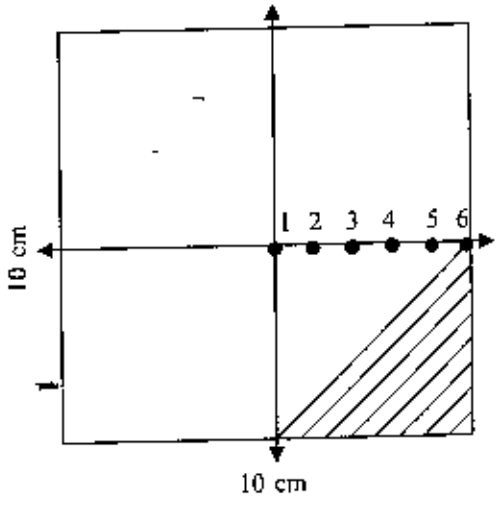

3 (iii) : Corner Block

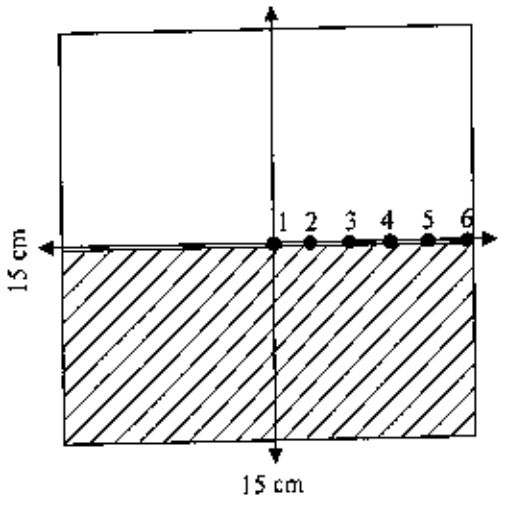

3 (iv) : Half Beam Device

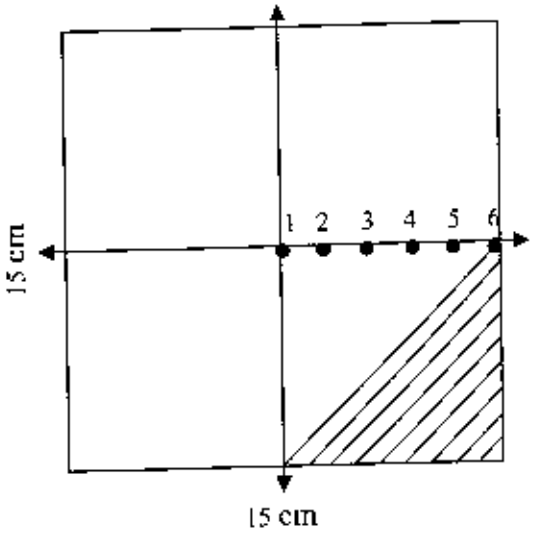

3 (v) : Corner Block

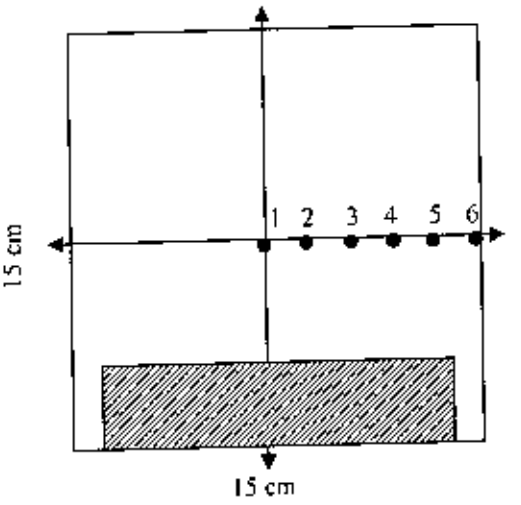

3 (vi) : Rectangular block

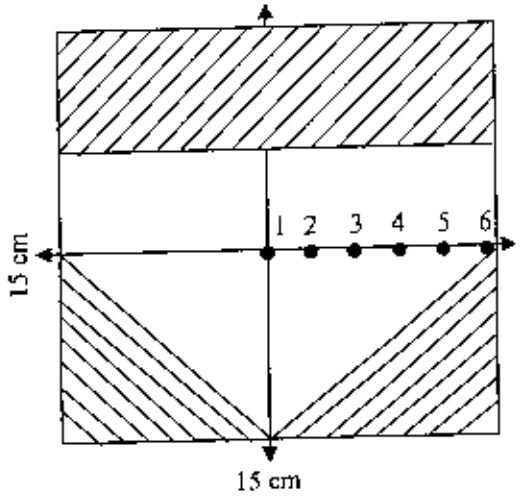

3 (vii) : Irregular shaped Block
(Rectangular + Double Corner Block)

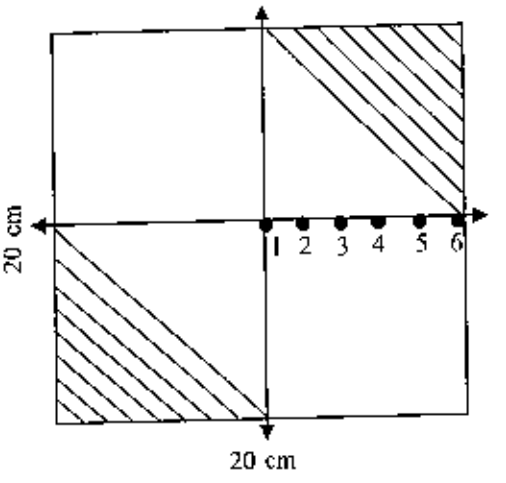

3 (viii) : Double Corner Block

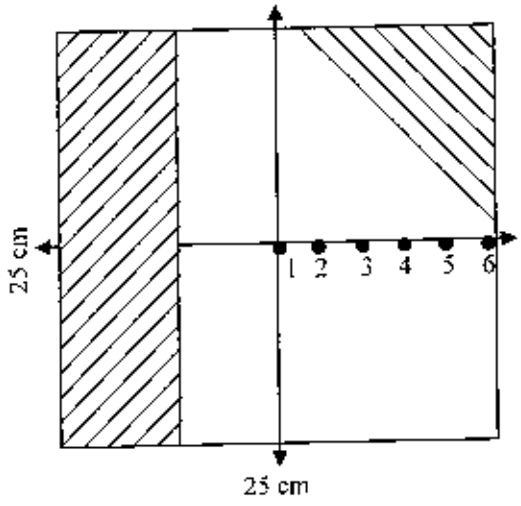

3 (ix) : Irregular shaped Block (Rectangular + Corner Block)

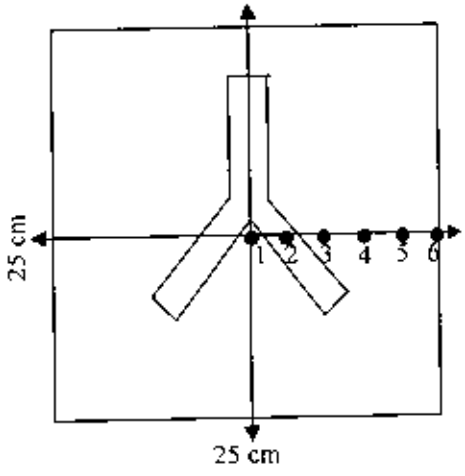

3 (x) : Inverted –Y Block

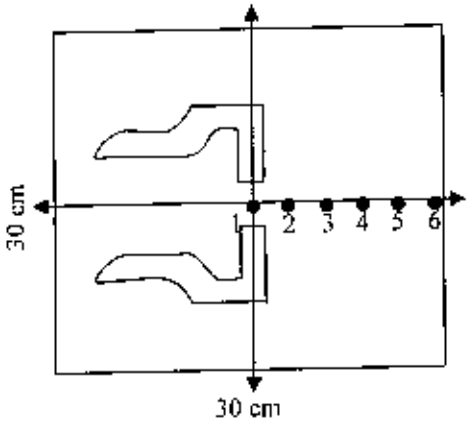

3 (xi) : Mantle Block

APPENDIX-3:

Dose calculation formulism used in irregular fields:

Dose calculation in Clarkson's method:

$$D_{cal} = (OFD)(PEF)\left(\frac{SSD + d_{max}}{SSD + d}\right)^2 \cdot \left(\frac{TAR}{BSF}\right)\left(\frac{1}{TF}\right)$$

Where

OFD = Open Field Dose rate

PEF = Phantom Exposure Factor

SSD = Source to Surface Distance

d_{max} = Depth of maximum dose

d = Dose calculation depth

TAR = Average value of Tissue Air Ratio

BSF = Back Scatter Factor

TF = Tray Factor

Corrected calculated dose.

$$D_{cal,w_{corrected}} = D_{cal} \times PW_{con.} \times K_{TP}$$

Where

PW_{con} = Phantom to water conversion factor

K_{TP} = Temperature- pressure correction factor

Dose measured in experimental method:

Corrected measured dose:

$$D_{F,w_{corrected}} = D_F \times PW_{con} \times P_c \times K_{TP}$$

Where

P_c = Phantom scatter factor

Dose calculation in Empirical relation:

$$D_{Lm,w_{corrected}} = D_{cal\ w_{corrected}} \times CF_i$$

Where

$$\text{Correction Factor, } CF_i = \frac{D_{L,w_{corrected}}}{D_{cal\ w_{corrected}}} \quad ; \ i = 1,2.3.....n$$

$$D_{Lm\ w_{corrected}} = \left[(OFD)(PEF)\left(\frac{SSD + d_{max}}{SSD + d}\right)^2 \cdot \left(\frac{TAR}{BSF}\right)\left(\frac{1}{TF}\right) \right] . PW_{con_i} \times K_{TP} \times CF_i$$

$$D_{Lm,w_{corrected}} = \left[(OFD)(PEF)\left(\frac{SSD + d_{max}}{SSD + d}\right)^2 \cdot \left(\frac{TAR}{BSF}\right)\left(\frac{1}{TF}\right) . PW_{con} \right] . K_{TP} \times CF_i$$

$$\boxed{D_{Lm,w_{corrected}} = (OFD) \times C'_{j\times k} \times CF_i \times K_{TP}}$$

Where

Correction Factor,

$$C'_{j\times k} = \left[(OFD)(PEF)\left(\frac{SSD + d_{max}}{SSD + d}\right)^2 \cdot \left(\frac{TAR}{BSF}\right)\left(\frac{1}{TF}\right) . PW_{con} \right] ; j,k = 1,2....n$$

APPENDIX-4:

Normalization of calculated dose values* of Empirical relation to the corresponding open fields

Fields	3(i)	3(ii)	3(iii)	3(iv)	3(v)	3(vi)	3(vii)	3(viii)	3(ix)	3(x)	3(xi)
Points	% of calculated dose values of Empirical relation in irregular fields at different points to central axis dose in the respective open fields.										
1	65.72	65.78	91.59	50.44	96.09	95.29	91.25	91.078	91.14	82.07	90.81
2	93.69	91.08	91.57	50.78	96.19	95.66	91.30	91.09	91.51	75.23	80.01
3	81.10	82.01	91.55	50.71	96.05	95.61	91.08	91.06	91.52	60.96	81.14
4			91.16	50.66	95.76	95.42	90.79	90.78	91.39	44.33	87.95
5			88.48	50.49	95.31	95.05	90.38	90.49	91.12	32.57	91.15
6			38.88	50.23	94.79	94.35	89.55	89.88	90.77	18.41	92.84

*The calculated dose values of Empirical relation using the correction factors C'_{fxk} and CF_i at different points in irregular fields was found to be exactly equal to the directly measured dose values, which is normalized to the central axis dose values in the corresponding open fields.

APPENDIX-5:

Different lead blocks used in the experimental work.

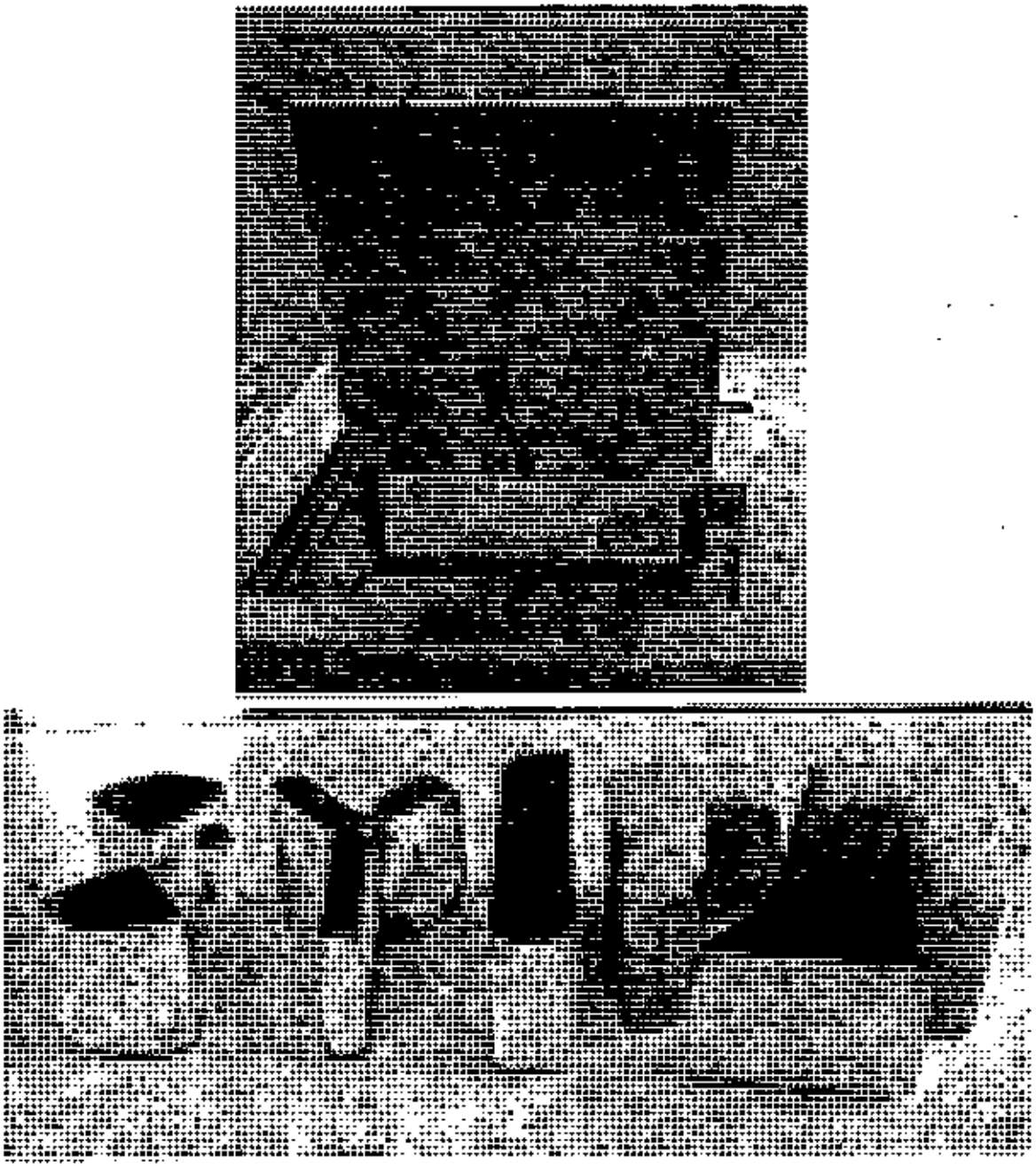

Fig. 31: Different lead blocks used to produce different irregular shaped photon fields

APPENDIX-6 :

Definition of certain relevant terms:

Absorbed dose:
The absorbed dose is a measure of energy imparted to matter by the ionizing radiation per unit mass of the material at the place of interest.

Back Scatter Factor (BSF):
It is defined as the ratio of the dose on central axis at the depth of maximum dose to the dose at the same point in free space.

Build Up:
The region between the surface and the point of maximum dose is called as the dose build up region and the dose as build up dose.

Calibration factor (CF):
The quotient of the conventional true value of the quantity being measured divided by the indicated value corrected to the reference condition.

Collimator scatter factor (S_c):
The ratio of the output in air for given field to that for a reference field (e.g.$10\times10cm^2$).

Correction factor:
A dimensionless factor by which the indicated value is multiplied to compensate for as assumed systematic error or to convert from the value when operated at a particular condition to the value when operated at a stated reference condition.

cGy: Subunit of Gy known as centigray (cGy) and is equivalent to rad.

Gray: It is the ratio of 1 joule of absorbed energy to 1 killogram of material. i.e. 1 Gray (Gy)= 1 J/Kg.

Indicated value:
The value of a quantity derived fro the scale reading of an instrument by application of any scale factors indicated on the instrument panel i.e. uncorrected value.

Ionizing radiation:
X-ray, γ-ray, neutron, alpha, beta and other heavy charged particles lose their energy in the medium through ionization and or excitation along their traversing path in medium and termed as ionizing radiation.

Kerma:
Kerma stands for kinetic energy released in the medium.

Leakage current:
Any current arising in the ionization chamber or measuring assembly that is not produced by ionization in a sensitive volume.

Measured value:

The best estimate of the true value of a quantity, being derived from the indicated value of an instrument together with the application of the calibration factor and all other relevant correction factors.

Non-ionizing radiation:

Light wave, ultraviolet light, microwave, radio-wave etc. refers its name as can not produce any ionization in the medium through which they are moving and causes no known or observable biological effects in living organisms.

Port film:

The purpose of port filming is to verify the treatment volume under actual conditions of treatment usually done using a diagnostic or simulator in radiotherapy practices and preserved as a legal record.

Primary standard:

An instrument of the highest metrological quality that permits determination of the unit of a quantity according to its definition, and accuracy of which has been verified by comparison with the comparable standards of other institutions participating in the international measurement system.

PSDL:

The primary Standard Dosimetry Laboratory is a national standardizing laboratory designated by the government for the purpose of developing, maintaining and improving primary standards in radiation dosimetry.

Penumbra:

The region, at the edge of a radiation beam, that is partially shielded from primary photons from the source, and over which the rate changes rapidly as a function of distance from the beam axis (usually region having dose rate of 80% to 20%).

Phantom:

A volume of tissue equivalent material usually large enough to provide full scatter conditions for the beam being used.

Phantom scatter ratio (S_p):

Ratio of the dose rate at the same depth for the reference field size (e.g., 10×10cm), with the same collimator operating.

Quality of radiation beam:

A term referring to the ability of a radiation beam to penetrate matter. For low and medium energy X-ray beams in radiotherapy, it is usually expressed in terms of the half value layer, for high energy ×-ray beams, it is expressed as TPR (20/10) and for radiation protection dosimetry, it may be expressed as equivalent energy.

Rad:

Unit of absorbed dose or simply dose which represents the absorption of 100 ergs of energy per gram of the absorbing material.

Roentgen:

Unit of exposure and is a measure of the ionization ability of a photon beam (x or γ) in air with photon energy not higher than 3 MeV. Roentgen was originally as the amount of x or γ radiation required to produce 1 esu (electrostatic unit) of charge of either sign in 1 cc air at STP (standard temperature and pressure). The current definition of roentgen is equivalent to 2.58×10^{-4} coulomb/kg dry air at STP which is equal to the original definition if the charge is expressed in coulombs (1 esu = 3.33×10^{-10} coulomb) and the volume of air is changed to mass (1 cc of weight 1.293×10^{-6}kg at STP).

Radiation:

It is the emission and propagation of energy through space or material medium.

Radioactivity:

The phenomenon in which energy is given off by disintegration of the nuclei of radioactive atoms is termed as radioactivity.

Reference standard:

A standard of the highest metrological quantity available at a given location from which measurements made at that location are derived.

Response:

The quotient of the indicated value divided by the conventional true value of the quantity being measured.

Secondary standard:

An instrument calibrated in comparison with a primary standard, either directly or indirectly by the use of a working standard.

Secondary Standard Dosimetry Laboratory:

A dosimetry laboratory designated by the competent authorities to provide calibration services, and which is equipped with at least one secondary standard that has been calibrated against a primary standard.

Standard:

A measuring instrument used to present physically the unit of a quantity in order to transmit it to other measuring instruments in comparison.

Simulation:

It refers to the procedure for combined trail set up and verification of the designed treatment plan using a simulator.

Simulator: A simulator is an apparatus that uses a diagnostic X-ray tube but duplicates a radiation treatment units in terms of its geometrical, mechanical and optical properties.

Scatter-Maximum-Ratio (SMR):

Ratio of the scatter dose at a given point in phantom to the effective primary dose at the same point at the reference depth of maximum dose.

Scatter-Air-Ratio (SAR):

Scatter-Air-Ratio is defined as the ratio of the scattered dose at a given point in the phantom to the dose in free space at the same point

Tissue-Maximum-Ratio (TMR):

Ratio of the dose at depth'd' to the dose at D_{max}.

Tissue-Phantom-Ratio (TPR):

Ratio of the dose at a given point in phantom to the dose at the same point at a fixed reference depth, usually 5 cm in the same phantom.

Tissue-Air-Ratio (TAR):

Ratio of dose at a given depth in a phantom at SAD to the dose without phantom at SAD.

References

References

1. **American Association of Physics in Medicine.** RTC Task group 21. A protocol for the determination of absorbed dose from high-energy photons and electron beams. Med. Phys 1983; 10: 741.
2. **Alison P Casarett.** Radiation Biology. Pub. Prentice-Hall Inc. Englewood Cliffs, New Jersey, 1968; 32 – 72.
3. **Almond P, Roosenbeek E V.** Browne R, Milcamp J, Williams C B. Variation in the position of the central axis maximum build up point with field size with high energy photon beams (Letter to the Editor). Br. J Radiol. 1970; 43 : 911.
4. **A E Nahum.** Extension of the Spener – Attix cavity theory to the 3 Media situation for electron beam. Dosimetry in Radiotherapy Proceedings of a Symposium, Vienna, Astria, 31 August – 4 September 1987, Organized by IAEA in Co-operation with WHO. Vol. 1, IAEA, Vienna, Austria 1988; P87.
5. **Abu Saleh Mohammad Ambia.** Radiotherapy of Canceer patients and related measurement (Thesis), University of Chittagong.), 2000, P 1-3.
6. **British Journal of Radiology.** Supplement No. 25 . Central Axis Depth Dose Data for use in Radiotherapy. Pub. British Institute of Radiology. 1983; P 45 – 59.
7. **Barnard G P.** Dose – exposure conversion factors for megavoltage X-ray dosimetry. Phy Med Biol. 1964; 9:321.
8. **Belli J A. and Andrews J R.** Relationship between tumor growth and radiosensitivity. J Nat Cancer Inst. 1963 ; 31 . 689.
9. **Bjarngard B E, Cunninghum JR.** Comments on " Validity of the concept of separating primary and scatter dose" Med Phy. 1986; 13:760.
10. **Bange F.** Physical aspects of suppervoltage X-ray therapy. Med Phys. 1974; 1:266.
11. **C .k Bomford, I. H. Kunkler and S. B. Sherrif.** Walter and Miller's Textbook of radiotherapy, Radiation Physics, Therapy and Oncology. Pub. Churchill Livingstone Inc. 650 Avenue of the America, NY. 5th Ed. 993; P88, 253 – 256.
12. **Cunninghum JR.** Scatter air ratios. Phys. Med Biol. 1972; 17 : 42.
13. **Cundiff J H, Cunninghum J R, Golden R et al. IRPC / AAPM Compiler.** Dosimetry workshop on Hodgkin's disease. Houston, MD Anderson Hospital. 1970.

14. **Chernak E S, Antunez R A, Jelden G L, Dhaliwal R S, Lavik P S.** The use of computed tomography for radiation therapy treatment planning. Radiology 1975; 117:613.

15. **CIS Bios international users Manual.** CIRUS. A PARTIR DU No/Unit # 96001, Code J2472 vers : 1.0, 10 September 1988; P1-35;

16. **Design and Development of a Radiotherapy Programme :** Medical physics, Radiation Protection and Safety Aspects, IAEA – TECDOC 1040, Vienna, Astria, 1998; P1-5.

17. **Day M J, greene D, massey J B.** Use of a Perspex sheath for ionization chamber measurements in a water phantom. Phys. Med Biol. 1965; 10 : 111.

18. **Design and implementation of a radiotherapy programme :** Clinical, medical physics, radiation protection and safety aspects. IAEA, Vienna, Austria. September 1998.

19. **Day M J.** A note on the calculation of dose in X-ray fields. Br. J Radiol. 1950; 23:368.

20. **Du Sault L A.** The influence of the time factor on the dose response curve. Amer J Roentgen. 1962; 87:567.

21. **Dawson D J.** Percentage depth dose for high energy X-rays. Phys Med Biol. 1976 ; 21:26.

22. **D K Bewley et al.** Central axis depth dose data. Br. J. Radiol. Supplement No.25. 1983:P50-75.

23. **F M Khan.** The Physics of Radiation Therapy. Pub. Lippincott William & Wilkins, 351 West Camden St, Baltimore, 2nd Ed. 1994; P94, 98, 101,117,138,181,300 – 325, 328.

24. **F M Khan.** The Physics of Radiation Therapy. Pub. Williums & Wilkins, Baltimore, Mary land. 1984. P180 – 193.

25. **Fowler J F. and Stern B. E** Dose-time relationships in radiotherapy and the validity of survival curve models. Brit J Radiol. 1963; 36:163.

26. **Greene. D., Massey J B.** The use of the Farmer-Baldwin and Victrometer Ionization Chambers for dosimetry of high-energy X-radiation. Phys. Med. Biol. 1968; 13:287.

27. **Greene. D., Massey J B. and Meredith W. J.** Exposure dose measurements in megavoltage therapy. Phy. Med. Biol. 1962; 6:551.

28. **Gray L H.** An ionization method for the absolute measurement of gamma-ray energy. Proc. R Soc 1936, A 156-578.

29. **Harunar Rashid et al.** Investigation of doses in irregular photon fields, Bangladesh University of Engineering & Technology, Dhaka, 2003,P-31,33,36-46.

30. **Harold Elfrod Johns & John Robert Cunninghum.** The Physics of Radiology, 4th ed, 983, P 218.

31. **H E Johns.** The Physics of Radiology. Pub. Charles C Thomas. Illinois. 3rd Ed. 1978 ; P 272 – 303.
32. **Hospital Physicists Association** : A code of practice for dosimetry of 2 to 8 Mv x-ray and ^{137}Cs and ^{60}Co γ-ray beams. Phy. Med Biol. 968;13 : 287.
33. **Harold Elford johns and John Robert Cunninghum.** The physics of Radiology. Pub. Charles C Thomas, Springfield Illinois, 3rd Edi. 5th printing 1978; P 196 – 197.
34. **Holt J G, Laughlin J S, Moroney J P.** Extension of concept of Tissue – Air Ratio (TAR) to high energy X-ray beams. Radiology 1970; 96:437.
35. **Holt J G., Letter to the editor.** Am Assoc Phys med. Q Bull. 1972; 6:127.
36. **Holt J G, Laughlin J S, Moroney J P.** The extension of the concept of Tissue – Air Ratio (TAR) to high energy X-ray beams. Radiology. 1970; 96: 437.
37. **Hanson W F, Berkley L W.** Off-axis beam quality change in linear accelerator X-ray beams. Med phys 1980; 7:146.
38. **International Commission on Radiological Units and Measurements:** ICRU – 38. 1980.
39. **International Commission on Radiological Units and Measurements:** Physical aspects of irradiation, ICRU report 10b, US National Bureau of standards. 1964.
40. **International Commission on Radiological Units and Measurements:** Radiation quantities and units ICRU Report 33. 1980.
41. **ICRU Report 10b,** Hand book 85, US Nat. Bur of Standards Washington DC, 1962.
42. **ICRU Report 31:** Average energy required to produce an ion pair Washington DC. 1979.
43. **ICRU.** Determination of absorbed dose in a patient irradiated by beams of X or gamma rays in radiotherapy procedures. Report No. 24 Washington DC. US Nat. Bur of Stds. 1976.
44. **Instruction Manual PTW-**UNIDOSE, Universal Dosimeter, Firmware No.2.20(D196–131– 0/7); P7-52.
45. **James E.** Turner. Atoms, Radiation and Radiation Protection. Pub. Perganon Press Inc. Ed. New York, 1986, P225 – 238.
46. **Johns H E, Cunninghum J R.** The Physics of Radiology 3rd Ed. Springfield Illinois, Pub. Charles C Thomas 1969; P210 – 233.
47. **Johns HE, Bruce W R, Reid W B.** The dependence of depth dose on focal skin distance. Br. Radiol. 1958; 31:254.
48. **Johns HE, Cunninghum J R.** the Physics of Radiology 3rd Ed. Springfield IL Pub. Charles C Thomas 1969.

49. **Jones DEA.** A note on back-scatter and depth dose for elongated rectangular X-ray fields. Br. J. Radiol 1949; 22:342.

50. **Khan F M.** Replacement correction (P_{repl}) for ion chamber dosimetry. Med Phys 1991; 18 : 1244.

51. **khan F M, Levitt S H, Moore V C, Jones T K.** Computer and approximation methods of calculating depth dose in irregularly shaped fields. Radiology 1973; 106:433.

52. **Khan F M.** Computer Dosimetry of partially blocked fields in cobalt teletherapy. Radiology 1970; 97 : 405.

53. **Khan F M.** Dose distribution problems in cobalt teletherapy [Thesis] . University of Minnesota. 1969, P106.

54. **Karzmark CJ, Deubert A, Loevinger R.**Tissue – phantom ratios-an aid to treatment planning. Br. J. Radiol. 1965; 38:158.

55. **Khan F M.**, Sewchand w, Lee J, Williamson J P. Revsion of tissue maximum ratio and scatter maximum ratio concepts for ^{60}Co and higher energy x-ray beams. Med Phys 1980; 7:230.

56. **Kepka A G, Johnson P M, David J.** The effect of off-axis quality changes on zero area TAR for megavoltage beams. Phys Med Biol 1985; 30 : 589.

57. **Khan F M, Gerbi B j, Deibel F C.** Dosimetry of Asymmetric X-ray collimators. Med Phys. 1986: 13 : 936.

58. **Karl-Heinz Hoever.** Photon Dosimetry for Radiotherapy Proceedings of the workshop on medical physics in radiotherapy and nuclear medicine. Dhaka, Bangladesh, 5-10 December 1999; P135.

59. **Loshek D D.** Analysis of tissue maximum ratio / scatter maximum ratio model relative to the prediction of tissue maximum ratio in asymmetrically collimated fields. Med Phys 1988; 15 : 672.

60. **Mayneord W V, Lamerton L F.** A survey of depth dose data. Br. J. Radiol. 1944; 14 : 254.

61. **Mohan R, Chui C.** Validity of the concept of separating primary and scatter dose. Med. Phys. 1980; 12 : 726.

62. **Mohan R, Chui C.** Reply to comments by Bjargrand and Cunninghum . Med Phy.1986; 13 : 761.

63. **Nahum A E,** Water / Air mass stopping power radios for megavoltage photon and electrons. Phys. Med Biol 1978; 23-24.

64. **Niroomand-Rad A, Paliwal BR,** Effect of field irregularities on the dose distribution of 4 MV photon beam. Radiation and Oncology.1987; 8(1):43-8.

65. **Paliwal BR, Podgorsak MB et al.** Evaluation and quality control of a commercial 3-D dose compensator system. Medical Dosimetry.1994;19(3):179-85.

66. **Papanikolaou N, Paliwal B.** A study of the effect of cone shielding in intraoperative radiotherapy. Medical Phy.1995;22(5): 571-5.

67. **P M K Leung.** Physical Basis of Radiotherapy. Revised Ed. 1978; P 1-2, 84-85, 144, 212.

68. **Quast U, Glaeser, L.** Irregular field dose determination with the weighed beam-zone method Int. J Radiat. Oncol. Phys. 1982; 8 : 1637 -1645.

69. **Robert Stanton and Donna Stinson.** An Introduction to Radiation Oncology physics. Pub. Medical Physics Publishing Corporation, Madison Wisconsin, 1992; P109, P 219-258.

70. **Ragan D P, Perez C A.** Efficacy of CT-assisted two dimensional treatment planning : Analysis of 45 patients Am J Roentgenol. 1978; 131 : 75.

71. **Robert Stanton, Donna Stinson.** Applied Physics for Radiation Oncology. 1986, P 166-169, 173-174, 178, 194-195, 232-234.

72. **Safety report series No.** 17. Lessons learned from accidental exposures in radiotherapy. IAEA, Vienna, Austria, 2000; P6.

73. **Special Evaluation review.** The Agency's technical Co-operation. Activities related to Quality Assurance and Safety in Radiotherapy - Bangladesh. Evaluation section, TCPC. Department of Technical Co-operational Atomic Energy Agency IAEA – FER-98/03, Vienna, Austria, December 1998; P1-3.

74. **Spencer L V, Attix F H.** A theory of cavity ionization. Radiat Res 1955; 3 : 239.

75. **Saunders JE, Price RH, Hosley RJ.** Central axis depth doses for a constant source-tumour distance. Br. J Radial 1968;41 : 437.

76. **Sterling TD.** Perry H. Katz I. Derivation of a mathematical expression for the percent depth dose of Cobalt-60 beams and visualization of multiple field dose distributions. Br. J. radiol. 1964; 37 : 544.

77. **Saunders J E, Price R H, Horsley R j.** central axis depth doses for a constant source-tumor distance. Brt. J Radiol.968; 41 : 646.

78. **Suntharalingam N, Steben D J.** Physical characteristics of 45 MV photon beams for use in treatment planning. Med Phys 1977; 4 : 134.

79. **Technical Report Series No. 381.** IAEA, Vienna, Austria, 1997;P 24, 49-51.

80. **Technical Report Series No. 374.** Calibration of Dosimeters used in Radiotherapy. IAEA, Vienna, Austria, 1994; P 96-99.

81. **Technical Report Series No. 277.** Absorbed Dose determination in Photon and electron beams. An international code of practice. 2nd Ed. IAEA, Vienna, Austria.

82. **Technical Report Series No. 398.** Absorbed dose determination in external beam radiotherapy. IAEA, Vienna, 2000. P 39.

83. **Undbom L.** Method of dose planning on application of shielding filters in Cobalt-60 teletherapy. Acta Radiol Ther Phys Biol. 1965; 3:210.

84. **Ulrich Quast.** Dosimetry of non regular beams including TBI. Proceedings of the workshop on medical physics in radiotherapy and nuclear medicine. Dhaka, Bangladesh, 5-10 December 1999; P135.

85. **V O Parthiban, K Passi, L M Aggarwal et al.** Dosimetry of blocked beams and its comparison with empirical relations. Medical Phy. 1998; 23(3)

86. **William R.** Hendee and Geofrey. Radiation Therapy Physics. Pub. Mosby, Mosby Year Book Inc. 11830 Westline Industreial Park. St. Louis, missori. 2nd, Ed. 1996; P 428-429.

87. **Walter and Miller :** Text book of Radiotherapy, Radiation Physics, Therapy and Oncology. Pub. Churchhill livingstone, Longman Group UK Ltd. 1993; P 71, 84-85.

88. **Whitemore GF.**, Gulyas S. and Botond J. radiation sensitivity throughout the cell cycle and its relationship to recovery. In cellular radiation biology. 18th . Ann. Sym. M D Anderson Hospital Baltimore, Williams & Wilkins. 1965, P423.

89. **Wthers H R.** Dose survival relationship for irradiationship for irradiation of epithelial cells of mouse skin. Brt. J Radiol. 1967; 40 : 335.

90. **Wrede, D** E. Central axis – Tissue Air ratios as a function of Area / Perimeter at Depth and their applicability to irregularly shaped fields. Physics in Medicine and Biology, Vol. 17, 1972; 4, P 548 – 554.